T.C.

ALTINBAŞ UNIVERSITY

Electrical and Computer Engineering

IMPACT OF SOLARCELL ON SYSTEM LOSSES ON DISTRIBUTION NETWORK

HASSNEN SNOUSSI H. SNOUSSI

Master Thesis

Supervisor

Prof. Dr. Dogu Cagdas Atilla

Istanbul, 2019

IMPACT OF SOLARCELL ON SYSTEM LOSSES ON DISTRIBUTI ON NETWORK

by

HASSNEN SNOUSSI H. SENOUSSI

Electrical and Computer Engineering

Submitted to the Graduate School of Science and Engineering

in partial fulfillment of the requirements for the degree of

Master of Science

ALTINBAŞ UNIVERSITY

2019

This is to certify that we have read this thesis and that in our opinion it is fully adequate, in scope and quality, as a thesis for the degree of .

_____
Asst. Prof. Dr. Dogu Cagdas ATILLA
Supervisor

Examining Committee Members (first name belongs to the chairperson of the jury and the

second name belongs to supervisor)

Asst. Prof. Dr. Dogu Cagdas ATILLA

School of Engineering and Natural Sciences,

Altinbas University

_____

Asst. Prof. Dr. Cagatay AYDIN

School of Engineering and Natural Sciences,
Altinbas University

_____

Asst. Prof. Dr. Cahrtt KARAKUS

Engineering and Architecture,

Esenyurt University

_____

I certify that this thesis satisfies all the requirements as a thesis for the degree of

_____
Asst. Prof. Dr. Cagatay Aydin
Head of Department

_____
Prof. Dr. Oğuz BAYAT
Director

Approval Date of Graduate School of

Science and Engineering: ____/____/____

I hereby declare that all information in this. I also declare document has been obtained and presented in accordance with academic rules and ethical conduct that, as required by these rules and conduct, I have fully cited and referenced all material and results that are not original to this work.

Hassnen Snoussi H. SENOUSSI

DEDICATION

I would like to dedicate this work to my first teacher, my mother, my first supporter and role model, my father and my companion throughout the journey. Without you, this dream would never come true and to my brother and my sister who stood with me in order to achieve my dream.

ACKNOWLEDGEMENTS

All praise and thanks are due to Allah, the most gracious and most merciful, the lord of the worlds, who taught man what he knew not. I would like to thank him for bestowing upon me the chance, strength and ability to complete this work.

I submit my heartiest gratitude to my respected supervisor: Prof. Dr. Dogu Cagdas ATILLA for his sincere guidance and help for complementing this project, without him, ending this research would not be possible.

My sincere gratitude and honour go to my parents who have provided me with invaluable love and support in every way possible. Finally, and most importantly, special thanks are due to my beloved family, my dear wife for her patience, and support, she has provided me with love and encouragement, when I needed it the most. Gratitude goes to my children for their love and for their prayers for me which have been the driving force that enabled me to finish this thesis.

ABSTRACT

IMPACT OF SOLARCELL ON SYSTEM LOSSES ON DISTRIBUTION NETWORK

SENOUSSI, Hassnen Snoussi H.

M.Sc., Electrical and Computer Engineering, Altınbaş University,

Supervisor: Asst. Prof. Dr. Dogu Cagdas ATILLA

Date: July, 2019

Pages: 98

Photovoltaic systems nearly become an essential part of every power system, or to give electrical power on standalone systems for rural reigns far from power transmission lines. The electrical power from the PV systems affected by the surrounding environment such as solar irradiance and temperature. Therefore, most of this system uses maximum power point tracking methods. In this project, we provide a full study of a grid-connected PV system, starting from the equivalent circuit of PV cell, then a Buck DC-DC converter works with Perturb and observation P&O algorithm for MPPT applied on the 120kW PV array. All the previous components connected with utility power grid through a three-phase converter which uses two control loops (voltage-current) to synchronize the PV system with grid then to inject active power with unity power factor to the utility grid. All the simulation performed with MATLAB-Simulink.

Keywords: Photovoltaic, Five Parameters, MPPT, P&O, Buck, Park, SPWM.

TABLE OF CONTENTS

Pages

LIST OF TABLES

Pages

LIST OF FIGURES

Pages

LIST OF ABBREVIATIONS

CE : Component Extractor

CCM : Continuous-conduction mode

CSI : Current source inverter

DCM : Discontinuous-conduction mode

GMPP : Global Maximum Power Point

GCC : Grid-Connected Converter

IEC : International Electra technique Commission

IEEE : Institute of Electrical and Electronics Engineers

IGBT : Insulated gate bipolar transistor

LF : Loop Filter

LPF : Low Pass Filters

MPPT : Maximum Power Point Tracking

MV : Medium-Voltage

NEC : National Electrical Code

OV : Open Circuit Voltage

P&O : Perturbation and Observation

PF : Power factor

PI : Phase Detector Indicator

PLL : Phase Locked Loop

PV : Photovoltaic

PWM : Pulse width modulation

RCC : Ripple Correlation Control

RSC : Resonant Switched-Capacitor

SEPIC : Single Ended Primary Inductor Converter

SL : Super Lift

SPWM : Signal pulse width modulation

SRF : Synchronous rotating frames

STC : Standard test conditions

THD : Total Harmonic Distortion

VOC : Open circuit voltage

VL : Voltage-Lift

VSI : Voltage source inverter

VCO : Voltage Controlled Oscillator

ZCS : Zero Current Switching

1. INTRODUCTION

Renewable energies refer to energies that are not exhausted and they are generally available in large quantities. Consequently, they provide an economical as well as a sustainable solution in the form of clean and sustainable energy, which is better than fossil fuels. New energy resources include solar energy because it exists in magnanimous amounts; it is free from toxicity; so, it is environment-friendly. The DC-DC converters are applied for power generation through solar photovoltaic generation (PV) systems, fuel cells, and wind power.

The solar power generation system uses both grid-tied and off-the-grid appliances. The grid-connection between the PV generation units and the solar photovoltaic installation is generally direct. Such units only operate during the daytime from sunrise, and since the daylight isn't constant, it affects the equipment and power stability. While producing clean energy, it is important to make it sustainable for the utilization of the consumers. A solar PV generation system optimizes the equipment utilization for managing the power quality. It performs like a harmonic funnel for avoiding power outages and reactive power compensation.

1.1. PROJECT BACKGROUND

Accuracy and reliability are important features of any applied photovoltaic (PV) system. We can conduct simulations to identify merits and the electrical dynamics of the PV power plants, which operate under various conditions, temperatures, and locations. The solar power generation efficiency is location-specific.

The PV system designers can optimize the designs and sizes of PV power sources, which are used to test and verify the performances of MPPT algorithms.

The collection of different photovoltaic (PV) panel types is termed as the PV collective that forms the PV array, which provides the loads. A solar PV module has a connection in a series to assure the required output voltage from a PV. In case of solar PVs, low DC voltage output exists within the range: 12V-75V.

In this case, the interfaces of the power electronic converter and the power for DC-DC or voltage regulating converter are compulsory because they convert the low DC voltage of the solar PV to the desired voltage. Rating is provided by the public electricity grid, or any other voltage

utilization mechanism. The low DC output voltage is locally used with opposite connection before the excessive energy is supplied to the utility grid.

The PV module or the solar arrays charge batteries with the help of a PV battery charging system,, and the obtained electricity is used for diverse purposes including street-lights, off-grid transceiver stations, solar vehicles, satellites, and building-integrated PVs; therefore, it is possible to store solar energy for rainy or winter seasons, and during nighttime and cloudy weather.

Charging solar PV modules or arrays damages the batteries, and reduces their lifespan. Besides the solar PV array or the solar panels, the DC-DC converters regulate it depending on the batteries' specifications. In order to avoid the issues, several DC-DC converters should be used.

The output voltages are generated in the form of low DC voltages from the PV array that depends on the irradiation while abrupt changes depend on the shadow effects, temperature, PV system mismatch, and the purity of the PV model surface.

There is always critical need to design the DC-DC converters to regulate low and discrepant DC output voltages in the arrays; therefore, a DC-DC converter has a critical function of extracting MPP under different conditions during the day. The PV arrays' output power depends on the PV's I-V merits, and the MPPT algorithms.

Thus, a DC-DC converter system is integrated with PV systems and other sources of energy, which have not been studied so far; however, it has been observed that integrating the solar system promotes optimum utilization of energy.

1.2. PROBLEM STATEMENT

Obtaining the maximum capacity of solar cells is not an easy procedure because there are many obstacles; however, many studies and experiments have been conducted to deal with them. The results were different depending on more than one factor (quality of cells used, type of control equipment, and DC-AC conversion equipment). Attempts were made to obtain the full capacity (actual capacity) and to eliminate any losses from the surrounding environment (reactive power), and most of such attempts/experiments were successful but with a ruthless capacity at different rates; so, getting rid of fusty power is a problem. Other problems include large active power rate

that reduces the fusty power and disposal of all the wastes, which are generated during the transformation stage like DC–AC inverter, DC-DC converter, MPPT, and frequency.

1.3. OBJECTIVES

Now we'll focus on the principal components for the grid connecting with the PV systems, which are given in Figure 1.1.

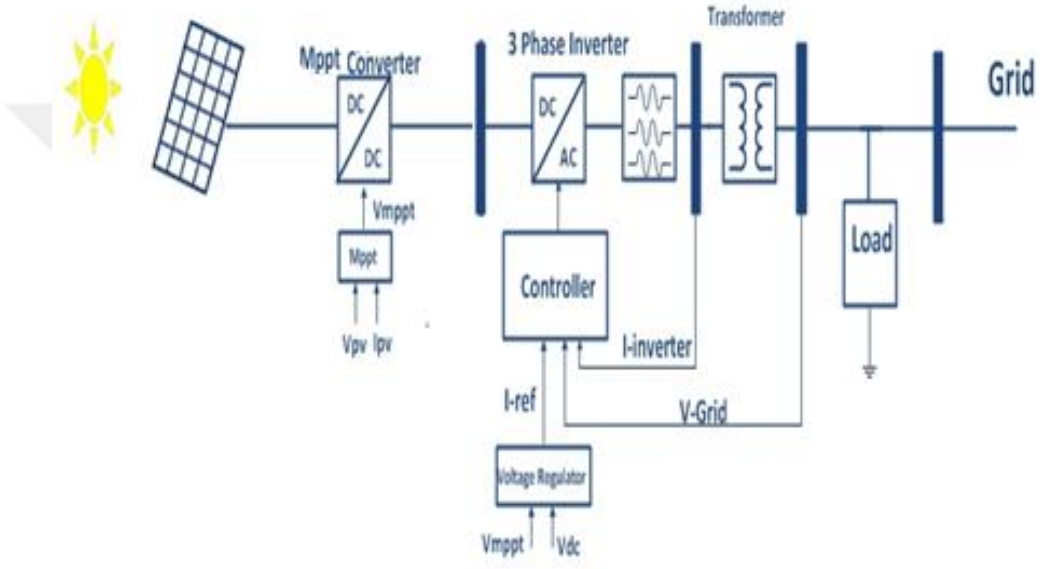

Figure 1.1: Main components of the PV- equipped Grid.

a) The main part of utility Grid and parameters of power quality.
b) Power losses during voltage drop in the transmission lines.
c) Excitation system control in the power plant to avoid overvoltage or voltage sag at different electrical loads.
d) Issues in connecting two or more power systems together.
e) PV panel parameters and collectives that affect the output of the PV and modeling that displays the performance of PV collective depending on a five-parameter model (solar irradiance, temperature, ideality factor, parallel resistance, and series resistance).
f) Different DC-DC converter types (Buck, Boost, Buck-Boost) that show the value of output voltage in the DC-link.

g) The MPPT algorithms and how to implement them to the DC-DC converters for gaining most of the generalized power from the PV.

h) The DC-AC inverter is one of the most important components for the Grid; so its study depends on the following:

- Control strategies of voltage regulation maintain synchronization between the utility grid and the PV system.
- The current controller, which controls active and reactive power provided from a PV.
- Park transformers (3-phase current wave) form and d-q-axis in the control algorithm.
- Different types of pulse generation for the transistors of the inverter such as SPWM or PWM and hysteresis.

A. Output filter of the inverter or connecting reactors for maintaining the THD on its accepted values.
B. Using active power curtailment to mitigate the impact of overvoltage.
C. Using the predicted value of irradiance temperature for forecasting the output power setup and simulated (PV) panel collective.

1.4. SCOPE OF THE RESEARCH

In this work, we will model a PV panel depending on five parameters; so, we'll be able to study its performance at different irradiance and temperature values, and then compare the results using MATLAB/SIMULINK.

We will model DC-DC converters with a PID controller to study the response of each one. It will operate with MPPT techniques, P&O, and connect it with the modeled PV panel. The final step for modeling the full PV system is placement of grid-connected inverter, which will control the synchronization between the system and PV, and then, the active and the fusty power will be controlled. Finally, we'll study the effect of PV on the utility grid with full and detailed modeling for each part of this system.

1.5 THESIS STRUCTURE

The thesis consists of five chapters:

1- Chapter 1: This chapter will introduce the problem that needs to be investigated and its relevant topics.

2- Chapter 2: It describes the background of the PV system, basic principle, DC-AC inverter, DC-DC converter, classification of solar photovoltaic system and advantages and disadvantages of the system.

3- Chapter 3: It discusses the inverters, grid-connected inverter technology (centralized, string, multi-string, and collective) inverter, the merits and classifications of inverter, half and full-bridge of inverter, IGBT and MOSFET power, voltage support for grid-connected PV systems, firm power factor, αβ transformation, Park's Transformation, grid synchronization, PLL algorithm, and control structure.

4- Chapter 4: It encompasses the test system and simulated results. The test has been mentioned in details and the complete simulated results are shown in it. A practical inverter involving the effects of power factor will be simulated using a Mat lab package.

5- Chapter 5: It includes the conclusion of the work presented in this thesis and recommendations for future work.

2. LITERATURE REVIEW

2.1. INTRODUCTION

In this thesis, we have described five equivalent parameters, and circuits with a single diode, which is simple and it gives a good explanation for studying the PV cell performance. The components of the modeled PV cell were assessed using MATLAB Simulink (Samsung SDIPV-MBA1CG255). Consequently, we can compare the results of the modeling with an interactive system.

2.2. PHOTOVOLTAIC CELL

Recently, the manufacturers have supplied the markets with commercial photovoltaic (PV) modules with up to 25% efficiencies [1]. Even now in large markets, the PV cells mainly consist of crystalline silicon, and their economy ranges from 15% to 20% [2]. The most significant advantage of the PV generation is the bigger amount of energy, and besides, it is versatile and can be placed on rooftops, open fields and the surfaces of windows.

The photovoltaic cells are evaluated for behavior under the standard test conditions (STC), with PV spectrum AM: 1.5, at 1000 Wh/m^2 irradiance and 25C cell temperature. For fulfilling the temperature and irradiance requirements under STC, in general, the testing procedure needs the kind of environment and special equipment (for example expensive solar simulations).

Depending on the version of physical PV cell, which forms the PV module, we'll find two relations between the electrical models to be built based on solar cells with single and double-diode. In case of single-diode model [3], the requirements are as follows:

- Photo generated the current from the source.

- Parallel diode (two adjustable diodes).

- The parallel and series resistances.

The model has been commonly applied in the available technical literature because it established reasonable relevance between the accuracy and simplicity [4]. Assessment of five unknown parameters is provided through manufacturer's data sheets [5], [6], [7].

The double-diode model [8] presents more data pertaining to diodes (two highly adjustable diodes) that improves the curve for fitting and the system accuracy.

To increase complexity of the model, the development of system's parameter rating is required; therefore, the method to do so won't be simple or straight forward [9],[10], and besides, the double diode design will be neglected.

I-V merit curves for the single-diode electrical model have been presented, which show the nonlinear supreme relation, which has five mutually coupled unknown parameters.

Because of some reason and difficulties, the parameters can't be determined by using simple analytical methods or by using a single approach. It can be solved by developing the ideal electrical model and the PV collective method [11]. It does not use the series and parallel resistances because most of the researchers recommended using diverse parameters in the models [12]. These diverse parameters include irradiance or temperature [3]. The collective was developed through multi-physical processes for the PV energy conversion.

The second approach is using the optimized numerical process to handle the artificial intelligence algorithms, and finding the parameters for minimizing the error that emerges between the I-V curves, and it is generated by the electrical case; so, the curves are based on the PV module [9], [13], [16].

In this case, our approach in is finding accurate solution, which has three significant drawbacks:

(a) The process needs the experimental I-V curves.

(b) A different set is obtained for every theoretical I-V curve for obtained parameters (for example, the lack of rated parameters which defines the physical realities such as irradiance and temperature, and besides, some other parameters increase or decrease when the temperature or irradiance changes.

(c) The interactive systems have error between I-V curves at minimum, and it will be desirable to get the accurate P-V curves for MPPT algorithms.

2.3. MPPT TECHNIQUES

Many researches have been conducted on MPPT methodologies, and how to implement them keeping in view the advantages and drawbacks of each one of them. The idea mainly consists of boosting equipment, which is digitally controlled to handle perturb-and-observe (P&O) algorithms [13]. P&O shows the maximum power, which reaches the minimum oscillation curve because it adapts the P&O of the MPPT algorithm for running the PV system [14].

The steady-state has limitations for oscillation in terms of divergence in the direction. The open circuit voltage is set without utilizing sensors.

The execution algorithm was compared with four technical aspects of MPPT technique (artificial bee colony, cuckoo search, modified Inc, and the hybrid ant colony through optimization of P&O). The evaluation of results was accomplished using buck-boost converter at the dSpace DS1104 DSP board junction, which improved the tracking speed by 2 or 3 times, and the efficiency is possible up to 99%.

The refined form of P&O is based on MPPT techniques [15]. The mentioned technique boosts the P&O.

V. R. Kota et al. [16] conducted a research on MPPT algorithms. The popular algorithms enhance adequacy, make a steady case for power but their dynamic behaviors cannot be defined for MPPT arrangement for improving the linear tangents of the P&O, [17] slant vitality, and power generation source, which is critical for every country. Hence the frameworks' executions are forwarded by irritating and watching the technique employed in case of the buck converter

Besides, MPPT, the variable-step InC technique is also applied to the PV [18]. This technique has been developed, and it is effective in the less steady case in terms of oscillation power for the MPP. The simulations were conducted to test the validation of the technique, for which, low-cost Atmega 328 microcontroller was used.

The investigation was carried out for the INC algorithm, which has been setup for MPPT for the PV to assure benefits at low-frequency [19]. The content of MPPT techniques has an understandable algorithm for the PV power creation system. For setting down enforcement of the InC, the PV needs to show the best functionality of current in terms of power output.

To determine a constant voltage for MPPT algorithm, which automatically adjust to the reference voltage for different values of environmental variations [20]. The pulse width analogue feed-forward modulator was developed for continuously tracking MPPT for the cell arrays [21]. The exhibit of MPPT has been designed for the overall application of the PV. The intention to prepare the voltage exploits the proportion of the controller along with the gains of the diagram.

The ANN collective has been occupied by the MPPT mayor [22]. The tracker of ANN estimation, and the currents and voltages correlating with the MPPT are affected by the PV power plant because the cell doesn't remain stable at varying temperature and radiation. The tracker uses a set for 124 arrangements in the algorithm for back-propagation.

A research article [23] includes simulation for fuzzy logic control, which is designed based on MPPT modules called as Takagi and Sugeno (TS) fuzzy module. The knowledge-dynamics for the PV include advanced TS representation, and the convex polytypical transformation. The role of exact TS representation, which is observer-order of a TS controller, had taken to accomplish MPPT in case of changing the atmospheric variations. The (TS) fuzzy MPPT state reflects the testing capability [24]. To explain the MPPT for the adaption arrangement, a novel plan was developed to fix the routine. It was compared with conventional direction, in additional to planting indirect TS to MPPT arrangement, and to display the advantages of the suggestions routine of the conventional MPPT.

Analysts [25] have described the GA for the MPPT at the PV-array, which is integrated to a battery storage unit, like a power generation unit on a standalone mode. In order to assure the system compatibility (between a resistive, reactive and asynchronous induction motor, and the non-linear load), the circuit was switched at different instances for the variables such as temperature and solar irradiance. For consistent voltage, the MPPT collective can be indefinitely put to pre-owned techniques in the PV system.

Investigators [26] have recommended that the MPPT should be operated at partial slashes because that modifies the PSO module. For evaluating the method after the simulation of a PV cell, Siemens (S75) has been used for three different graded states. The module was better for an adequate and faster performance as compared to the PSO. The benefit for the module can be witnessed in the form of reducing the oscillatory steady-state, in which, the MPP operates.

Furthermore, during the process of shading, large and partial fluctuations emerge because of temperature and irradiance. This shows the tracking capability of the MPP. It was observed when the algorithm was applied to the dSPACE-1104 controllers.

In our simulation, we'll use the P&O technique for tacking MPP, because applying it is simple, and besides, it can be applied to any kind of photovoltaic panels. The implementation of this technique is possible through variable values of irradiance and temperature.

2.4. PV CELL EQUIVALENT CIRCUIT

The analysis of photovoltaic cells is done through a simple strategy [29]. The result is obtained from important information, which depends on the electrical outputs of a PV cell [$I_{pv\ cell}$- V_{pvcell} – $P_{pv\ cell}$]. The semiconductor of a photovoltaic cell operates like a diode; and the process involves the following collectives:

- The ideal model.
- The simple diode model.
- The double diode model.

The purpose behind mathematical modeling of photovoltaic cells modeling obtains accurate characteristic curves as displayed in Figure.2.1 [5], and finding the electrical parameters values for a PV power system in different states.

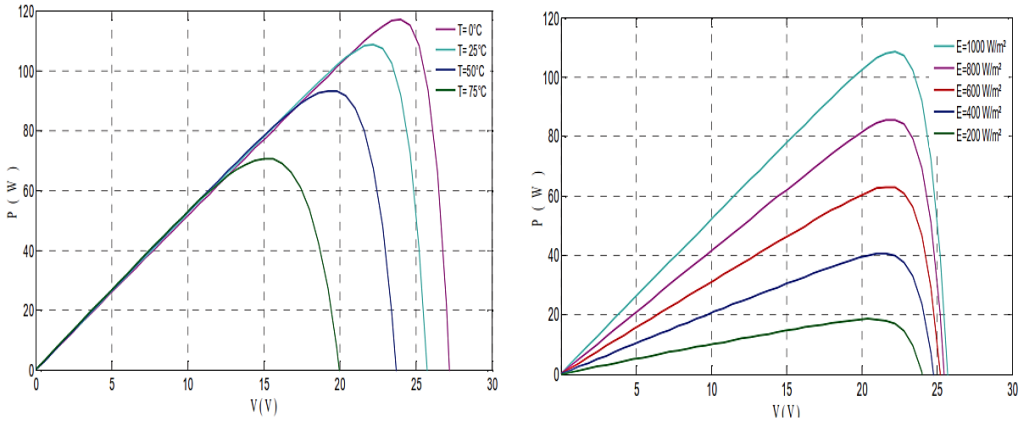

Figure 2.1: A – IV Curve, B – PV Curve .

(a) (b)

2.4.1 Ideal Model (Simple Diode)

In Figure.2.2, a diode-based circuit [3] has been presented that represents the parallel source of electricity for a diode. This circuit is simple, which could be seen in general form at the PV solar cell.

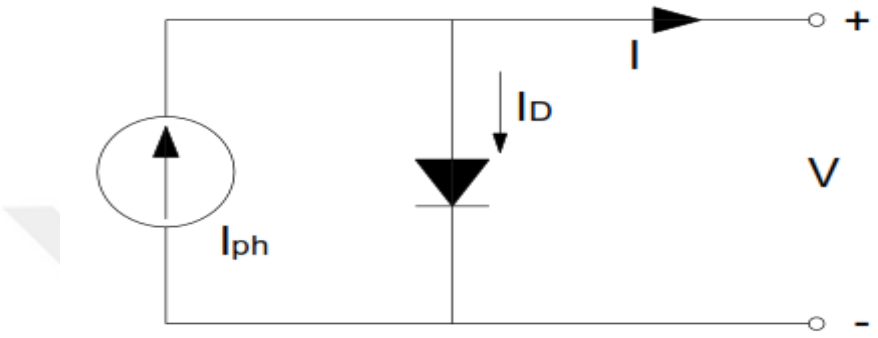

Figure 2.2: Equivalent circuit of the PV solar cell.

This equivalent is formed when:

$$R_{sh} = \infty \quad \& I_{ph} = I_{sc} \tag{2.1}$$

2.4.2. The Simple Diode Model With R_s

In the operating variations, the electric circuit's case and the PV cell have the special resistance R_s [7]. The model has been upgraded by adding a resistance, so, it will be accurate and ideal, and it will not make a comprehensive case, as shown in Figure 2.3.

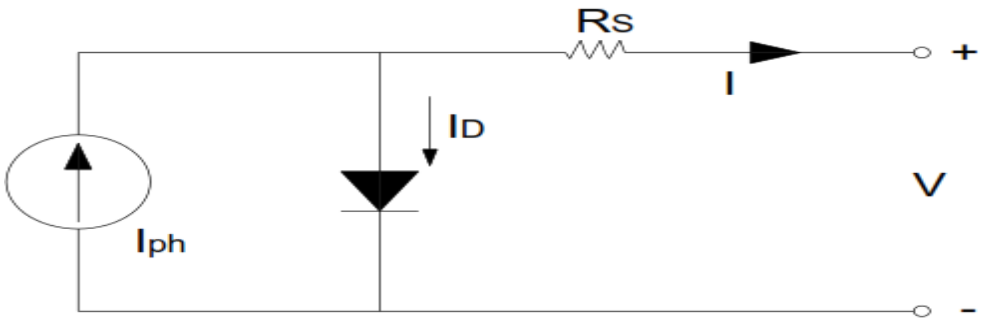

Figure 2.3: Equivalent of the circuit with Rs**.**

This circuit is called as the four-parameter model for a PV cell.

2.4.3 Simple Diode Collective With R_s And R_{sh}

The collective with R_s and R_{sh} is the spreading model for simulation of the operation of photovoltaic panels. The model takes into account both a series resistance R_s and R_{sh} for the PV array. By using this model, we expect to obtain more realistic results. The equivalent circuit is given in Figure 2.4 [9].

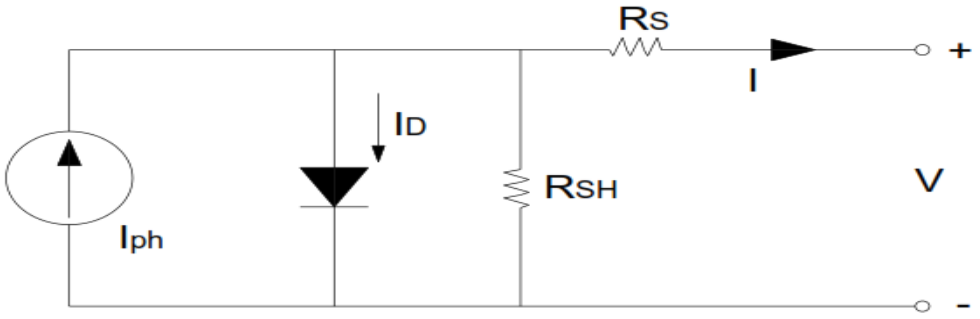

Figure 2.4: The equivalent circuit with R_{sh} and R_s .

The output current value is determined by the following expression [10]:

$$I = I_{ph} - I_d - I_{sh} \tag{2.2}$$

The expressions for the I_d and I_{sh} will be solved while the rigor of current electric will be generated in the photovoltaic cell, which forms the following equations:

$$I_d = I_0 \left(exp \frac{q(V+IR_s)}{n\ K\ T_{op}} - 1 \right) \tag{2.3}$$

$$I_{sh} = \frac{(V+R_s I)}{R_{sh}} \tag{2.4}$$

$$\boldsymbol{I = I_{ph} - I_0 \left(exp \frac{q(V+IR_s)}{n\ K\ \text{the}\ T_{op}} - 1 \right) - \frac{(V+R_s I)}{R_{sh}}} \tag{2.5}$$

Here: K Boltzmann is a constant, n is the diode factor as $1 < n < 2$, q, electron charge is $1.6021X10^{-9}$ with I_0 Diode saturation current, I_{ph} photocurrent, and T operational temperature.

We obtained a simplified case of high R_{sh} values with 100kΩ resistance. The photovoltaic current I_{ph} should be considered similar to the short-circuit current I_{sc} [15]. When we apply the assumptions for the standard test conditions:

$$I = I_{ph} - I_0 \left(exp \frac{q(V+IR_s)}{n\,K\,T_{op}} - 1 \right) \quad (2.6)$$

- **The solar radiation effect:**

The solar power and radiation intensity have important effect on the power generation by the photovoltaic (PV) cells [4], [8]. The variation in solar radiations determines the change in photovoltaic current that is represented by I_{ph}

$$I_{ph} = \left[I_{\mathrm{sc}} + K_{\mathrm{i}} \left(T_{op} - 25 \right) \right] \frac{G}{1000} \quad (2.7)$$

- **The impact of cell temperature:**

Since T_{cell} is a significant parameter of the PV cell temperature, it affects the power output. Its effect will be seen on the reversed saturation of the current I_0 [21], and for the voltage of the open circuit V_{oc}. Here the current of reverse saturation for the diode depends on the cubic temperature function:

$$I_0(\mathrm{T}) = I_0 (\frac{T}{T_{op}})^3 \exp[(\frac{T}{T_{op}} - 1) \frac{E_g q}{n\,K}] \quad (2.8)$$

The voltage of the open circuit varies with the temperature as a law:

$$V_{\mathrm{oc}}(\mathrm{T}) = V_{\mathrm{oc}}(T_{nom}) - V_{\mathrm{oc}}(\mathrm{T} - T_{nom}) \quad (2.9)$$

- **The series resistance R_s effect:**

When the series resistance increases [25], the voltage drops down at the junction while rigor increases at the terminals. This result drops the terminal voltage as a result of insignificant short-circuits. When the value of R_s is high, the PV cell behaves like a resistor [11]. Losing the power will be determined via R_s, which is given below:

$$P_{loss} = I^2 R_s \quad (2.10)$$

This power loss depends on the photocurrent, and it will increase in case of the high levels of solar radiation.

The fill factor (*FF*) reduction is based on the total resistance series, which can be evaluated by the following formula:

$$\Delta FF = \frac{-I_{SC}}{V_{oc}} FF_{ideal} \quad (2.11)$$

- **The shunt resistance R_{sh} effect:**

When the R_{sh} resistance reduces, the current will deflect and raise a certain voltage level [3]. The results significantly reduce for terminal current. In addition, a small reduction in the $V_{oc}$is observed. At a state with a high resistance, a PV cell has low shunt for the resistance that operates as a resistor.

- **The reverse saturation current:**

This type of current I_0 represents the circulation for charging at the *p-n* junction in the reverse path [5]. The leak ageing will be determined by the recombination phenomenon for charging the carrier for the zone neutral for both sides of the junction.
The current I_0 is high, the voltage of the open circuit is V_{oc}, and the reduction of symmetry in the logarithm raises. The function of the diode is subjected to the effects of recombination of the charging carriers. The phenomenon cannot be described with a simple diode model. Another term in this context is the idealist factor "*n"* [9].

The relation of the real module of the diode occurs where the recombination of the mass for the cell exists and not in the junction zone. The recombination is developed by the other cell zones, which maintains the ideality factor at value 1 [6]. Practically, when the ideality factor is raised, the product voltage decreases; however, most of the photovoltaic cells are made of silicon, and a conventional diode has an impact on the behavior of ideal factor (n ≈ 1). The entire behavior of the photovoltaic panel is modeled when I_{ph}, I_0, R_{sh}, and R_s are known for two external parameters including the cell's operating temperature and the solar radiation [2].

2.5 MPPT ALGORITHMS

The power generation through photovoltaic modules depends on solar irradiance and the temperature. A PV system operates at a higher cost and lower efficiency, if it is operated at MPP; it will change with load variations or solar irradiance. The MPPT technique has been developed for controlling the PV modules [14].

The drawback of a PV cell is its low efficiency for optimizing the operation; so, the system will be operating all the time at MPP that uses maximum energy [17][26].It is more essential to utilize the MPPT system because it automatically allows the MPP to get the value.

The PV systems' major challenge is how to handle non-linear factors out of the current-voltage (I-V); it generates the unique MPP in terms of power-voltage (P-V). The MPPT procedure becomes complex when the P-V relation varies because of weather-related inconsistencies. The MPPT collectives do not allow power increase, as the increase is delivered by PV systems to the load, which assures long-life operations for the system [20]. For this purpose, a wide MPPT variety has been developed.

The mentioned collectives should be classified depending on the benefits such as sensors type, MPP convergence speed, popularity and hardware efficiency.

The PV systems are improving by the continuous MPP operational research and development despite variations in the temperature and solar radiation. Operating the MPPT collective assures smooth PV operations despite weather changes, and it maximizes the power, which is extracted by a PV plant [4]. It is important to automatically track the MPP in terms of current and voltage.

The MPPT technique creates the required voltage and current values in a PV panel that computes the MPP, it can modify the power converter's duty cycle, and it extracts the maximum available power. In some conditions ,the PV collectives provide the maximum points but only one of them represents the MPP, which corresponds to the GMPP, and assures the maximum power generation.

2.5.1 Perturbation, observation and hill climbing

Perturbation and observation (P&O) method refines the collective for MPP, which operates depending on the periodic measures in terms of voltage and current in a PV. The resulting value

can be compared with the value of the past power, and by using the information and the voltage for operating of the system, it can be modified.

When the PV of array power value increases (dP/dV>0), adjustment will take place in the control system for the PV cell operating point in a likewise direction, or the operating point will be moved to the opposite path. The process will repeat until the MPP is reached while the system will continue oscillating among the operational points [13] [24].

The length of voltage perturbation can be a small value; however, the MPPT system responds slowly to the MPP but when the perturbation value is large, the system will quickly reach the MPP point, the oscillation around the MPP will be higher that leads to power loss. In order to solve this problem, the P&O system design should be enabled to handle varying perturbation sizes for reducing the perturbation length.

The advantage of this technique is its simplicity, and besides, the past PV knowledge isn't needed. The two main drawbacks of the P&O include oscillation at the MPP point and existence of failure values because of abrupt weather changes. The P&O collective is illustrated in Figure 2.5 [14], [16].

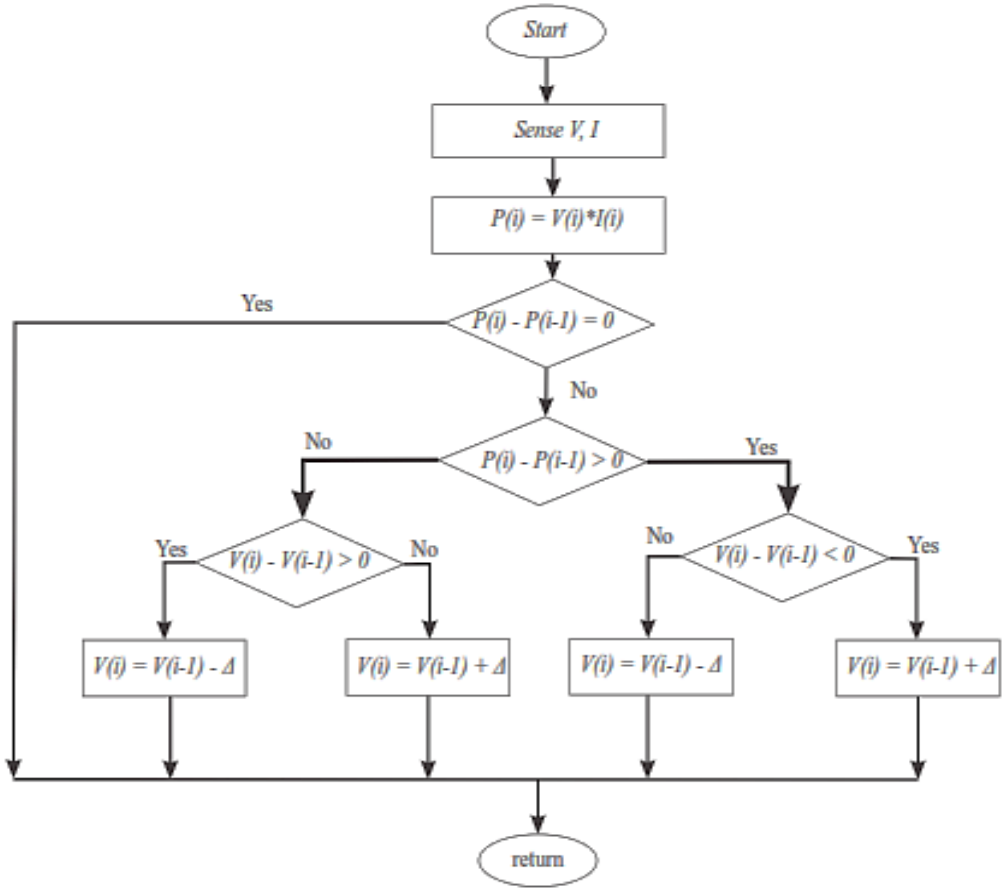

Figure 2.5: (P&O) MPPT method.

The operation of "climbing the hill" technique is the same as the P&O technique, and the only difference between them is that the P&O technique changes direction during the duty cycle of a power converter that reaches the MPP. By doing that, the voltage and current of the PV will be calculated in terms of power, and then, they are compared to the past power value to modify the power converter for getting the desired MPP. The disadvantage for this technique is its inability to detect the MPP point when abrupt weather changes take place. Figure 2.6 shows the flow diagram for the Climbing the Hill technique [15].

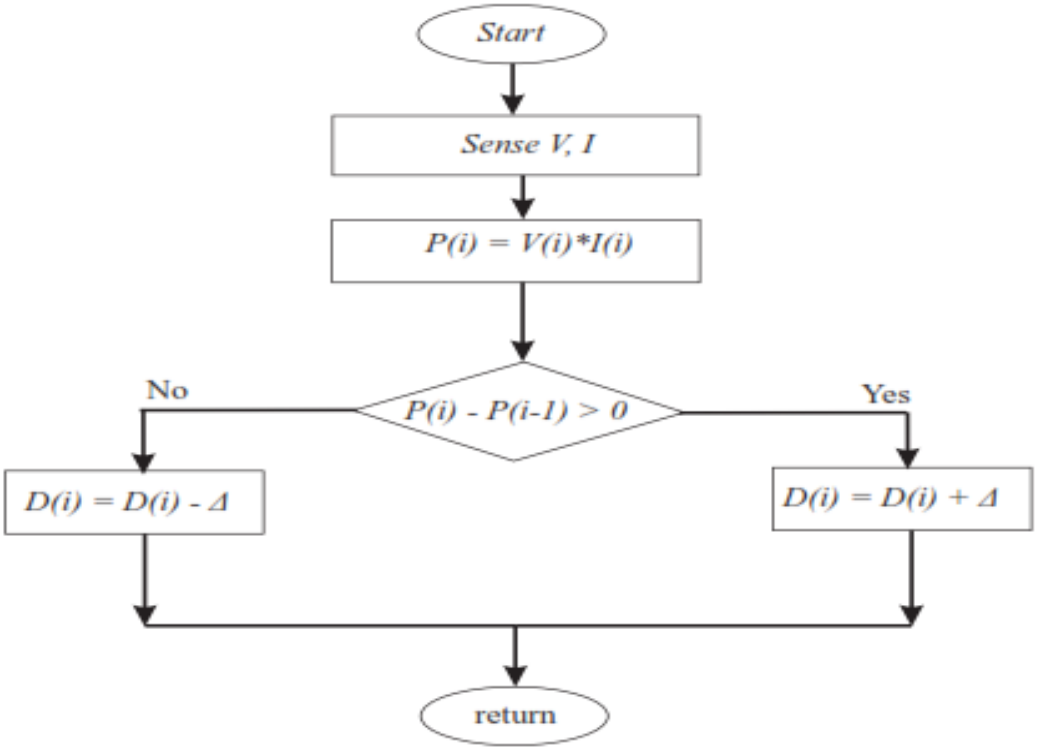

Figure 2.6: Hill Climbing Technique.

2.5.2. Incremental Conductance

Incremental conductance or IncCond technique involves the zero value of the slope of the P-V curve, and the MPP that reaches the positive value on the left while the value is negative on the right side for MPP:

$$\begin{cases} dP/dV = 0 & \text{at MPP} \\ \mathrm{dP/dV} > 0 & \text{Left of MPP} \\ dP/dV < 0 & \text{Right of MPP} \end{cases} \tag{2.12}$$

Where:

$$\frac{dP}{dV} = \frac{d(IV)}{dV} = I + V\frac{dI}{dV} \cong V\frac{\Delta I}{\Delta V} \tag{2.13}$$

$$\begin{cases} \Delta I/\Delta V = -I/V & \text{at MPP} \\ \Delta I/\Delta V > -I/V & \text{Left MPP} \\ \Delta I/\Delta V < -I/V & \text{Right MPP} \end{cases} \tag{2.14}$$

The MPP is planned to be obtained through comparing the incremental conductance INC (ΔI/ΔV) with the instantaneous conductance (I/V), while the reference voltage (V) range is modified for obtaining the MPP point [9], as Figure.2.7 indicates. The MPP approximates to the point while the system is likely to operate at that point until some variation ΔI is detected. It is used because of weather variations while the V_{ref} has been re-modified to reach the MPP point.

A drawback of the mentioned IncCond technique becomes obvious when the reference size is small; so, the system will reach the slow point MPP, and since variable increments exist in the system; it is likely to converge to the MPP point. In case when there are abrupt weather changes, the IncCond technique provides a satisfactory response when it has a stable and steady-state. The IncCond technique might lose the oscillatory behavior at the MPP point if it is compared to the P&O technique [16],[20].

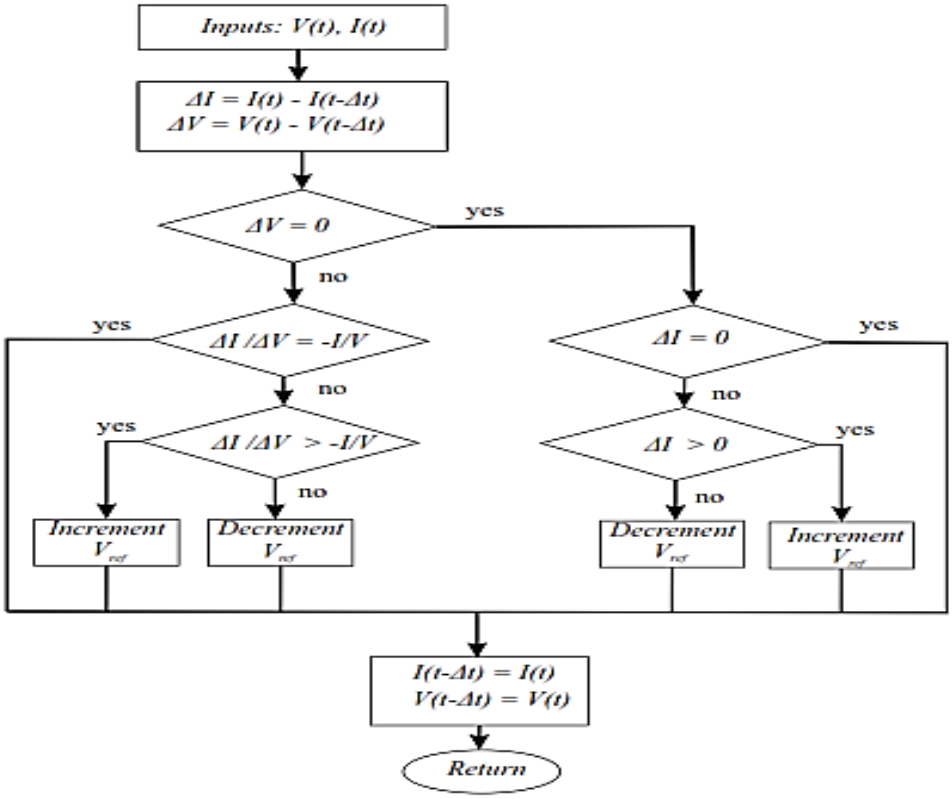

Figure 2.7: IncCond MPPT technique .

2.5.3. Fuzzy Logic Control

These techniques help tracking the MPP in the PV systems, which get more the accessible [24] and improve the performance of low-cost micro-controllers. There are three stages of Fuzzy logic control, which are shown in Figure.10:

- Fuzzification.

- Fuzzy inference processes.

- De-fuzzification.

In the fuzzification state, the numerical value of the input variables converts in the linguistic variables, which are based on predefining functions, and better performance for fuzzy logic [23]. Defuzzification acts as the output controller for linguistic variables because it converts the analogue signals into numeric variables by controlling the duty cycle of the converter and obtains the MPP point, as Figure 2.8 indicates.

The two advantages for this technique include the mathematical nature of the technique [25], and the ability to handle non-linear situations. This technique accurately tracks the MPP despite climatic variations. They have a major controlling disadvantage because its effectiveness depends on the calculation error that affects the fuzzy inference mechanism.

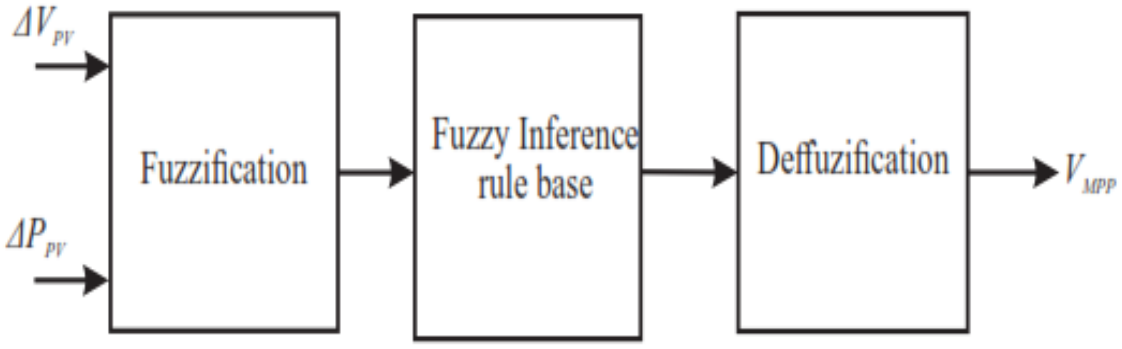

Figure 2.8: Fuzzy logic control technique.

2.5.4. Neural Network

In general, the neural networks technique has three layers, as Figure.2.9 indicates. They include:

- The input layer
- The hidden layer
- The output layer

The nodes for all the layers depend on the user. The input variables of the parameters of a PV cell include short circuit current (I), open-circuit voltage (VOC), and atmospheric data, etc. The output system corresponds to numerous reference signals; one of the signals modifies the duty of cycle for maintaining the power converter at the MPP [22].

The hidden layer obtains the MPP point but the chaining of the neural network will be required for the path of rigor that depends on the processing. The neural networks can be retrained by applying different PVs because they have different allotments. On the other hand, it is significant to note that the PV system parameters can be periodically modified, which means that it is important for periodically chain the neural network for ensuring the effectiveness of the path in the MPP point.

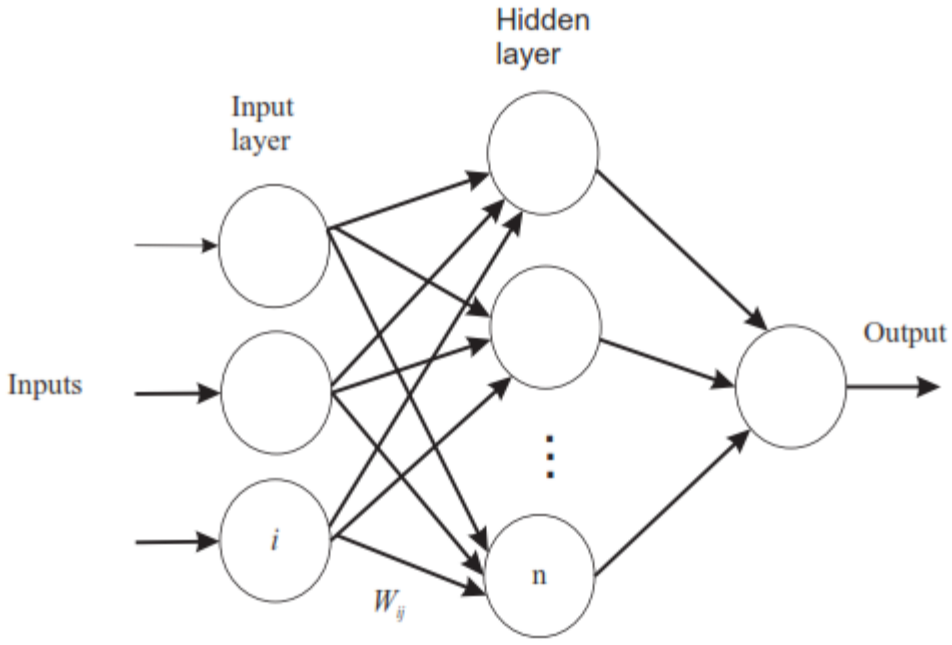

Figure 2.9: Neural Network Control Technique.

2.5.5. Ripple Correlation Control

This control technique helps obtaining the MPP point by the ripple of voltage or current in a PV array for switching power converters. The RCC technique primarily depends on the time derivative power (Ṗ) of the PV array and the current of time derivative ($\dot{I}$). The voltage of time derivative (v̇) drives the gradient to zero that reaches the MPP point [9]. When the current or voltage is high ($\dot{v} > 0$ *or* $\dot{I} > 0$) at a specific time, the power increases ($\dot{P} > 0$), and the system operates below the MPP point ($V < V_{MPP}$ *or* $I < I_{MPP}$). If the power drops ($\dot{P} < 0$), the operation will take place at the MPP point ($V > V_{MPP}$ *or* $I > I_{MPP}$). When the MPP point is obtained; the left side is positive, and the right side is negative. This technique has certain benefits including fast concourse to the MPP point despite abrupt weather changes [16].

2.5.6. Sliding Mode Control

The sliding mode control is separated from the feedback control technique. The collective is favorable for regulating the system of switching control, [20] (for example the electronics of power devices), and the emptiness of class for electromechanical and mechanical systems (robots, motors, and satellites). The sliding mode control sends a signal (on-off) to turn on or off a power converter, which obtains the MPP point for a PV system. A commutation function "u" influences dP/dV>0 on the left MPP point while dP/dV<0 on the right. It can be expressed as follows:

$$\begin{cases} u = 0 & S \geq 0 \\ u = 1 & S < 0 \end{cases} \tag{2.15}$$

S will become:

$$S = \frac{dP}{dV} = I + V\frac{dI}{dV} \tag{2.16}$$

At u =0, the commutation function is similar but the switching converter must be open. At u =1, the switching converter should be closed. It consists of different devices (FPGA, DSP, and microcontrollers). Other possibilities include existence of non-zero steady-state error [28].

2.5.7. Open-Circuit Voltage

This (OV) technique applies to the MPPT control point, which is set up when the voltage is measured at the terminal and PV arrays. Generally, the OV collective utilizes 76% of the open-circuit voltage [7].

The real-time open-circuit voltage measurement predefines the PV for the I-V curves. It is important to perform the static switching and converting it into the PV array. The switch is connected in the series that opens a circuit. At I_{pv}=0, the PV system won't supply the power. The features of the approach are relatively fast for the response and the oscillations won't be in a steady-state [11].

2.5.8. Short-Circuit Current

This method is employed when the value for I_{sc} approximates the I_{mp}.The process, in general, is used for short-load pulse to generate a short circuit. It is important to observe that the time during the short circuit pulse V_{pv} should be zero [9]. Consequently, the power will not be supplied through the PV system, and there will be no power generation; so, the power conversion circuit needs to be powered through other sources. For creating a short circuit state, it is necessary to put the static switching in a parallel state with the PV array. The optimum operating current I_{PV} has maximum output power that is actually the short circuit current $I_{sc.}$ The irradiance level G is as follows:

$$I_{op}(G) = K.I_{sc}(G) \tag{2.17}$$

Here, k represents a supposed constant.

This technique has a definitive benefit in terms of the input capacitance tolerance when it is compared with the V_{oc} process [16].

2.5.9. Merits of the MPPT Techniques

For comparing different attributes for each technique, and the MPPT techniques' essential features have been summed up in Table 2.1.

Table 2.1: The main merits of the MPPT technique

MPPT Technique	PV array Depends?	Analog Digital	Periodic Tuning?	Convergence speed	complication	Sensed Parameters
P&O	Nope	Both	Nope	Differs	Low	Voltage, Current
Hill Climbing	Nope	Both	Nope	Differs	Low	Voltage, Current
Incremental Conductance	Nope	Digital	Nope	Differs	Medium	Voltage, Current
Fuzzy Logic	Sure	Digital	Sure	Fast	High	Varies
Neural networks	Sure	Digital	Sure	Fast	High	Varies
Ripple Correlation	Nope	Digital	Nope	Fast	Low	Voltage, Current
Sliding Mode Control	Nope	Analog	Nope	Fast	Medium	Voltage, Current
OPEN CIRCUIT VOLTAGE	Nope	Both	Nope	Varies	Low	Voltage
MERITS OF MPPT TECHNIQUES	Nope	Both	Nope	Varies	Low	Current

2.6. TOPOLOGIES OF DC-DC CONVERTER

A DC to DC converter sends a specific request of the direct current (DC) loads. We have several DC-DC converters, which depend on the collective regulators' switching functions. It enables an operator to regulate the non-regulated DC voltage for conversion that is suitable for utilization during the increase or decrease in the DC output when the power-switching devices are used for PWM at a fixed frequency, which are called the buck, boost, buck-boost, cuk, and Single Ended Primary Inductor Converter (SEPIC) [25]. Every converter needs power switching devices to turn on/off. The devices of power switching include BJTs, MOSFETs, thrusters, and IGBTs, which are used for various applications as well as circuit-design parameters. Despite the fact that the power switching devices are triggered, the appropriate gate drives signals through the driver circuit gate. A DC-DC converter performs through Pulse Width Modulation (PWM) process for controlling the frequency, converter voltage, and phase delays [27].

2.6.1. DC-DC Boost Converter

Figure 2.10 describes the circuit of a non-isolated DC-DC boost converter that comprises:

- Diode (D)
- Capacitor (C)
- Power Switch (M)
- Inductor (L).
- Switching Controller.

The topology cell will be applied for connecting interface from low PV to the higher battery bank for input voltage for any DC load [31],[32]. The DC-DC boost collective boosts the output voltage that exceeds the input voltage. The controller adjusts the switches to turn on/off the input voltage, which yields the required output.

When the switch is turned on, a diode is in the opposite state while the electrical energy stores in the inductor. At the same time, the capacitor supplies current to the load. When the switching process is turned off, electrical energy in the inductor transfers to the capacitor and the load.

A DC-DC boost converter has two operating modes, including a discontinuous and a continuous conduction mode (DCM and CCM). When the DC-DC boost operation is carried out in the CCM, inductor current exceeds zero. During DCM, the indicator's switching cycle drops down to zero. The research bearing of a DC-DC boost converter has current, which is reported for harmonic elimination. The correlation power factor, zero regulation voltage, and load balancing are significant [36].

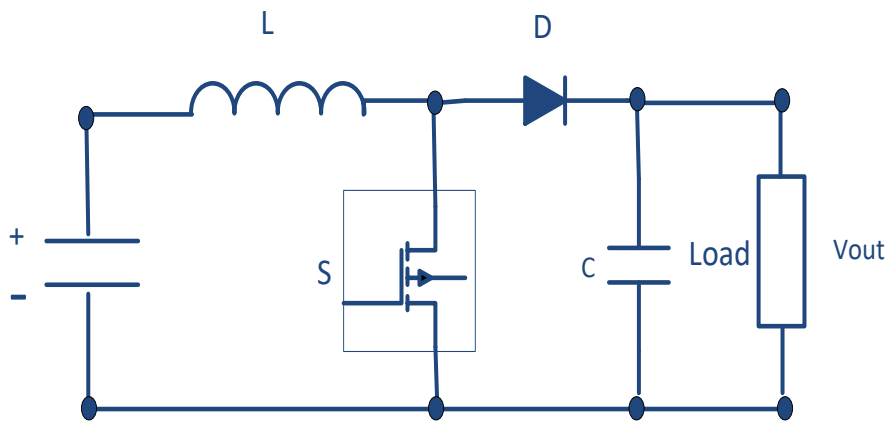

Figure 2.10: The DC boost converter.

Output voltage:

$$V_{out} = \frac{1}{1-D} . V_{in} \quad (2.18)$$

D is the duty cycle.

2.6.2. DC-DC Buck Converter

The intrinsic DC-DC buck converter circuit consists of the following [33], [37]:

- Diode (D).

- Power Switching (M).

- Inductor (L).

- Switching Controller and the Load.

- Capacitor (C).

Figure 2.11 shows that the DC-DC buck converter operates by stepping, which means that it shifts from the high input voltage to the low output voltage; therefore, its output is lower as compared to the input. The circuit gives purely DC output when LC is added to the low-pass filter to a basic circuit.

The DC-DC buck converter either connects to low voltage DC load or the battery storage at high PV array voltage. DC-DC buck converters are reliable step-down converters, and they regulate

low power range. A simple collective is used with the low control, no isolation and minimum number of components.

Most DC-DC buck converters are part of the battery storage that has high input voltage modulation through PWM for generating low required output using batteries. In addition, the MPP races for maximizing the output power, which is obtainable from the PV cells. Numerous PV solar applications have DC-DC buck converters and standalone solar PV pumping systems, which supply water to the solar battery charger, rustic areas, grid-tied MPPT racing and off-the-grid PV systems. Figure.1.3 shows the basic circuit collective (DC-DC Buck Converter).

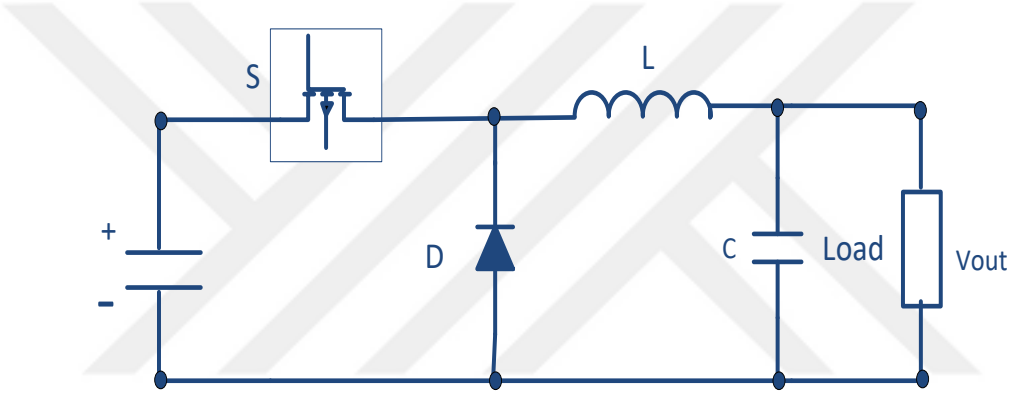

Figure 2.11: DC-DC buck converter.

The output voltage dc is given by:

$$V_{out} = D.V_{in} \tag{2.19}$$

2.6.3. DC-DC Buck-Boost Converters

This type of converters is similar to non-isolated (boost) converters. They switch the element before the inductor (L), as Figure 2.1 indicates. The DC-DC buck-boost converters are also called step-up/down converters. A bidirectional converter generates either the lower or the higher output voltage when it is connected to a suitable-voltage PV array, the battery input voltage, or the DC load. The DC-DC buck-boost converter cascades the connection between the two basic buck and boost converters.

The output is adjustable because it is possible to change the duty of a cycle D. When D is less than 50%, it will operate in the buck mode, and the voltage output will be lower than the input. In

case D is more than 50%, the converter functions in the boost mode, and the output is more than the input [1].

The parameters are part of the design process, and the converter operates at an indicator frequency, maximum voltage, and current. The inductor's voltage value can be resisted, and this resistance may be other than the one on the driver gate of the circuit. The PWM switching signals trigger the power switch. Figure 2.12 is a basic circuit collective [33], [39].

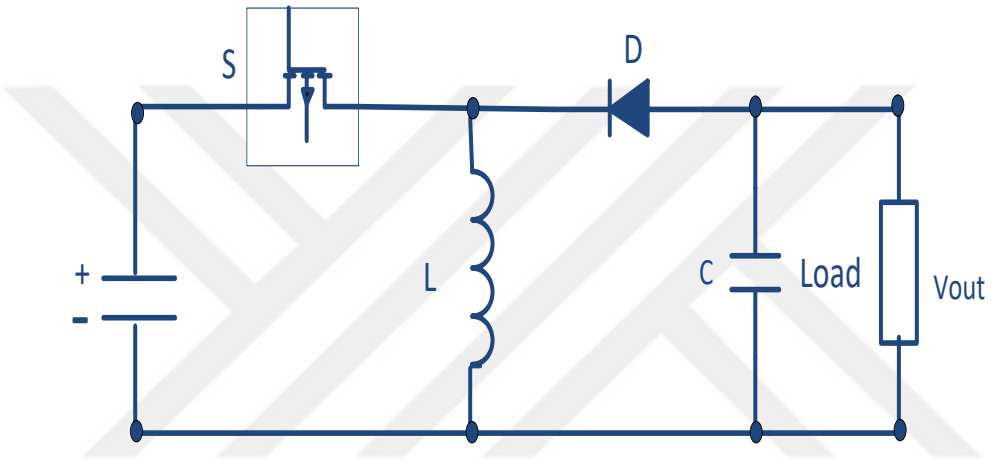

Figure 2.12: The DC-DC buck converter.

The output DC voltage will be:

$$V_{out} = \frac{D}{1-D} . V_{in} \quad (2\text{-}20)$$

2.6.4. DC-DC Cuk Converter

Figure 2.13 shows a basic collective circuit of a DC-DC converter. A Cuk converter has a specific magnitude of the output voltage [33] [36], which may be greater or lesser than the magnitude of the input voltage. A converter can be low-switched for losses and it has higher adequacy. The converter gives better output current of the inductor during the output stage.

The output voltage has the opposite polarity as compared to the input voltage. When the input voltage is turned on, the MOSFET (SW) switches off. When a diode D works in the forward path, the capacitor Cl charges through Ll-D.

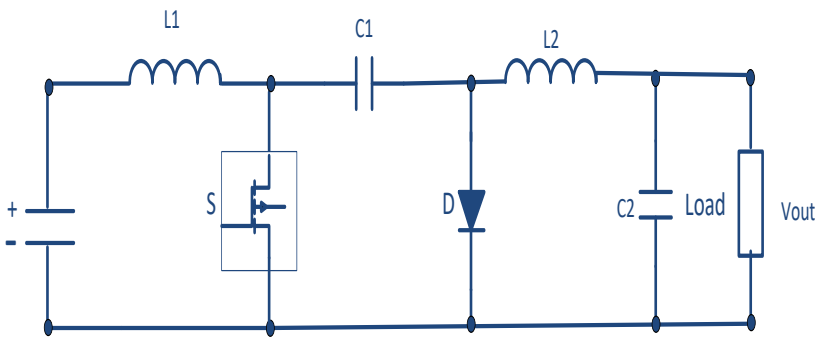

Figure 2.13: The DC-DC Cuk converter.

The output voltage is:

$$V_{out} = \frac{-D}{1-D} . V_{in} \quad (2\text{-}21)$$

2.6.5. SEPIC Converter

The SEPIC DC-DC converter allows lower/greater output voltage as compared to the input while the output voltage is controlled through D switching. A SEPIC stand for Single-Ended Primary Inductance Converter and it has no inverting buck-boost feature. The converter has the gate for the drive construction for landing the terminal switching, and besides, it has no pulse for current input. The SEPIC operates by transferring the energy between C1 and Ll, which means that it reduces the stress of voltage on C1, which is lower than the cuk converter; so, it provides better input and output for isolation, low rippling input and noise. Figure 2.14 describes the basic circuit collective of a DC-DC SEPIC converter [32].

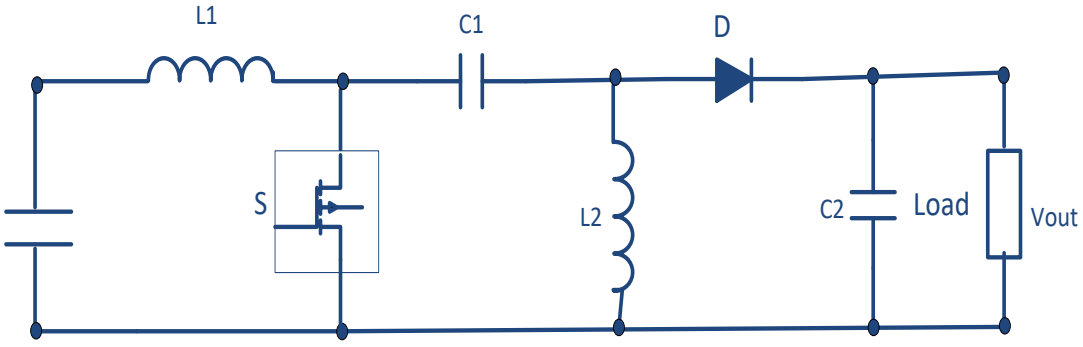

Figure 2.14: The DC-DC SEPIC Converter .

2.7 CONTROL DESIGN

Figure 2.15 shows how a controller performs with the buck-boost converter through closed-loop PID control [31]. The output voltage V_R has the opposite direction in terms of input voltage V_E while the reference voltage is a positive solution to adjust the error of rising E. For the negative solution, the feedback will be the negative unit of gain for output of the converter. The signal error will enter the PID controller, and it will provide the output value. The output controllers are connected to the element of saturation and the output has pulses of the generator.

The element of saturation limits the signal error at the value of upper-lower saturation [28] [32] while the input signals exists within the range. The ideal switching case at the lower saturation level is zero while the upper is one. When the one takes the time for necessary switch opening and closing, such limitations should be moved forward for reducing the range. This range has the active control, and it uses the outward signal control that doesn't affect the behavior of the system. To perform the full-time system control, it is essential to control the signal within the saturation range.

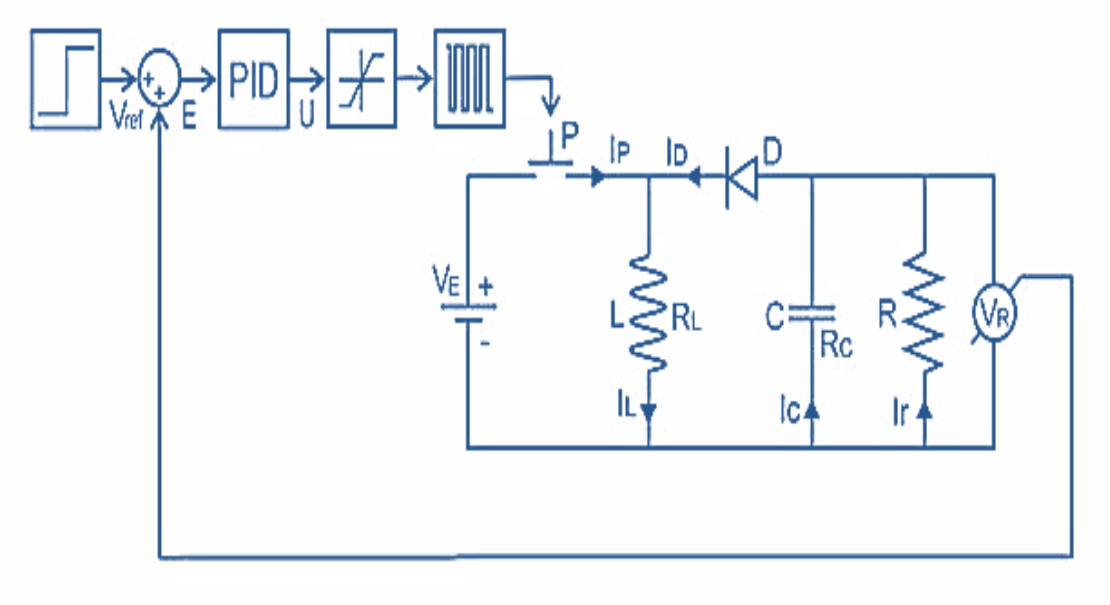

Figure 2.15: PID control through a buck-boost converter.

The maximum gain for an ideal buck-boost converter may be beyond limits. The real converter has limited gain, and the parasitic resistances will be lost. Maximal gains for the physical properties in an electric circuit can't be overcome. Figure 2.16 is a graph that represents the

dependency of maximal gain on a duty cycle D for real and ideal-state buck-boost conversion. In the designing control, the maximal value of the reference signal should have a certain limitation and the gain will never exceed the maximal.

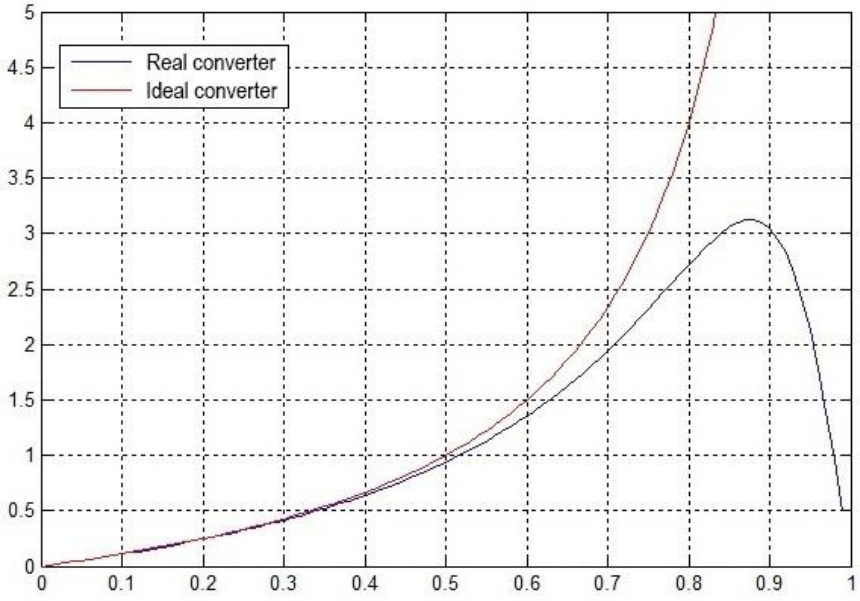

Figure 2.16: Maximal gain for buck-boost .

The form of PID control law can be expressed through the following relation:

$$u(t) = K_p e(t) + K_i \int e(t)dt + K_d \frac{de(t)}{dt} \tag{2.22}$$

The function of transfer for the PID controller is:

$$C(s) = \frac{U(s)}{E(s)} = K_p + \frac{K_i}{s} + K_d s \tag{2.23}$$

Where K_p, K_i, and K_d symmetrical, integral and derivate gains, respectively.

The PID controller indirectly uses a pulse generator and controls the duration for switching in a single period. The control level is limited in case of theoretical, zero and one. The symbol has been represented by the saturation on the block diagram (Figure 2.10).

For the moment of step bounce to the reference signal, the voltage output stills at zero, while the signal E error is likely to be similar to the reference voltage. In order to prevent the control of the

signal to the upper limit of the saturation [25], the maximal is allowed for symmetrical gain, which should be similar to the inverse of the reference signal.

$$K_{pmax} = \frac{1}{V_{ref}} \tag{2.24}$$

Any value with higher gain would result out of the higher signal control than the upper saturation limit, and the control signal will get disturbed. The proportional gain shows a critical value $K_{cr,}$ that is applicable to the PID design, and it can be calculated by multiplying the maximum allowed gains from the duty cycle D with the desired gain of converter:

$$K_{Cr} = dK_{pmax} = \frac{d}{V_{ref}} \tag{2.25}$$

The influence of the converter gain M on the law of control has been given, and it provides a uniform response step in the scope of the possible gains for a converter. The critical oscillatory period T_{cr} can be obtained by measuring the oscillation time that relates to the maximal point, which assures symmetrical gain K_{pmax}. For a buck-boost converter, the minimal oscillatory period is measured through all-time uninhibited oscillations of the output value [20].

The alternative approach is evaluated through a critical oscillatory period for the standard equivalent of a system for transferring a function [22]. This approach is adapted to the shortest possible periodic oscillations in the circuit of the converter. The minimal possible oscillatory period corresponds to the zero value for duty cycle D. After the lapse of all the parasitic resistance, the critical oscillatory period will be given by the expression:

$$T_{Cr} = 2\pi\sqrt{LC} \tag{2.26}$$

By using the adopted values for K_{cr}, and Ziegler-Nicholas recommendations for the PID tuning in Table.2.2, the unknown parameters of the PID controller can be evaluated as follows:

Table 2. 2: Ziegler-Nichols recommendations for PID tuning

Controller	K_p	K_i	K_d
PID	$0.6\ K_{Cr}$	$\frac{2K_p}{T_{Cr}}$	$\frac{K_p T_{Cr}}{8}$
PID small overshoot	$0.33\ K_{Cr}$	$\frac{2K_p}{T_{Cr}}$	$\frac{K_p T_{Cr}}{3}$
PID without overshoot	$0.2K_{Cr}$	$\frac{2K_p}{T_{Cr}}$	$\frac{K_p T_{Cr}}{3}$

2.8 DC-DC CONVERTERS

The large scale PV is a single DC to AC converter that reduces the system cost, power loss, and the size of the system. The overall efficiently reduction depends on the partial tenting. Hence, the two stages of conversion have higher adequacy, especially when MPPT is used for algorithms; however, the high cost and power quality are some issues in the AC grid connecting with PV systems. In addition, long distance transmission and fusty power compensation are some important challenges, which affect the grid stability [27].

For effective solution, it is proposed that the DC power grid should be connected to the PV system [28].

For more direct conversion of PV power to MV DC-grid, a simple structure increases the adequacy value and reduces the cost, when it is compared to other MV AC grid-connected systems. Moreover, like MV AC systems, it is possible to convert the voltage through a DC-DC voltage converter. In the MV of DC grid-connecting to PV systems, the important part for high gain is the high frequency of the DC-DC conversion system that converts the adaptable and non-regulating PV for DC voltage in order to regulate the MV DC voltage [29].

Many studies are conducted to test the use of DC-DC converters in the MV DC grids for developing as well as deploying renewable energy sources such as PV plants and wind turbines [27],[28]. Many collectives were investigated based on their applications; so we can divide them into two main forms:

-The isolating module requires the low voltage for semiconductor devices on the input side, by adding galvanic input to assure isolation. The converter design for MV and high power levels are more complex [30].

- The DC-DC converter of non-isolated system provides the step-up of voltage without needing any transformer [31].

The DC-DC converter of the non-isolated collective, which based on the boost converter collective, was introduced, while the devices of silicon carbide are used to boost the efficiency of the transformer. The results of silicon carbide MOSFETs showed 98.5% power rating conversion adequacy at 30kW. The device has rating of current and voltage ratings 10A and 10kV,

respectively. In this case, of the connection between the strings of PV will be parallel for greater current transmission.

Another collective [32] was set up on hybrid union for boost and buck/boost converters to assure higher voltage. The high voltage gains will be achieved by using multiple collectives for a single switching and single-inductor converter if the single collective has failed the converter that would continue to operate with less power level.

The resonant step-up (RS) was introduced, it steps-up the ratio using a capacitor and an inductor. A converter collective reduces losses through soft switching, ends the turn-off, and reverses the loss recovery [33].

The Resonant Switched Capacitor (RSC) is used with a DC-DC up converter [34] to reduce the losses across the soft switching in all diodes and switches through Zero Current Switching (ZCS). The zero-current switching is possible when all the currents in the puffy inductors are zero. Then, the soft switching becomes possible, and the switching losses are reduced, which is possible to attain a higher switching frequency.

The parasitic elements affect the DC-DC converters for voltage and power output that restricts the transfer adequacy; therefore, the Voltage-Lift (VL) process has been widely used for boosting the DC-DC converters when it increases the voltage output [33].

The VL converters have a simple design with high voltage gain value as it increases the voltage stage value for mathematical progression. VL is applicable to the Luo-converters [34].

The conversion of the DC-DC voltage takes place at high adequacy, high power density, and higher voltage output with small ripples and simple chipping structure. The converters are classified depending on power stages. A basic circuit has a single power stage, a Re-Lift circuit has two power stages, and a triple-lift circuit has three power stages etc.

A converter has the Super Lift (SL) technique with full power as compared to a VL technique. For gaining several traits, the SL technique is used with Luo-converters. The mentioned traits include:

- Very high gain of voltage transferring,

- Increasing output voltage

- Higher efficiency

- Higher power density

- Reduction in ripple current and voltage [34].

For simulation, we will study three DC-DC (buck and boost-buck/boost) converter types with MPPT techniques, and the use of a PID controller to study the response for each type of selected converter. Then, the converter will be used at a DC-DC stage before adjusting the active/fusty power in the PV-system.

2.9. GRID CONNECTED DC-AC INVERTERS

There are many types of PV plants [35]. The Microgrids provide efficient solutions to contain the electrical grid for more stability and less fluctuation [36].

The multiple parallel PV-inverters increase the power quality, and the system efficiency [37]. For load-sharing through a PV-system with the grid, currents' circulation is reduced between the power converters.

The simplified VAR control is a single-phase PV-inverter, which is connected to the grid [38]. The alteration techniques are set up on the asynchronous-sigma-delta with current-mode to reduce the THD.

The strategy of current control for the LCL-filter of the inverter of a grid reduces the THD [39], and improves the unity power factor. The phase of line current is supplied by a solar-inverter. It contributes to the grid voltage as the LC-filter does. The power-factor circuit connects in parallel state to the PV-inverter to improve the power factor for the grid feed, and to improve the power transfer to the PV panel. The synchronization changes in an orthogonal manner, while the power factor adjusts the fusty power (VAR) in a grid-connected system. The results of the proposed techniques improve the performance of solar cell power inverter to supply highly inductive loads.

3. METHODOLOGY

3.1 INTRODUCTION

In this chapter, the methodology for research has been discussed based on results of previous researches which provided the best solutions to make the investment feasible. Moreover, it results in higher output capacity, puts the power in the public electricity network, and tries to avoid losses in large reactions of power resulting from the equipment during the DC conversion process from low power to high power [1].

In the first stage, we will discuss the methods of continuous conversion from low values to intermediate power values. In the second stage, the styles of converting from continuous intermediate efforts to the three-phase alternating intermediate stage. Converting from alternating intermediate power to high alternating power, and synchronizing are essential in order to connect to the public network.

The appropriate styles for these stages, which we can obtain the maximum values of actual capacity, will be drawn, and how to get rid of reaction capacity in the best way. Later, we will propose the best model and appropriately apply the model parameters [2] [4], by proposed and most appropriate modifications to get results for the best actual capacity. We have tried not to get the reaction capacity resulting from the equipment, which will assure maximum utilization of the stored energy.

3.2 THE PRINCIPLE

The inverters are the heart of a PV system, and it is important for all the utility of the interconnection codes with standards. The solar or the PV inverter power needs an electrical inverter, which changes the DC electricity from the array of photovoltaic to AC for using it in houses and industries [3].

The photovoltaic (PV) arrays are a DC source because it requires the conversion of DC to AC power. The PV array runs at the time when the sun rises up and locates way from the cold areas for directing sunlight. The PCU is a general term used for the equipment between the inverter

and the interface of the PV (battery of system) in a grid system. The important thing for the inverters is their safer design which is better than rotating generators [9].

During the same period, the PV system is connected to the grid; so, the generated power needs to be at specific standards, depending on the regulated utility of countries.

The main factors in grid-connection to the inverters include [6] [8]:

- The Total of Harmonic Distortion (THD).
- Power factor control (P.F).
- The injection power for DC current level.
- The range of voltage and frequency for standard operation.
- Detecting islanding or non-islanding functions
- Automatic synchronization and linking.
- Protecting the system from grounding

Markets of distributed resources have several standards. A PV system is important because it has all the wiring. The rolls are ordered by IEC (International Electro Technical Commission), IEEE (Institute of Electrical and Electronics Engineers) and NEC (National Electrical Code).

The standard codes are designed for proposed PV systems in the NTNU electronics for using PVs for electrical installations and interfacing to the grid [7]. The IEEE 929-2000 standard has a recommended practice for utility interface of the Photovoltaic (PV) Systems to guide the PV system for practices. These practices include the power quality and protection of functions. The IEEE: 929-2000 standard has another UL-1741 standard, which is the key to choose the inverters in the design.

The code (690) describes the information for aspects of designing and composition, which includes:

- The PV system for coding and conductors.

• The grounding system and collective connection.

• The (PV) source of circuits. The PV power inverter, which is used for output circuits and circuit routing.

• The identification of equipment is used for understanding the circuit requirements (open-circuit voltage and the short-circuit current) [9].

3.3 GRID–CONNECTED INVERTER TECHNOLOGY

The technologies and topologies' for the network of connecting to the PV systems have been categorized, and set up for a number of power stages. The PVs of plants have diverse technological utilization that uses the connection of an array of the PV to the utility grid. Every technology has its own advantages or disadvantages in terms of efficiency, and the same is true for grid-connected inverters.

3.3.1. Centralized Inverters

This technology is old, which is obvious in Figure 3.1. The centralized inverters are interfaced with large number of PV collectives, and the mentioned PV collectives are divided into strings. The generator has processes to deal with high voltage or higher amplification. When the connections are established in the parallel state through the string of diodes, they reach higher power levels. This diagram shows the parallel connections to a central inverter [13].

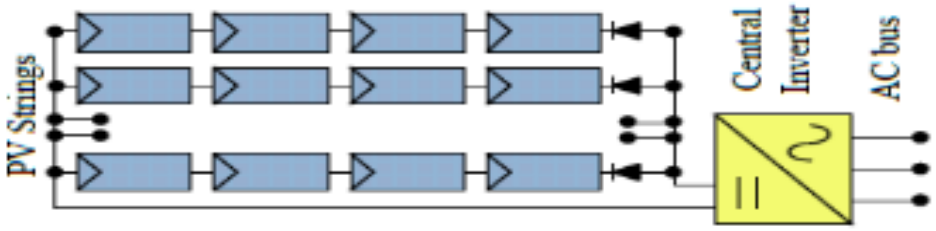

Figure 3.1: Centralized inverters

In parallel strings, the PV plants are bigger than 10 kWp, which connects them to a single central inverter (Figure 3.1). The first line is linked to a transistor that has an inverter setup, which has

been used for our research. We used IGBTs as they are efficient and low-cost [16]. It has the following disadvantages:

- Need a cable for (high-voltage) DC.
- The power losing setup of MPPT.
- The power losing setup due to collective mismatch.
- Losing power in the diode strings.
- Dependence of the whole system on a single inverter.

3.3.2. String Inverters

Today, the technologies involve multiple series of inverters and the AC collectives. The series of inverters reduce the centralized inversion at the single of string for PV, which is connected to the inverter, as shown in Figure 3.2. The input voltage is high enough to avoid voltage amplification. The purpose of this technique is reducing the drawbacks of the central inverters, which apply to the PV system in markets since 1995.

This collective string of PV connects to the separating inverters when the level of voltage is lower before the inverter, and the DC-DC converter uses it for boost collective.

The collective of strings has its own inverter and a string of diodes, and it needs to eliminate the total reduction. The system improves depending on the action, which is not only separated by one inverter [27].

The configurations improve efficiency as compared to the centralized converter, for reducing the price with the ability to produce the mass.

The PV module defines the structure, and it ends up forming the string, and the PV array voltage will be in the range 150-450V.

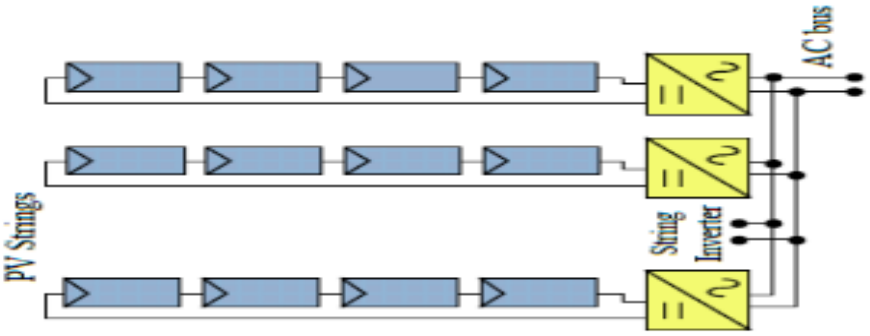

Figure 3.2: String inverters.

The central inverter has several advantages as compared to the string inverter, which are:

- There are no losses in a string of diodes.
- Separate MPPTs for every string.
- The lower price of producing the mass.

3.3.3. Multi-String Inverters

Some forms of advanced technologies including the multi-string inverters, mixed collectives, and configuring equipment are available in the PV market since 2002. The multi-string inverter is displayed in Figure 3.3, which is more developed as compared to the string of the inverter, the several of diode strings interface with their own converters and DC-DC or DC-AC inverters [36].

If it is compared to the centralized system, it is more beneficial because every string is individually controlled. The power of ranges is 5kW for the configuration of the strings, which are used for DC-DC conversion before connecting it to the inverter.

Many strings allow the converters to connect with the others depending on the power and the PV system that connects with different current-voltage (I-V) ratios. The MPPT is implemented to each string and that improves the power adequacy. This collective has a flexible design with high adequacy, and it may probably become a standard instead of the centralized and string converters, which are used now [9] [10].

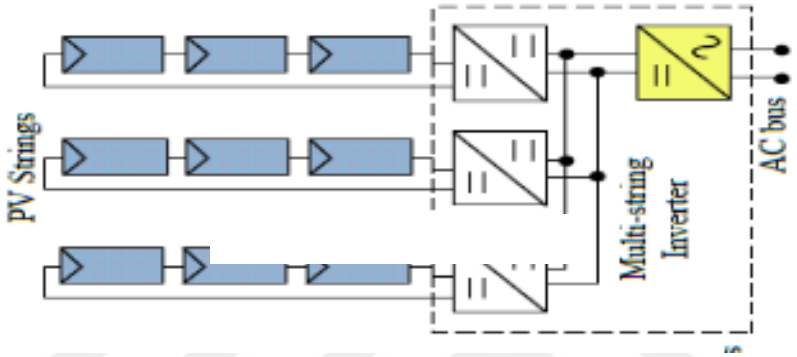

Figure 3.3: Multi Level String Inverter.

3.3.4. Collective of Inverters

The inverter collectives are shown in Figure.3.4, which belong to the present time and future. They contain a single solar panel connecting to the grid through the inverter. Efficiency can be best obtained by comparing with the series of inverters as the MPPT incorporates the PV system collective and the converter with a similar device that improves the performance of the “plug and play” devices [13] [16].

Using this configuration, losses can take place because of the mismatch of the PV system collectives, which optimizes the converter of the PV module.

This needs more than one device, and its major benefit is its low cost. The input voltage will become so low that it needs high voltage for amplification, which reduces the performance.

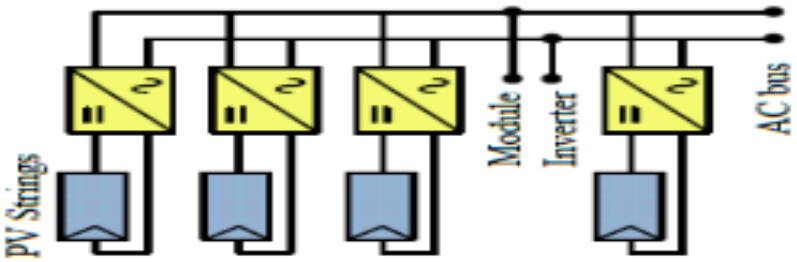

Figure 3.4: Collective Inverters. 1

3.4 THE INVERTER

Inverters are circuits of power electronics, which are used to convert the DC voltage to AC voltage (one or three phase) with other frequencies and amplitudes; so, it is a necessary component in the PV systems. The AC loads or grid-connected systems are synchronized and the standalone systems have battery-powered uninterruptible power supplies [29].

3.4.1. Inverters Merits and Classifications

We can categorize inverters in many classes according to the input source, output phases and number of the power electronics switches.

A. Input Source

Converters can be divided according to the input source into single-phase current of the source of the inverter (CSI), and single-phase voltage for the source of the inverter (VSI).

1- The current of the single phase of the source of inverter CSI.

A studding inverter is used as a DC current input source. It is applied with power AC motor drives; so, it isn't included in the photovoltaic systems, which can be described as the DC voltage source.

2- The voltage of single phase for the source of the inverter (VSI).

The inverter is connected to the DC voltage source. The voltage is kept stable by using the capacitor in parallel to the input. The AC current side is fixed up by the current loop control [30] [29].

B. Output Ac Load Phases

The most important types of inverters are categorized into single and three-phase inverters as shown in Figure 3.5.

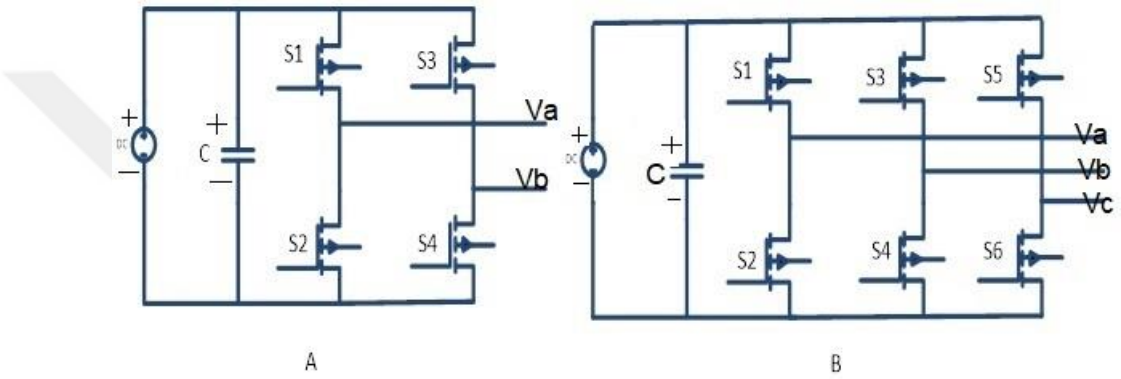

Figure 3.5: A-Single-phase Controlled In Inverter. **B-** Three-phase Controlled Inverter.

A three-phase inverter has been used for this purpose, and it is a medium-voltage grid-connected PV system.

C. Number of Switches

Inverters used for single-phase have two legs; so, it is divided into half or full-bridge inverters, as Figures 3.6 and 3.7 indicate.

3.4.2 Half-Bridge Inverters

This type of inverters only has two power electronics switches, and a couple of similar capacitors, which are linked in series to the DC input. It divides the input voltage into $\frac{V_{dc}}{2}$. The junction of these two capacitors is the medium voltage point. The circuit of the inverters is shown in Figure 3.6 [18].

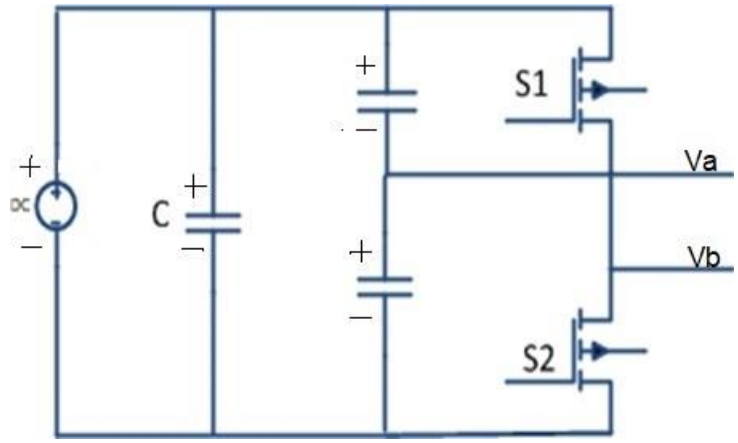

Figure 3.6: A Half-Bridge Inverter.

We can see in Figure 3.6 that it is the cheapest option since only two switches use it because it has only two switches but the output voltage has high THD, and the switching losses are very high because it has to handle twice as much output voltage when it is open.

3.4.3. Full-Bridge Inverters

The inverter has two legs and four power electronics switches, which are coupled in the same branch. It is used in applications, which consume high power. The numerous probabilities for controlling energy are within the range for input and output voltage, and the inverter for full-bridge is for the collective use. This kind of inverters needs a high level of controlling techniques to control the period of open and close for each switch. Figure 3.5a shows a full-bridge inverter circuit [22].

3.4.3.1. Full-bridge inverters collective

In this chapter, we will discuss the function of Full-Bridge Inverters by controlling the duty cycle of each power electronic switch, as shown in Figure 3.7. When S2 and S3 are driving the output, V_{AB} equals V_{DC} but when S1 and S4 drive the output, V_{AB} equals $-V_{DC}$. The switches must follow two main rules; first the two switches of same legs will not open at the same time, or we will have the short circuit in the input source side; second, in the opposite situation, the two switches in the legs will not turn off at the same time since the inductors (LCL filter) are located at the output of the circuit (indicator Va-Vb) [12], [26].

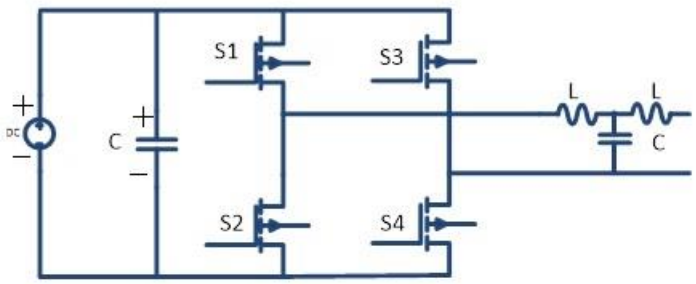

Figure 3.7: Full-Bridge inverters with LCL filter.

The output voltage, in this case, will be a square wave; so, we can use different topologies for driving these switches depending on the control technique; therefore, we can get sinusoidal output wave voltage and current. The main control techniques are:

- **The Square wave inverters**

The output voltage technique is in squared waveform, and the controller won't adjust the amplitude voltage for the output, and it has the control of the DC input voltage in this case. This kind of inverters can be used to control only the output voltage frequency. The switching frequency of this inverter is the least as compared to the PWM inverters [16].

- **The Pulse width modulated (PWM) inverters**

The PWMs are the most common control technique for inverters. The output voltage of these inverters is in a square waveform; so, we have to use passive filters to get the sine wave in the output.

DC voltage is transformed into AC voltage through these inverters to feed the AC load or connecting PV to the utility power grid. In PWM inverter, we can control the amplitude and frequency for the output voltage.

This type of modulation can be obtained by comparing a carrier signal with triangular waves for generating the pulses for power electronics switches. Other kinds of inverters combine the merits of the inverters mentioned above. The voltage cancelling technique only works with the single-phase inverters. The output voltage is nearly in a square waveform.

- **SPWM inverters**

The SPWM or Sinusoidal Pulse Width Modulation is the best common way to gain sine (modulated signal). This collective technique of carrier signal is in a triangular wave form as compared to the sinusoidal signal, if we detect the intersection between both the signals to gain the pulse for switches.

The sinusoidal signals are larger for triangulating the signal (the corresponding switches are ON) and vice versa. The ON time of a switch couple is the variable called duty cycle (D), as Figure 3.8 indicates [23].

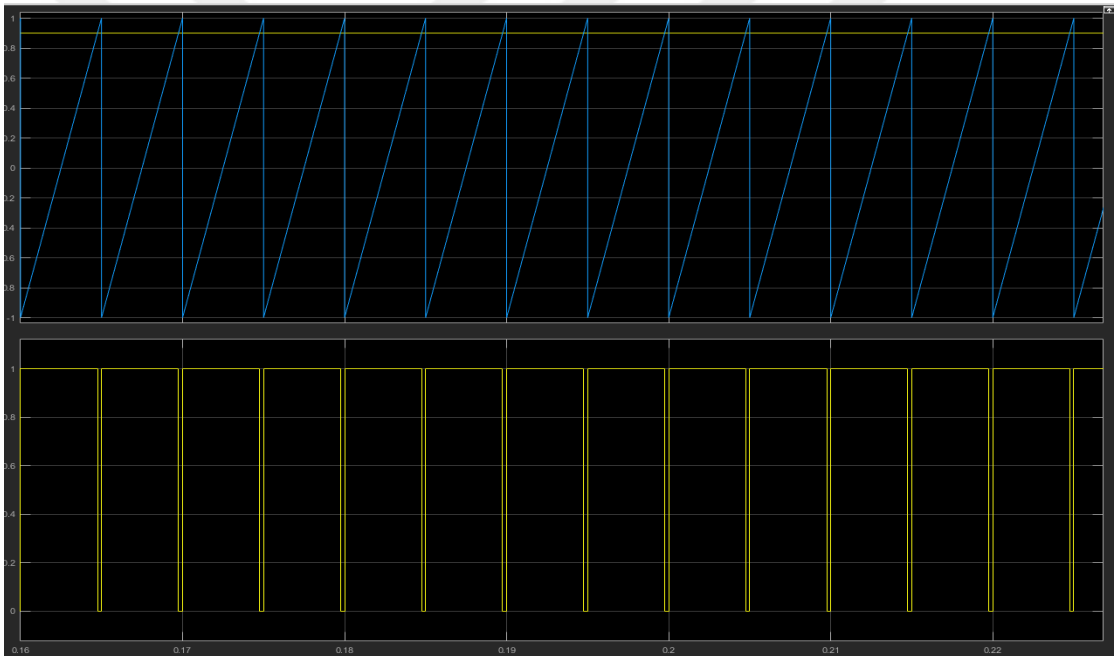

Figure 3.8: SPWM Technique.

We can also use two sinusoidal control signals to generate the duty cycle signal. The two signals have opposite turns as shown in Figure.3.9. It depends on the number of control modulation signals:

1- Bipolar: A single control sinusoidal signal is used. The inverter output of voltage is at +V, as Figure 3.9 indicates.

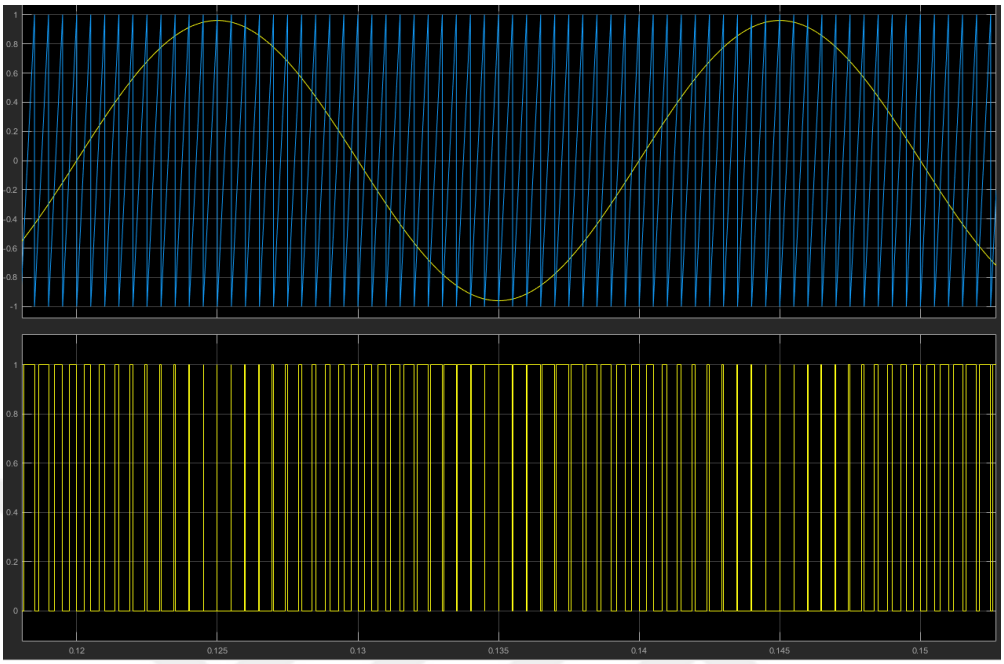

Figure 3.9: Bipolar PWM.

2- Unipolar: Two opposite sinusoidal signals are compared with a DC or $-V_{DC}$ triangular signal. The output voltage is at +V or 0 for the positive part of sinusoidal signals at 0 or $-V_{DC}$ for the other part of the sine. V has been shown in Figure 3.10.

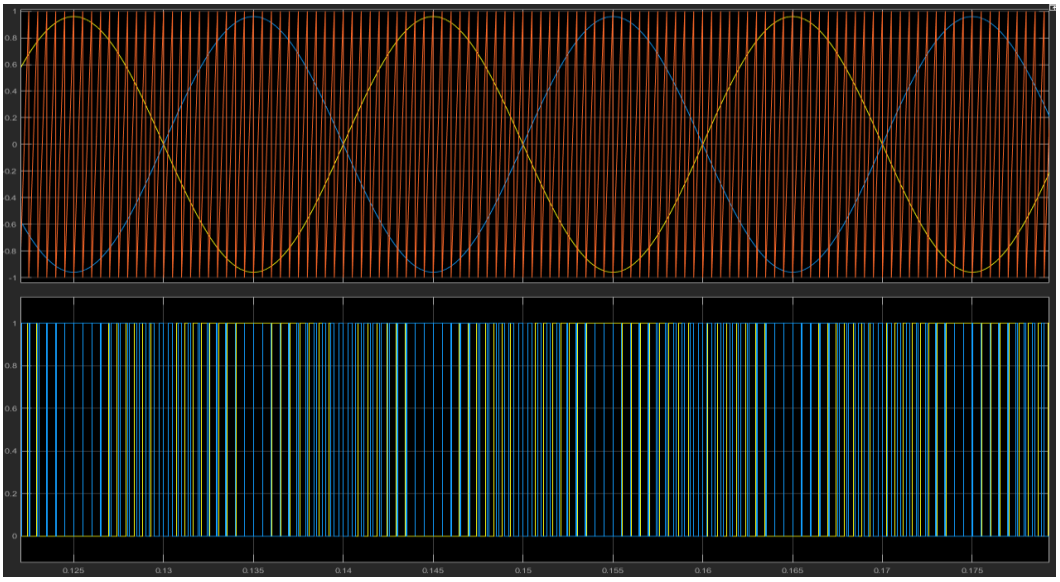

Figure 3.10: Unipolar PWM.

The Unipolar technique is oriented with a number of possibilities for the output voltage (positive or negative) and not used with several control signals. The bipolar modulation technique isn't used in this work, and it has following disadvantages:

• Complexity of the controller to correctly control the zero-crossing sides.

• The current in the DC side has elevated frequency.

The inverters can't store electrical energy; so, the power input for the photovoltaic system should be similar to the output power. When there are losses in the power switches and the output filters, the adequacy of the inverter is below 1. While the load has a utility of the grid or AC loads both for load current I_{load} and voltage V_{AB}. It will be sinusoidal and have a shifting power factor. The voltage will lag from the current, which is represented by Φ. The current and voltage on the load side can be described as follows [10] [15]:

$$V_{AB} = \sqrt{2}V_{AB\,rms}\,sin(w_1.t) \tag{3.1}$$

$$I_{load} = \sqrt{2}I_{load\,rms}\sin(w_1.t - \Phi) \tag{3.2}$$

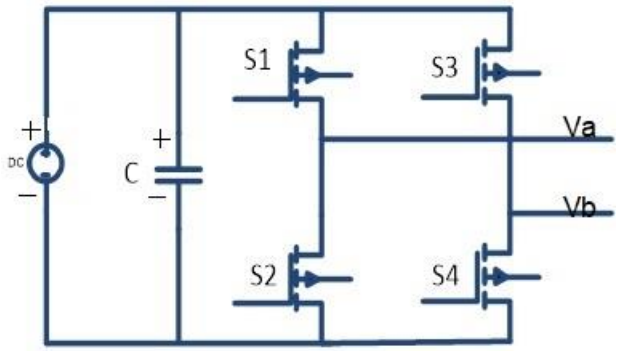

Figure 3.11: Full bridge inverter with AC load.

The input power for the inverter is DC and the power factor on this side is unity. But the output values (current and voltage) will have different rms and tip values we can see as follows:

$$P_{in} = V_{AB}.I_{load} \tag{3.3}$$

$$P_{in} = \sqrt{2}V_{AB\,rms}\sin(w_1.t).\sqrt{2}I_{load\,rms}\sin(w_1.t - \Phi) \tag{3.4}$$

By using trigonometric formula, the equivalent will be:

$$P_{in} = V_{AB}.I_{load}\cos(\Phi) - V_{AB}.I_{load}\cos(2.w_1.t - \Phi) \tag{3.5}$$

From Equation 3.2, 3.3, 3.4, and 3.5, the input power relations have two terms, a term of DC minus the second-order harmonic component (twice the fundamental frequency with the output inverter voltage).

$$P_{dc} = V_{AB}.I_{load}\cos(\Phi) \tag{3.6}$$

$$P_{ripple} = V_{AB}.I_{load}\cos(2.w_1.t - \Phi) \tag{3.7}$$

P_{ripple} represents the harmonic components power, which has to be managed by filters for reducing ripples on the input side; so, we used a DC link capacitor.

3.5 IGBTS VS. MOSFETS POWER

The in-circuit inverter design with two main switching collectives has been set up based on the electronic power. The first is MOSFET of power, and it is standard, but its design handles massive voltages and currents. The second is the gate insulation for a bipolar transistor IGBT. Both of them have the advantages and many useful specifications.

IGBTs in general work with normal-voltage applications, which is almost 200V or more, and above 600W. They have no high-frequency switching for MOSFETs, and they can work under 29 kHz. They work with high current; so, the output will be greater up to 5KW and have excellent thermal operations because they operate up to 100 degree Celsius. Some important drawbacks of IGBTs is the turn-off function because when the IGBT is turned off, the flow of the current to the transistor doesn't immediately stop that results in power losses [32].

IGBTs can be used for high-power applications, which require uninterrupted power supplies higher than 5kW, soldering application, or low-power lighting.

MOSFETS of power have a higher frequency for switching through IGBTs; it works up to 200 kHz. The capability of high-voltage and high-current applications is limited to 250V or 500W. Both MOSFETs and IGBTs sloped up and down for voltage when there are power losses during the turning on-off processes (dV/dt losses). The dissimilar IGBTs and MOSFETs have the diode frames.

The IGBT's are used for high voltage, and the low frequency (>1000V, <f20kHZ) and MOSFETs are used for low-voltage applications with high frequency (<250V, >f200 kHz). In the mentioned

range, there is a large grey area. In this area, there are different duty cycles and different factor availability [37]. The simulation has been designed for a 600W inverter with 340 bus VDC, and the switching frequency 5kHz. In this case, the MOSFET is the ideal choice, but the switches have a higher resistance in the turned on state and conduction will result in losses. The MOSFET is better for voltage-controlled equipment, and it is directly adjusted by 'CMOS or TTL' when the signal passes through the same gate. The opposite switching of the gate drive for the current is very low. When the system is large and requires high power output, IGBTs are the best.

3.6 VOLTAGE SUPPORT FOR GRID CONNECTING VIA PV POWER SYSTEMS

Inverters in the PV collective usually work to produce active power from the solar module at the unity power factor Cos (φ) =1, but just with high penetration PV systems in distributed generation power grid. With more and more penetration, the active power was generated from the PV that can adversely affect the grid. So, the need for regulations of Grid connecting with PV collective has been added to the standards to maintain stable and quality power specified by a coding grid. This needs many standards, which are used to distribute the generation of interconnection with the target PV systems in the LV network for distribution are: VDE-AR-N 4105, IEEE – 1547 and IEC- 617272.

For utility grid voltage support from the PV systems, the inverters are capable of applying controls to the active P.F or fusty power; so, the system has a leading and lagging phase angle φ. Mostly, the photovoltaic systems operate below the rated power using the inverters while converting the DC generated power to the AC active power. This operation gives the photovoltaic system the required flexibility to handle the fusty power depending on the power factor without affecting the produced active power. The voltage support can be done for controlling the fusty power flow in the grid (consume or produce), which is decided by the power factor in the inverters as they play the role of an interface between the grid and the PV module.

The active-fusty power feature is important for the PV inverter because it shifts PF, as shown in Figure 3.12. The active power is injected in the utility grid but the fusty power can be delivered to the grid or simply digested in the grid. The fusty power is negative; so, it's been absorbed in the grid. In low voltage networks, a moron power factor is needed to operate the load of inductive and fusty power-consumption from several loads

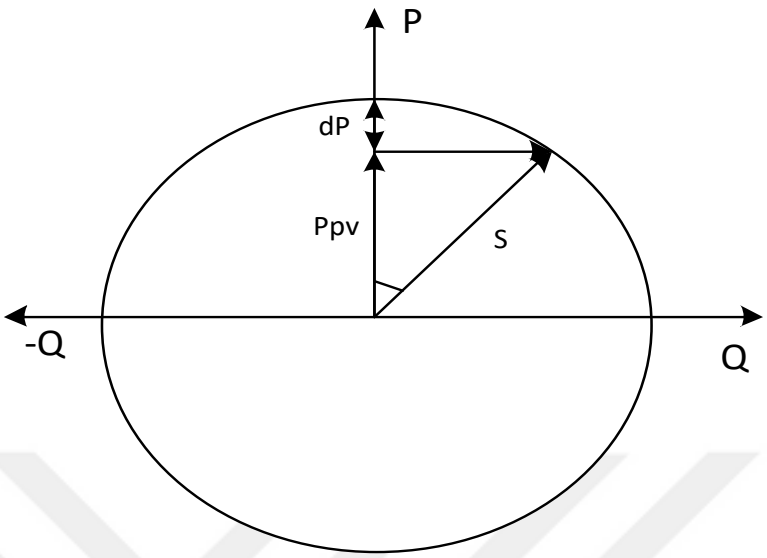

Figure 3.12: PQ an inverter with lagging PF.

There are many standards of voltage support, which are different to some degree when both the utility grid and the PV system work normally [19][24]:

- IEEE- 1547 state: There is no active regulation voltage for the type that performs; the network for voltage would not be affected.
- IEC- 617272: The PV system requires a specific power factor more than 0.9, at which, the output will be greater than 50% for the power rating.
- VDE-AR-N 4105 requires the voltage support if the DSO requires it. The fusty power has been mentioned with many possibilities in Table.3.1. VDE is the maximum voltage while the different voltage for the system with and without DG is 3%.

Table 3.1: Limiting of reactive power

Rated power of the PV power system	$S_{max} \leq 3.68$ kva	3.68 KVA $\leq S_{max} \leq 13.8$ kva	$S_{max} > 13.8\ kva$
P.F range	Firm P.F 0.95 Capacitive (Leading) 0.95 Inductive (Lagging)	P.F features 0.95 Capacitive to 0.95 Inductive	P.F features 0.90 Capacitive to 0.90 Inductive

3.6.1. Inverter Collective for Voltage Supported

Inverters can affect the voltage in the utility grid in two ways:

- The PV system is limited for activating the generated power.
- The fusty power is absorbed in the grid.

These two methods are used to mitigate the voltage, which increases in the utility grid. In this work, we used fixed power factor for central inverter in the PV collective due to the fact that the effect of active PV system power is too small on the utility grid.

3.6.1.1. Firm power factor

This strategy will lead to the photovoltaic inverter by creating fusty power with the active power through a PV system. Figure 3.13 shows firm power factor [14].

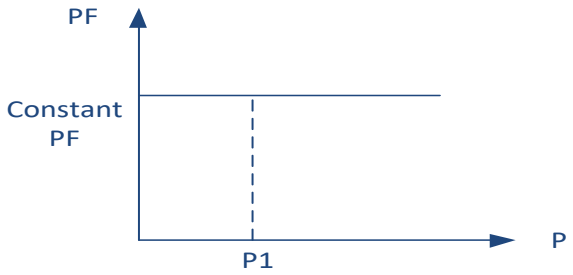

Figure 3.13: Firm PF Strategy.

Usually lagging power factor is used in this type; so, the photovoltaic inverter consumes fusty power and mitigates the voltage in the connected node.

As long as the power factor is close to one of the larger parts of the apparent power S_i, it is an active power.

We can calculate the amount of active power produced by the photovoltaic system P_m by multiple S_i $(\cos(\Phi))$. Based on the dimensions of the PV system, the rating of power for the inverter S_i is more than the rating of the solar collectives, and the fusty power, which is given by:

$$Q = tan\left(cos^{-1}(PF)\right).P_{Gen} \tag{3.8}$$

This strategy hasn't reacted to changes in the utility grid so far but only some experts believe that the power generation from a PV is a passive control method. The overvoltage risk is smaller when the production is lower but it is risky in case of bigger produced power and the less consumed power in the grid. The overvoltage risk might increase [37], if the fusty power is considered by the inverter that reduces with decreasing the active power-production. It may not be needed when the voltage has no value dangerous enough to override the limit.

3.6.1.2. Power factor dependent on PV for production of power

The power factor is also considered as a passive control strategy but it's more flexible than the previous method. This control strategy is shown in Figure 3.14, which clearly indicates that the active power of the inverter is modified in a certain band, which is determined by the upper and lower boundaries of the power factor because it maintains the voltage inside the acceptable range, and the values of power factor can be determined by:

- PF_1 and PF_2, determine the (PF) band at operating the inverter.
- P_1 and P_2 control the active power of the PF-loop for initiating and ending.

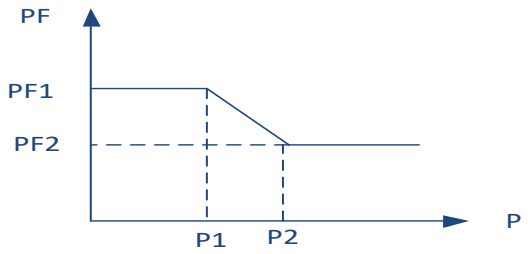

Figure 3.14: PF with PV power production.

The PF1 (upper boundary) works with no overvoltage risk and most of the time; it is similar to the lower boundary PF2, which is determined by the nominal power of designed photovoltaic system. In LV power grid standards, when PF_2=0.9 and the value is able to create an impact, so reduction in the fusty power is suggested [26] [33]. The band should guarantee that the PV should not have overvoltage, and it should be less than P_1. Then the generated power will be PF_1. P_{PV} is the nominal power of the PV module. P_2 produces the power factor, which can be calculated by:

$$PF = \begin{cases} PF_1 & P_{Gen} < P_1 \\ \frac{PF_1 - PF_2}{P_1 - P_2}(P_{Gen} - P_1) + PF_1 & P_1 \leq P_{Gen} \leq P_2 \\ PF_2 & P_{Gen} > P_2 \end{cases} \quad (3.9)$$

3.6.1.3. Fusty power exhaustion Q (U)

The simulation is quite flexible to support the voltage in the utility grid, as shown in Figure 3.15. It assumes that when the PV systems' real power production increases, the grid voltage increases as well, but it’s not correct when the generated power is injected to the grid. High irradiance levels coincide with higher order power, and the fusty power exhaustion for (PV) inverter should be high.

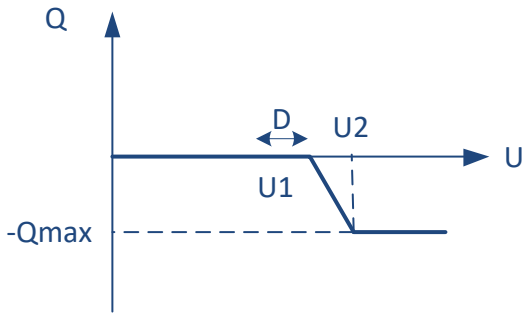

Figure 3.15: The reactive power.

The reactive power is controlled by the local voltage with the PCC; so, the total reactive power can be reduced. The voltage support to the inverter is not as strong as the power factor, and the fusty power grant of the PV inverters will disappear when the voltage is measured, which is

lower, and the loads at the end of the grid will get overvoltage problems without the fusty power exhaustion of the inverters.

The consumption of fusty power for the PV inverters affects the voltage of the PCC. U_n is nominal voltage; U_2 is voltage at the maximum fusty power compensation and performance. D is the band of the dead for natural voltage, where the voltage support is zero [38].

$$Q(U) = \begin{cases} 0 & U < U_N + D \\ \frac{Q_{max}}{U_2 - U_N - D}(U - U_N - D) & U_N + D \leq U \leq U_2 \\ Q_{max} & U > U_2 \end{cases} \quad (3.10)$$

For increasing the consumed fusty power in the inverters of the photovoltaic system, we use this process keeping in view the dead band and power factor of boundary, which will be ultimately lower than the voltage. The power factor will be limited and the shifting will increase it to the maximum fusty power. The inverter will depict the following inequality:

$$U_n + D \leq U \leq U_2 \quad (3.11)$$

3.6.1.4. Droop setup of power curtailment

Limiting the maximum installed power capacity of the photovoltaic system in a low-voltage utility grid can be used for avoiding overvoltage, as shown in Figure 3.16. This method is counterproductive for adding the penetration of PV system in the disturbed micro grids. The power curtailment does not directly limit the PV capacity of the grid, when the PV systems' production reduces. Economically, it is not very feasible.

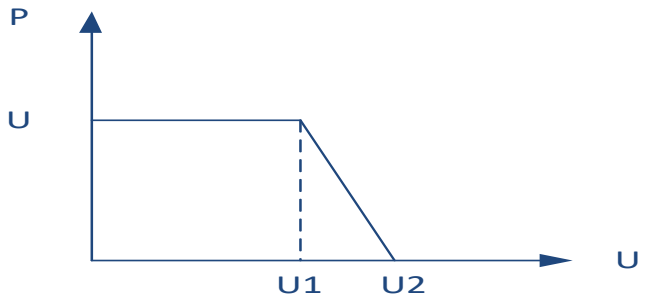

Figure 3.16: Droop setup power.

This state is frequently supported, and the reason is the frequency, which is linked to the active power. The droop describes the following relation:

$$P = \begin{cases} Pv & U < U_{lp} \\ P - Pv * \frac{U - U_{hp}}{U_{hp} - U_{lp}} & U \geq U_{lp} \end{cases} \quad (3.12)$$

P: The active power with the PCC.

P_{PV}: The power created by the PV collective.

V: Phase-to-phase voltage at the terminal of loading.

V_{hp}: Voltage for open point.

V_{lp}: Voltage at the point of reducing power.

The inverter uses the voltage at the PCC; it has a little change close to the transformer although the overvoltage at network ends [27].

3.7 COLLECTIVE OF INVERTER AND THE OUTPUT OF FILTER

For the inverter, the current inductor, and voltage capacitor ($[i_a, i_b, i_c, v_{dc} = v_{pv}]$), the variables state for three-phase grid-connected PV system, as Figure.3.17 shows, while the space state is indicated as follows:

$$\dot{\imath}_a = -\frac{R}{L} i_a + \frac{1}{L} e_a + \frac{v_{pv}}{3L}(2S_a - S_b - S_c) \quad (3.13)$$

$$\dot{\imath}_b = -\frac{R}{L} i_b + \frac{1}{L} e_b + \frac{v_{pv}}{3L}(-S_a + 2S_b - S_c) \quad (3.14)$$

$$\dot{\imath}_c = -\frac{R}{L} i_c + \frac{1}{L} e_c + \frac{v_{pv}}{3L}(-S_a - S_b + 2S_c) \quad (3.15)$$

Sa, Sb, and Sc are switching signals for all-phase (VSI), and their interrelation is as follows:

$$S_i(i = a, b, c) = \begin{cases} 1 & if \quad S_i^{Top} : on \;\; S_i^{Bottom} : off \\ 0 & if \quad S_i^{Top} : off \;\; S_i^{Bottom} : on \end{cases} \quad (3.16)$$

When applying the KCL to DC link node of the capacitor, the relation for voltage of the capacitor is as follows:

$$\dot{v}_{pv} = \frac{1}{C}(i_{pv} - i_{dc}) \tag{3.17}$$

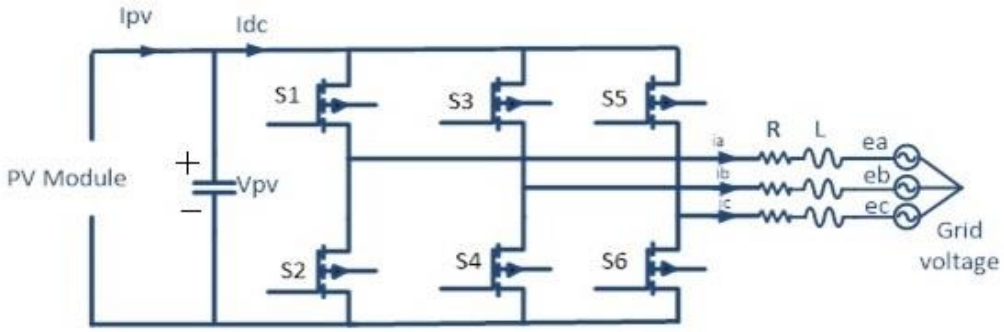

Figure 3.17: Three-phase grid-connecting form.

When conduction losses for the inverter are negligible, the inverter's current input will be like the output current [18].

$$i_{dc} = i_a S_a + i_b S_b + i_c S_c \tag{3.18}$$

Here, the output is as follows:

$$\dot{v}_{pv} = \frac{1}{C} i_{pv} - (i_a S_a + i_b S_b + i_c S_c) \tag{3.19}$$

From the relations, the system is non-linear because of different time-bound switching functions and the current of the diode.

3.8 TRANSFORMATIONS IN THE THREE-PHASE SYSTEMS

The design control handles a three-phase grid-connected system, which has two fundamental transformations for reducing the extra mathematical dimensions of a module, and it decouples the diverse relation. The transformations are as follows:

3.8.1. *Aβ* Transformation

The αβ transformation can reduce the state of space representation of the dimensions for three-phase systems. When the current loop model is described by three relations (each phase has the relation) and turns into two differential relations model, the three-phase αβγ transformation can be expressed below [25], [36]:

$$\begin{bmatrix} x_\alpha \\ x_\beta \\ x_\gamma \end{bmatrix} = \sqrt{\frac{2}{3}} \begin{bmatrix} 1 & -\frac{1}{2} & -\frac{1}{2} \\ 0 & \frac{\sqrt{3}}{2} & \frac{\sqrt{3}}{2} \\ \frac{1}{\sqrt{2}} & \frac{1}{\sqrt{2}} & \frac{1}{\sqrt{2}} \end{bmatrix} \begin{bmatrix} x_a \\ x_b \\ x_c \end{bmatrix} \tag{3.20}$$

x_a, x_b, and x_c are the currents of output, voltages, or powers of the three phase system, as Figure 3.18 indicates.

The three dimensions at the geometrical point of Cartesian coordinator with the vectors of three bases are as follows:

$$\begin{bmatrix} 1 \\ 0 \\ 0 \end{bmatrix}, \begin{bmatrix} 0 \\ 1 \\ 0 \end{bmatrix}, \begin{bmatrix} 0 \\ 0 \\ 1 \end{bmatrix} \tag{3.21}$$

This will change into another Cartesian coordinating with vectors of the different bases as follows:

$$\begin{bmatrix} 1 \\ -\frac{1}{2} \\ -\frac{1}{2} \end{bmatrix}, \begin{bmatrix} 0 \\ \frac{\sqrt{3}}{2} \\ -\frac{\sqrt{3}}{2} \end{bmatrix}, \begin{bmatrix} \frac{1}{\sqrt{2}} \\ \frac{1}{\sqrt{2}} \\ \frac{1}{\sqrt{2}} \end{bmatrix} \tag{3.22}$$

The basic vectors have orthonormal diagram of the inverse of the matrix while its αβγ transformation is similar to its transpose. This transformation is called “the power invariant” and it can be described by $I_{abc}.U_{abc}=I_{\alpha\beta\gamma}.U_{\alpha\beta\gamma}$ (vector of scalar product).

The uniform three-phase state, when $x_a+ x_b+ x_c= 0$, and $x_\gamma = 0$, the mean of the three phase indicates two vectors ($x_{\alpha,}$ x_β). That is the uniform three-phase, γ is orthogonal axis for the αβ collective, and cannot overturn it [39]. The αβγ transformation can be expressed in matrix form as follows:

$$\begin{bmatrix} x_\alpha \\ x_\beta \end{bmatrix} = \sqrt{\frac{2}{3}} \begin{bmatrix} 1 & -\frac{1}{2} & -\frac{1}{2} \\ 0 & \frac{\sqrt{3}}{2} & \frac{\sqrt{3}}{2} \end{bmatrix} \begin{bmatrix} x_a \\ x_b \\ x_c \end{bmatrix} \tag{3.23}$$

The inverse of αβ transformation is:

$$\begin{bmatrix} x_a \\ x_b \\ x_c \end{bmatrix} = \sqrt{\frac{2}{3}} \begin{bmatrix} 1 & 0 \\ -\frac{1}{2} & \frac{\sqrt{3}}{2} \\ -\frac{1}{2} & -\frac{\sqrt{3}}{2} \end{bmatrix} \begin{bmatrix} x_\alpha \\ x_\beta \end{bmatrix} \quad (3.24)$$

In this case, the stationary map of the two-phase system under the symmetrical slash is balanced for the three-phase system.

3.8.2. Park's Transformation

This transformation consists of three phases (three-dimensional) and it can be converted into two dimensional as the αβ transformation while the difference between them takes place through the coordinate rotations with a fixed frequency. Park's transformation consists of two rotating axis, d and q, where it can rotate around the αβ of the static axis with a constant angular frequency (ω), as Figure 3.18 indicates. For a three phase system, the synchronous frame will be operated by transforming the two-phase [14], [29].

At the first point, the three phases for the output vector (current, voltage) will change to the frame of αβ, while the Park transformation provides the rotating frame as given below:

$$\begin{bmatrix} x_\mathrm{d} \\ x_\mathrm{q} \end{bmatrix} = \begin{bmatrix} \cos(\theta) & \sin(\theta) \\ -\sin(\theta) & \cos(\theta) \end{bmatrix} \begin{bmatrix} x_\alpha \\ x_\beta \end{bmatrix} \quad (3.25)$$

As θ = ωt, ω is the utility of grid for frequency in the enforcement of grid-connection as stated below:

$$\overrightarrow{x_{dq}} = x_d + jx_q = \overrightarrow{x_{\alpha\beta}} e^{-j\theta} \quad (3.26)$$

Here, x_d is the real section and x_q is an imaginary section. We will find the following:

$$\begin{bmatrix} x_\alpha \\ x_\beta \end{bmatrix} = \begin{bmatrix} \cos(\theta) & -\sin(\theta) \\ \sin(\theta) & \cos(\theta) \end{bmatrix} \begin{bmatrix} x_\mathrm{d} \\ x_\mathrm{q} \end{bmatrix} \quad (3.27)$$

The complex form of the inverse transformation of Park's transformation is $\overrightarrow{x_{\alpha\beta}} = \overrightarrow{x_{dq}} e^{-j\theta}$. Two vectors are the result including d and q, which are called as the dq transformation.

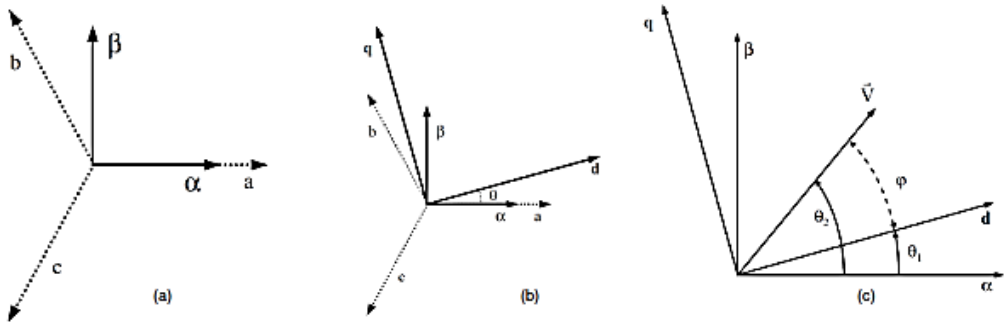

Figure 3.18: αβ transformation, αβ and Park's transformation in a synchronous frame.

3.9 GRID SYNCHRONIZATION DURING UNBALANCED SLASHES

The information of grid voltage is important for suitable operation for all the converters of the Grid connecting GCC. The synchronization process becomes a necessary part, for algorithm controlling the GCC applications, which is listed in Table 3.2. The correct dimension, especially the phase angle, is an essential consideration for power quality.

Table 3.2: GCC applications

Device Type	Applications
FACTS	Static Var Compensator (SVC), Static Compensator (STATCOM), and Static Series Synchronous Compensator (SSSC).
PQ Compensators	Active Power Filter (APF), Uninterruptible Power Supply (UPS), Dynamic Voltage Restorer (DVR).
RES	The PV plant, wind farm, ocean wave energy plants.
PWM Converters	Grid- Connected Converters (GCC) with unity power factor generation, Active Front End (AFE) in Adjustable Speed Drives (ASD), etc.

Every power converter setup device needs accurate grid synchronization; so it should be equipped with the synchronization algorithm. This is called Phase of Locked Loop (PLL) [17], [23], [30].

The PLL is a feedback algorithm; it automatically adjusts to the local phase of signal, which is generated to compare the phase with the input signal. It will be synchronized with the output signal in terms of phase frequency.

The main applications of the PLL are in radio of communications, which is shown in Figure.3.19. The PLL has three parts:

- VCO or Voltage Controlled Oscillator: It generates the output signal while the frequency depends on the input signal.
- PI or Phase Detector Indicator: It generates the signal, which is relative to the phase and the difference between the input and the VCO signal.
- LF or Loop Filter: It reduces the high frequency, which shows PD output and defines the dynamic control [35].

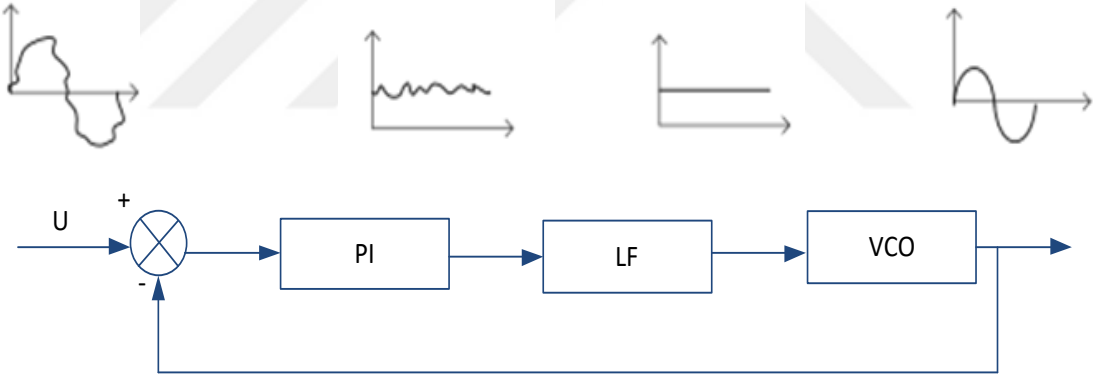

Figure 3.19: The PLL algorithm with PD Phase Detector, VCO (Voltage Controlled Oscillator), and LF Loop Filter.

The PLL has main objectivities to generate quiet phase angle for the signal at any voltage variation. Synchronization is necessary for:

- Parameters of voltage monitoring: grid frequency, amplitude, unbalanced harmonic distortion, and calculating the power factor.
- Grid monitoring: Detecting faults (angle-frequency), islanding detection, processing for connecting/disconnecting controls, and detecting fault.

- Current control: Higher harmonics and fusty power compensation.
- Active and fusty power controls
- Voltage regulation, dips and flickering.

3.10 PLL ALGORITHMS

There are some clear classifications of algorithms, and PLL operations. Three groups of PLL are as follows:

- Classical signals, three-phase structure, and abc coordination.
- The algorithms of utilizing αβ stationary frame.
- The algorithms for utilizing dq frames during the synchronous rotation (SRF).

The main things, which are used in the applications to achieve the digital implementation on DSP platform, have been shown in Figure 3.20. Diverse techniques are used for the synchronization of (one out of three phases of) PLL. We will use the three-phase method for analyzing and using in medium and high power applications [37].

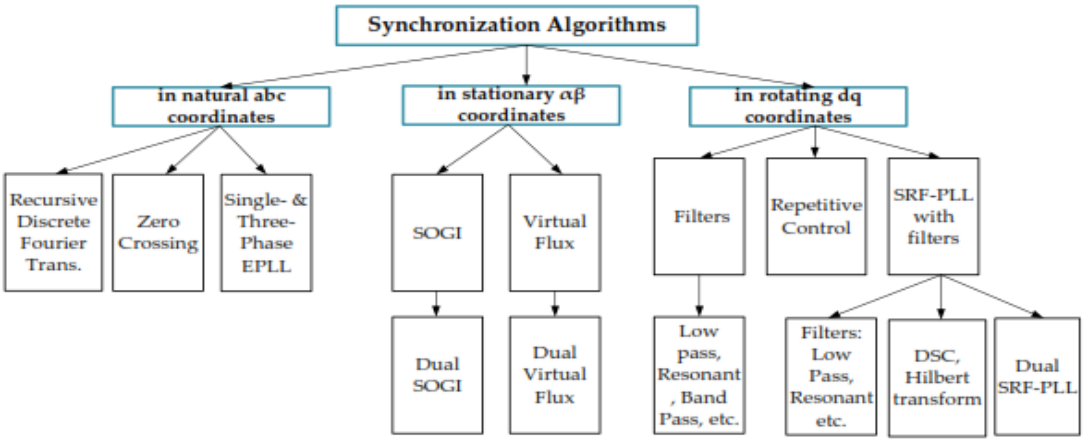

Figure 3.20: Classification of PLL algorithms.

We'll assume that the frequency of the analyzed signal is fixed. The zero-crossing method is applied in case of single-to-three-phase signals. Enhanced PLL won't give stable results, which depends on synchronization with the grid voltage.

The idea of algorithms for traditional PLL is good for the requested PLL algorithms. The synchronization in the electrical grid case is a challenge in case of voltage fluctuations. Phase detection is direct and generally has significant errors depending on zero voltage variations such as voltage dips, higher harmonics, and phase and frequency fluctuations. When there are fluctuations in the voltage grid, GCC algorithm of control is introduced. The wrong calculation or creation of marred phase angle can happen because of the PLL algorithm that badly amplifies and causes variations in the control algorithm.

This leads to “domino effect” that further leads to serious power deterioration. Studying helps creating signal-adaptive frequency and amplitude. There are different pre-altered methods to deal with the problems (imbalance, faults and higher harmonics). Band-pass filters, Low-pass filters (LPF) help solving the mentioned problems.

For the development of PLL algorithms with the component of extraction, the αβ and the dq cases are used as described in Figure.3.21 [24]:

- The block of coordination transformation (abc, αβ or dq).
- The extractor of filter or component (CE).
- Calculating and separating the positive and negative components of the voltage.
- Phase Detector Identification (PI).
- Voltage Controlled Oscillator (VCO) – calculates the phase angle.

In general, Phase-Locked Loop (SRF-PLL) is used to calculate the phase angle; however, the SRF-PLL is the best for calculating the phase angle from the grid voltage [25].

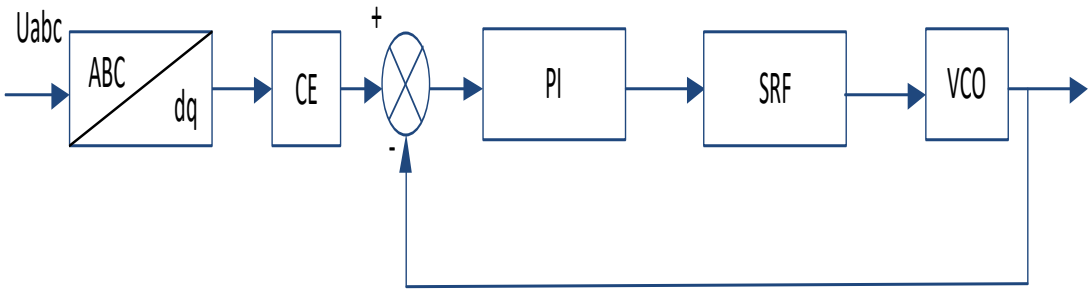

Figure 3.21: PLL in aß and/or dq frame.

3.10.1. Synchronous Reference Using PLL

The Synchronous Reference Frame PLL (SRF-PLL) is the best collective, and it is used to calculate the phase angle for three phases of the grid from voltage [Hsi]. The SRF-setup is used with the current control method and it has the most simple and reliable form.

The block of the SRF-PLL is described in Figure.3.22. For operating in sync with the loop, the process is described as Figure.3.23 indicates.

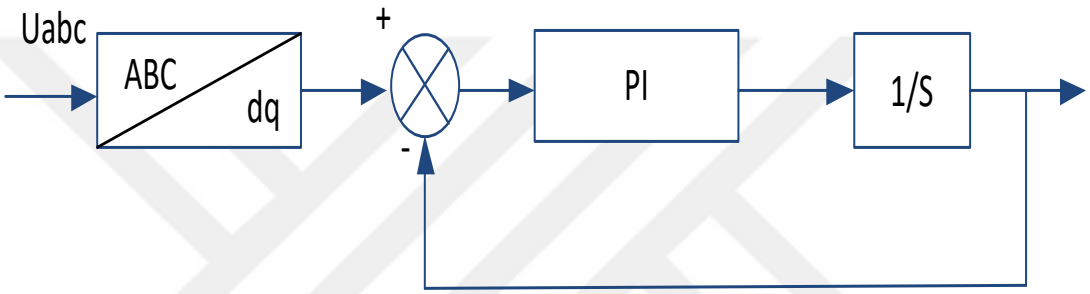

Figure 3.22: Scheme of Synchronous Frame PLL (SRF-PLL).

At natural frame of abc is in sync with the rotating frame dq, while the SRF-PLL setup transforms Park into three-phase grid voltage. The PLL use is aimed at adjusting the created phase angle for aligning d-axis of SRF with the vector of grid voltage. This will happen by adjusting q and reduces the grid vector to zero. The output controller of PI is the angular frequency. Integrating block transformation will show the phase angle value [23] [24].

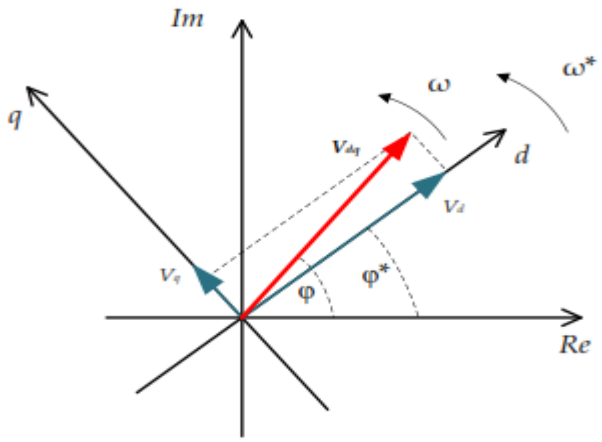

Figure 3.23: SRF-PLL.

The SRF-PLL is a standard, optimum, and symmetrical setup. A block form of the dynamic system is shown in Figure 3.24.

The digital sample for delay is considered, and Ts is the sample with respect to time. The digital control of delay and PWM of voltage generation is in the first-order of time, which is approximately similar to 1.5Ts.

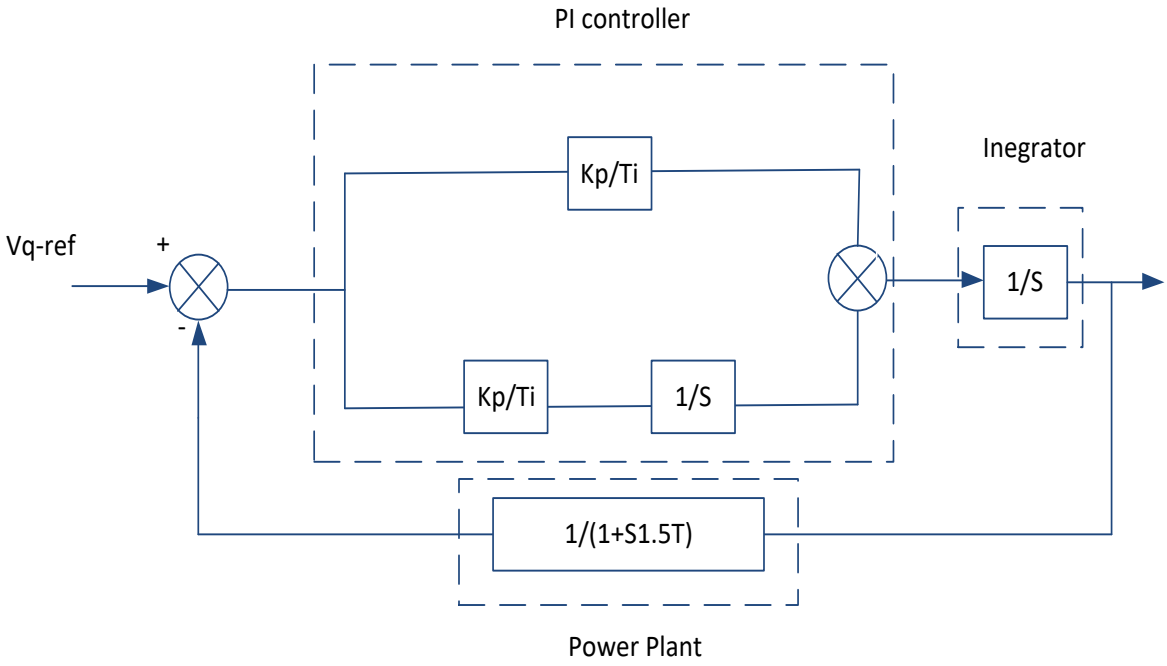

Figure 3.24: PI- controller based on SRF SRF-PLL with closed-loop.

3.11PROPOSED CONTROL STRUCTURE

The inverter controller consists of two loops; the first is the voltage regulator for controlling the amplitude of voltage supplied to the output by using two axes (d, q) transformation, and the second control loop is for current control, which is responsible for regulating the active system power taking power factor equal to 1 or less.

For using two independent loops in the controller helps the process of supplying voltage, regulating it, and separately injecting the active power or fusty power Figure 3.25.
The diagram of the general controller is used. It depends on the inverter modeling. Using the utility grid as a concept, the basic value of voltage and active power for using PU are determined. The voltage and current values from the photovoltaic system can be calculated using the PU system before conversion into rotating axis (d, q).

The phase-lock technique was used for obtaining the velocity angle while the controller worked based on the rotatory dq theory. This makes Park's transformations necessary for the voltage network, and the current will be generated by the PV system [28]. The voltage regulator adjusts the alternating current and the voltage, which means determining the reference value (i_{d-ref}) at the time of the active power, which will be provided by the system, and it depends on the current i_d and voltage v_d.

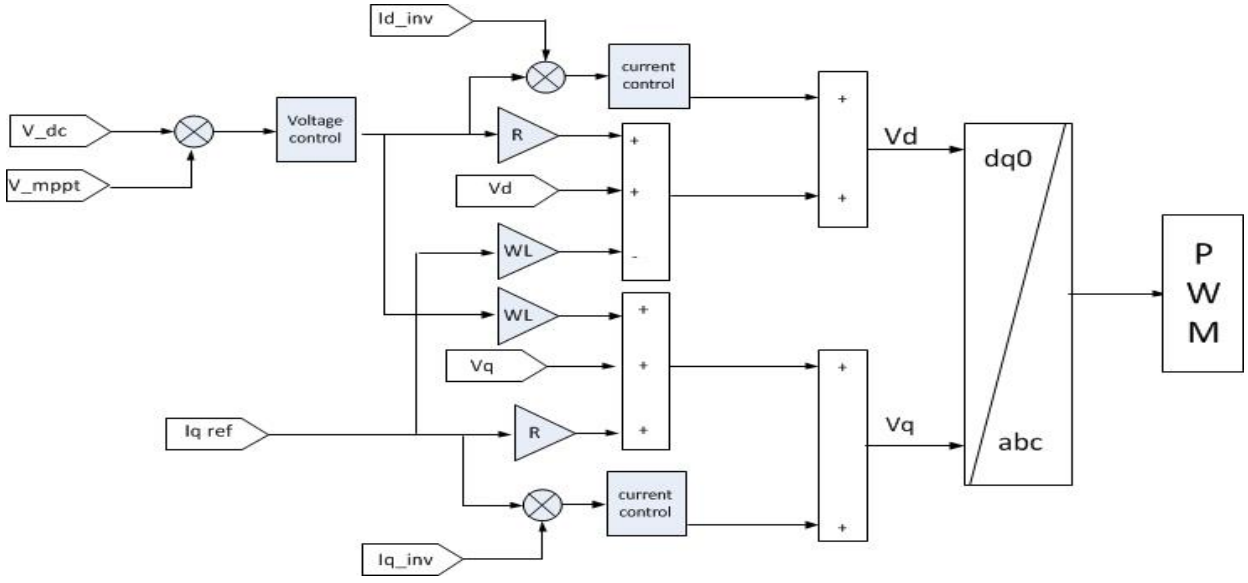

Figure 3.25: Proposed Control Structure.

The active power is provided to the utility grid by controlling the voltage amplitude and not allowing the power in the opposite direction, which is assured by a voltage regulator. The current controller will obtain the current values $i_d i_q$ and they will be taken from the PV system. Active and fusty power capacities have equations, which are given in the dq axis [38]:

$$P = V_d i_d + V_q i_q \qquad \& \qquad Q = V_q i_d - V_d i_q$$

The reference value is: $i_{q-ref} = 0$ that will provide the active power (Q) at the power factor (P.F). At the time of getting $V_q V_d$ values in the rotating axis, we will convert it into the other form (a, b, c) to adjust the reference sinusoidal signal (to create PWM pulses). The outline of the control key is given in Figure 3.26.

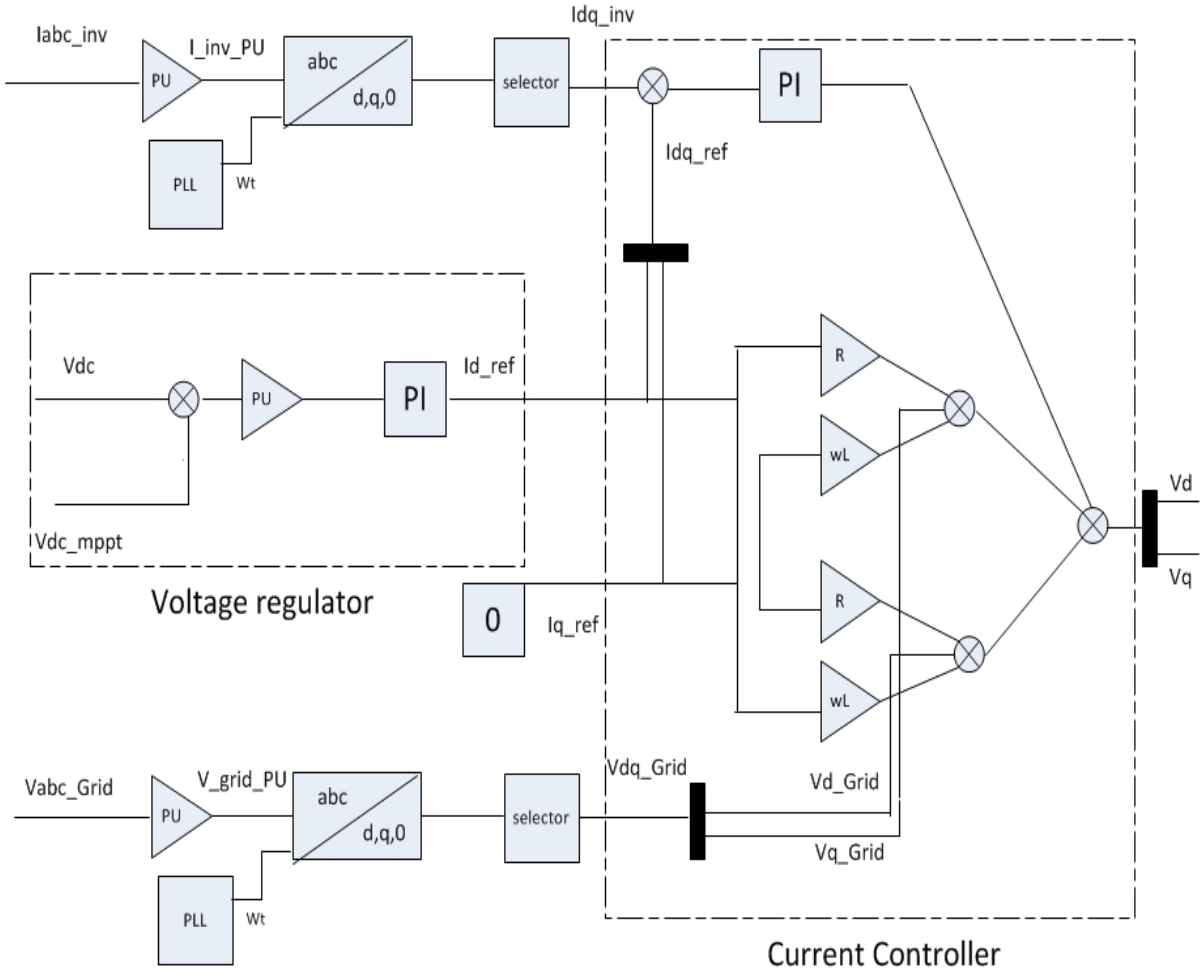

Figure 3.26: Detailed structure of the controller.

4. PRACTICE

4.1. INTRODUCTION

In this section, we are going to study a 120kW photovoltaic system that works at the maximum power using P&O of an algorithm with the DC-DC buck converter. After injecting the active power from the PV into the utility grid with unity power factor P.F using a full-bridge 3-phase inverter with two control loops for synchronizing with the utility grid and applying general electrical power system. Basically, we will study the effects of a PV system on a utility power grid. All the modeling was performed with MATLAB/Simulink.

At first, we studied modeling in detail and decided the following processes:

- Modeling of PV cell "5 parameters equivalent Circuit "
- Modeling of switch circuits DC-DC.
- ✓ Buck (step-down) with PID.
- ✓ Boost (step-up) with PID.
- ✓ Buck-Boost (step-up/down) with PID.
- Using the P&O Algorithm for MPPT with Buck converter.
- Modeling Grid Connecting via PV system with utility grid using closed-loop three-phase inverter.
- Injecting the active power generated from the PV module to the utility grid system and studying active power of load flowing through it.

4.2. MODELING PV PANEL

4.2.1 Five Parameters Model

Using five parameters' equivalent circuit and relations for studying the performance of PV panel under the different solar irradiance and the temperature values; we used the PV panel Samsung SDIPV-MBA1CG255 in MATLAB/Simulink 2017 which showed the following values:

$$I_{sc} = 8.89A \qquad V_{oc} = 38.1\ V \qquad V_{mpp} = 30.5\ V \qquad P_{max} = 255w \qquad n = 60\ cell$$

Figure (4.1) shows the simulation of PV cell relations:

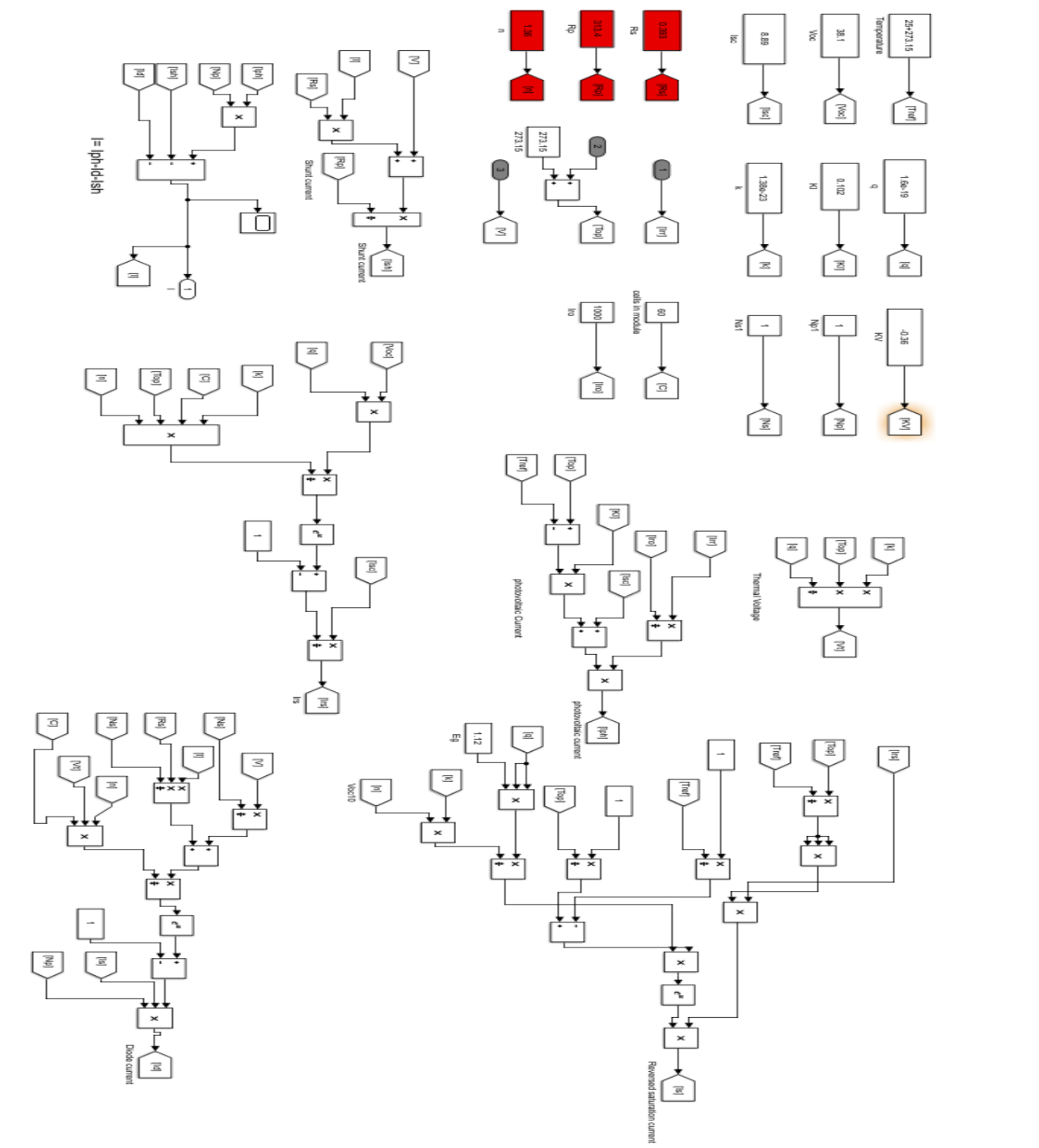

Figure 4.1: Simulation of the PV cell.

If we put all these relations in the subsystem, and connect it to the current source, then we will get the electrical output for the PV panel as shown in Figure 4.2.

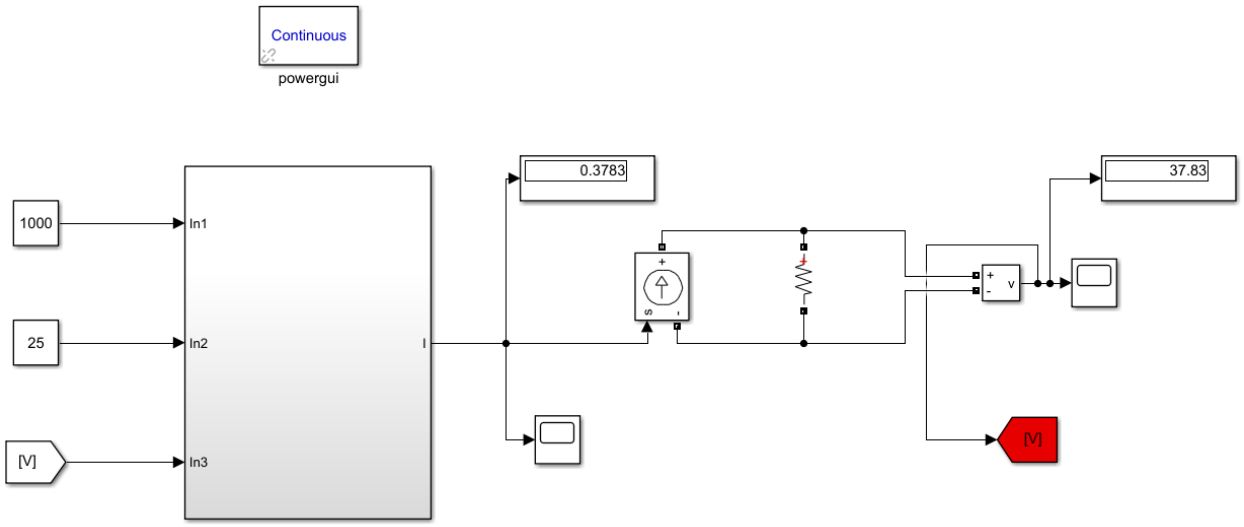

Figure 4.2: PV module simulation.

Using different solar irradiance values [1000-600-400], the output voltage is shown in Figure 4.3.

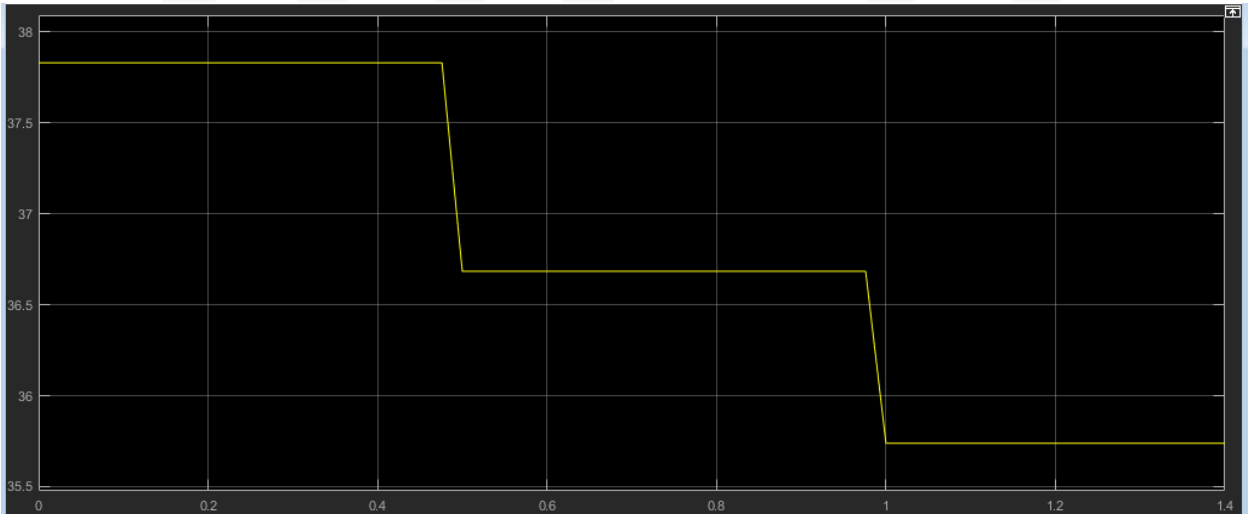

Figure 4.3: Output voltage.

Figure.4.3 describes the resulting voltage, which is affected by solar irradiance and stays lower than VOC.

4.2.2 Result Comparison

The MATLAB/Simulink module application has constant values as compared to the values of irradiance and temperature in an active solar system. In this case, we can compare the results using a five parameter model. Figure 4.4 shows the simulation for one of the PV power systems with three solar irradiance values [1000-600-400] at constant load.

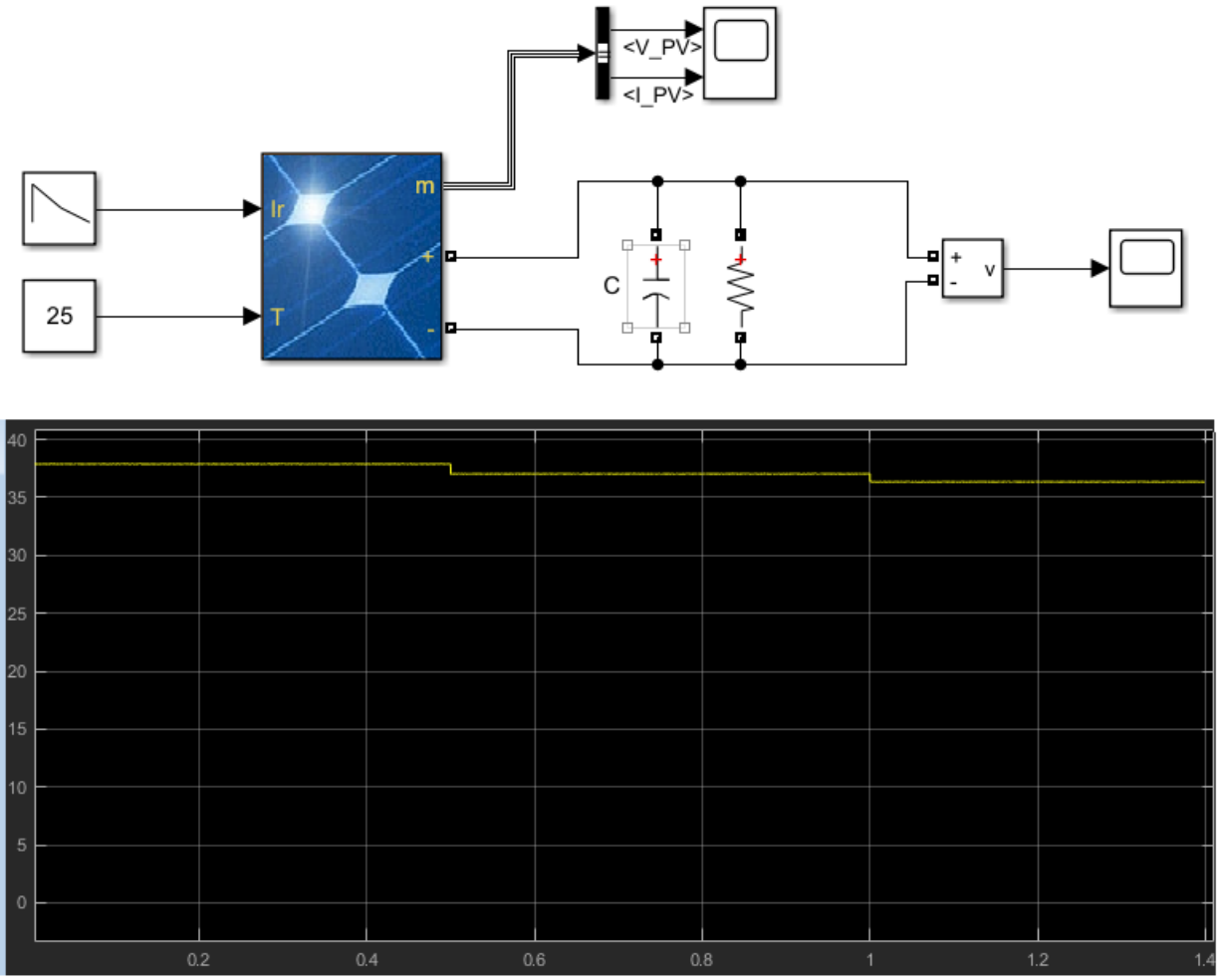

Figure 4.4: PV module in MATLAB/Simulink.

We can note that the output result is very close to the simulated model, and we will use it as the PV system's electrical source in our enforcement study.

4.3. DC-DC CONVERTERS

Using the "Nicole-Ziegler" method for calculating DC-DC component values of converters in continuous mode and tuning PID controller parameters, we applied the simulation for three types of converters in order to control the output voltage at 540Vdc using a three-phase inverter. We obtained 380Vac-RMS output voltage using the following formula: $380 * \sqrt{2} \approx 540\ V$

4.3.1. The Buck Converter

A DC-DC buck converter usually uses step-down output voltage according to the Duty Cycle D, which is controlled by PID, and the calculations of the capacity and inductor. We took PID as constant at 540V output voltage, as Table.4.1 indicates:

Table 4.1: DC-DC Buck converter components

F Hz	L hennery	C Farad	Kp	Ki	Kd
5000	5e-2	20e-6	0.0018	124.2813	1.8775e-08

The simulation for Buck converter controlled is given in Figure 4.5.

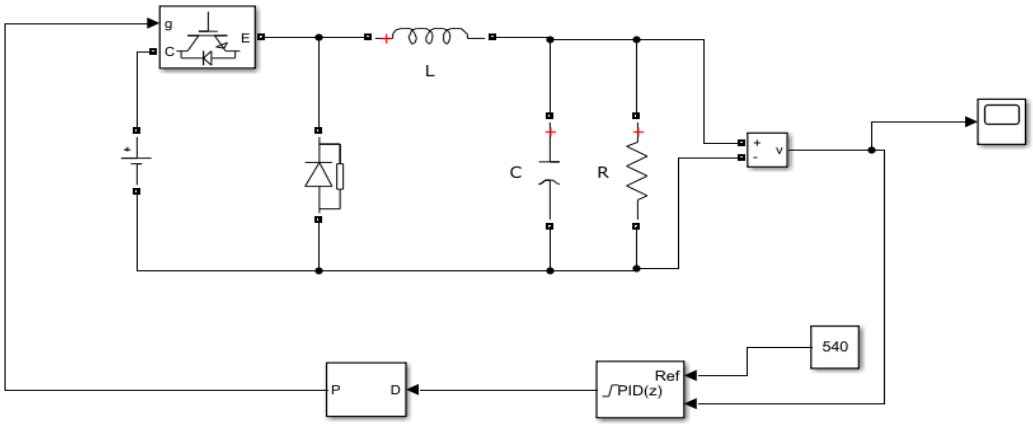

Figure 4.5: Buck converter with PID.

The output voltage is shown in Figure 4.6.

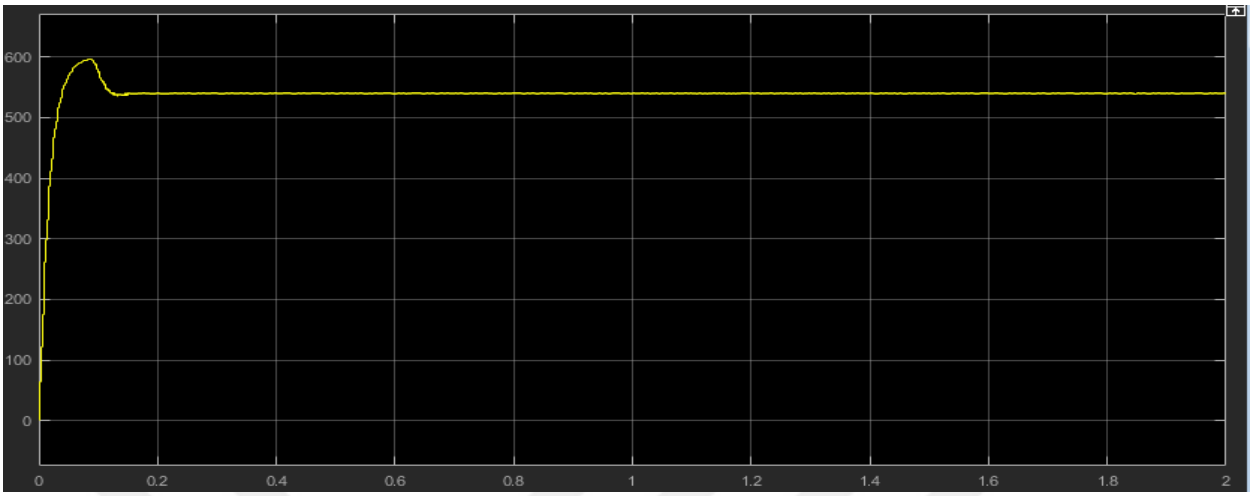

Figure 4.6: Buck converter - Output volt.

4.3.2 Boost Converter

The DC-DC boost converters are usually used to step up output voltage, and perform the inductor and capacity calculations. We have taken PID constant at 540V output voltage, as Table.4.2 shows below:

Table 4.2: DC-DC Boost converter components

F Hz	L hennery	C Farad	Kp	Ki	Kd
5000	5e-3	200e-6	0.0010	124.2813	1.8775e-08

The simulation for Boost converter controller as Figure 4.7 indicates.

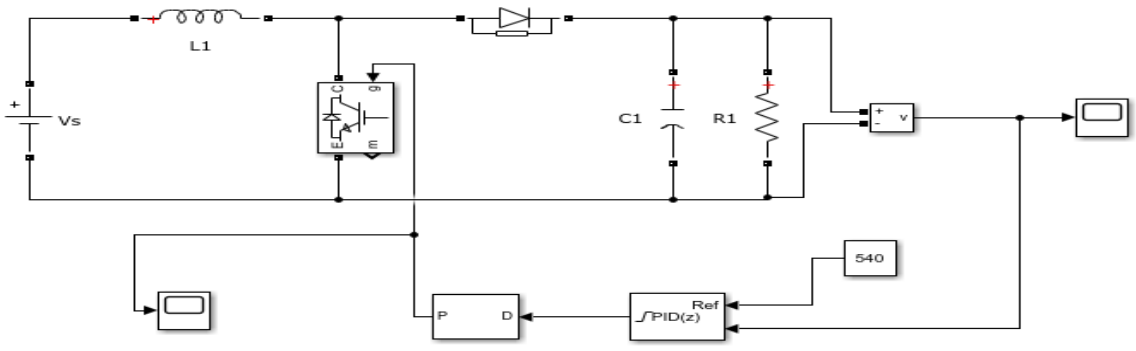

Figure 4.7: Boost converter with PID.

The output voltage is shown in Figure 4.8.

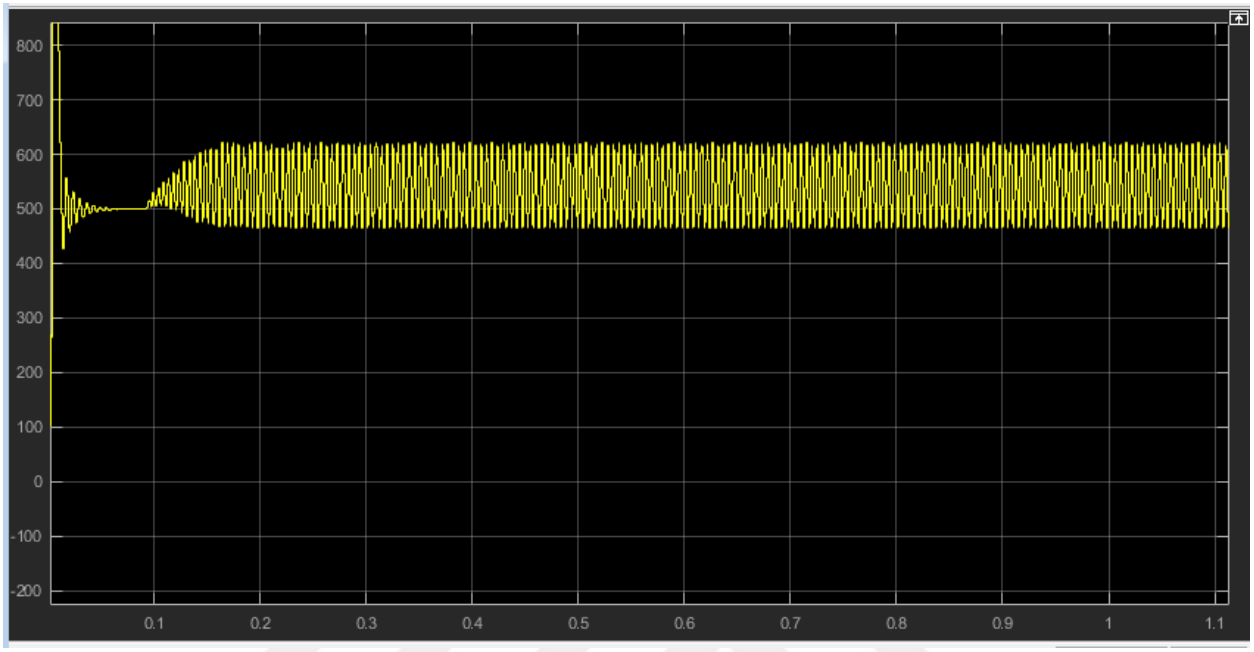

Figure 4.8: Boost converter – output voltage.

4.3.3 Buck-Boost Converter

The converters work for step-up or step down allowing the order of Cycle D; if D<0.5, it will step down for the input voltage; or at D>0.5, it will be step up for the input voltage. At this stage, we will study two cases, the first one for the input voltage - 700V, the converter has to step down for holdout, and the second for the input voltage - 450V, the converter has to step up the input. These calculations are focused on the inductor and the capacity, and we can tune the PID firms for 540V output voltage, as Table 4.3 indicates.

Table 4.3: Buck-Boost DC-DC converter components

F Hz	L hennery	C Farad	Kp	Ki	Kd
5000	5e-5	10e-6	0.0011	124	1.8775e-08

The simulation of controlled Buck-Boost converter is shown in Figure 4.9.

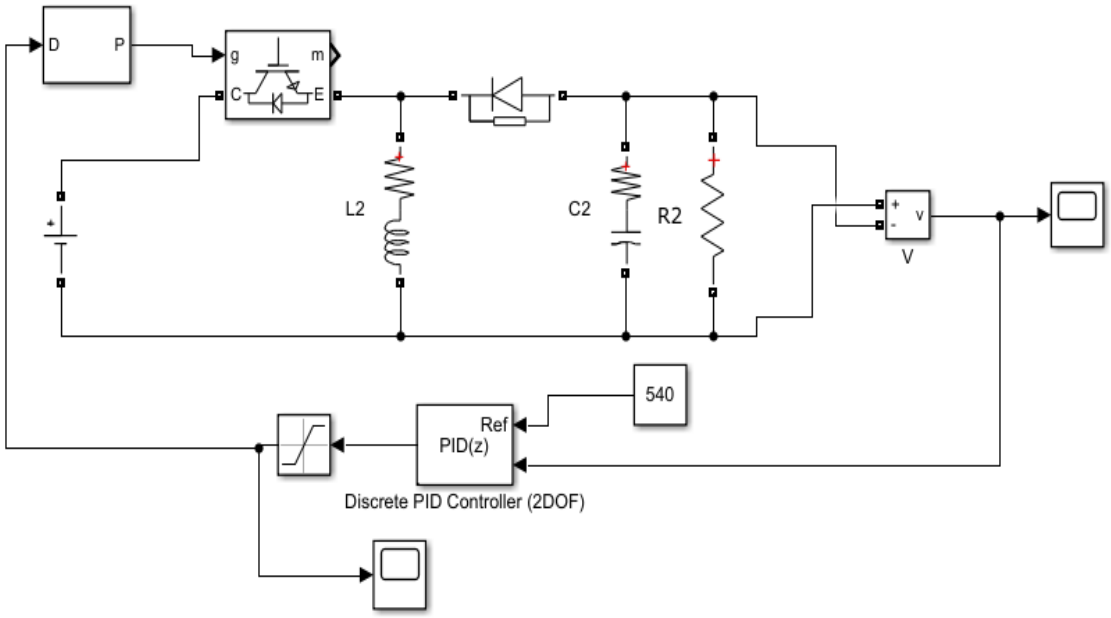

Figure 4.9: Buck-Boost converter.

- DC-DC (Step-Down) mode: The signal is shown in Figure 4.10 and the converter changes for the DC voltage from 700V to 540V.

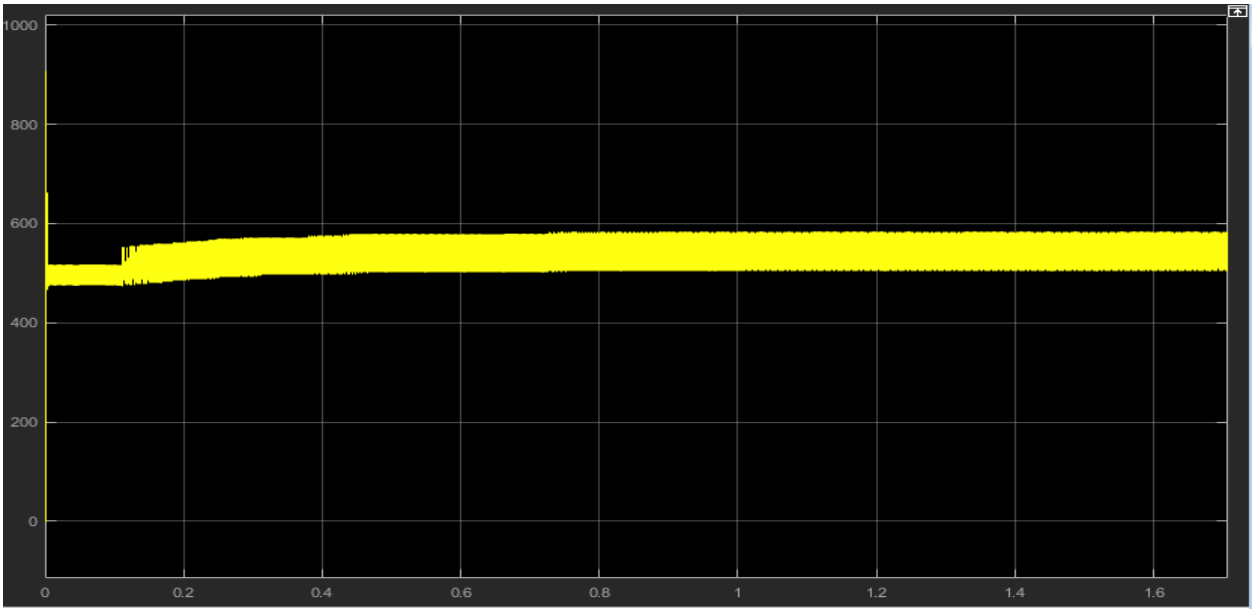

Figure 4.10: Buck-mode converter output voltage.

- Step-up mode: The signal is shown in Figure 4.11. The converter changes the DC voltage from 400V to 540V.

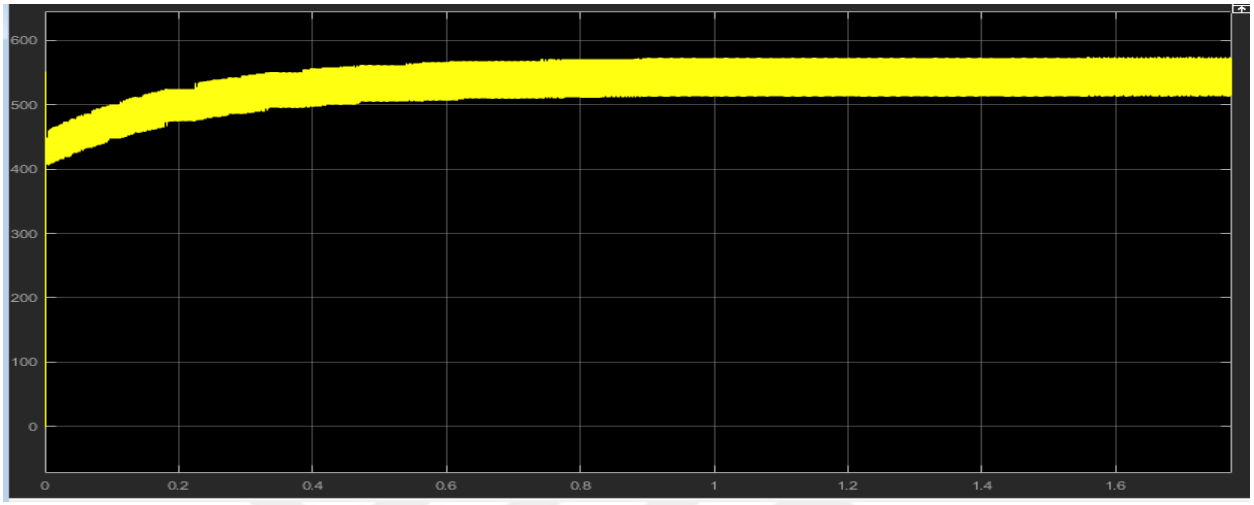

Figure 4.11: Boost-mode converter - output voltage.

We found ripples in the output voltage in boost and buck-boost; they are very wide range, which means that the enforcement can affect the MPPT technique in a negative way, so the VMPPT is lower than VOC, and the buck converter is significant for MPP tracking, especially when the PV system is connected to the utility grid.

4.4. MPPT ALGORITHMS

In our simulation, we applied two kinds of MPPT algorithms. The first one is Perturb and observation in P&O method, the other one is an open voltage method. Both of them were applied to a DC-DC Buck converter.

4.4.1 P&O MPPT Algorithm with Buck Converter

By applying P&O algorithm as a function in the MATLAB/Simulink to control the Buck converter, the variables of the input are I_{pv}, V_{pv}, and T (time of sampling), the function will compare the output power according to the changes in the duty cycle (D), and the result will either increase or decrease the voltage. In the second case, we will use the maximum load (resistance), although the P&O was directly applied to the transistor gate in state of the Buck converter. The full simulation of the PV systems with MPPT is shown in Figure 4.12.

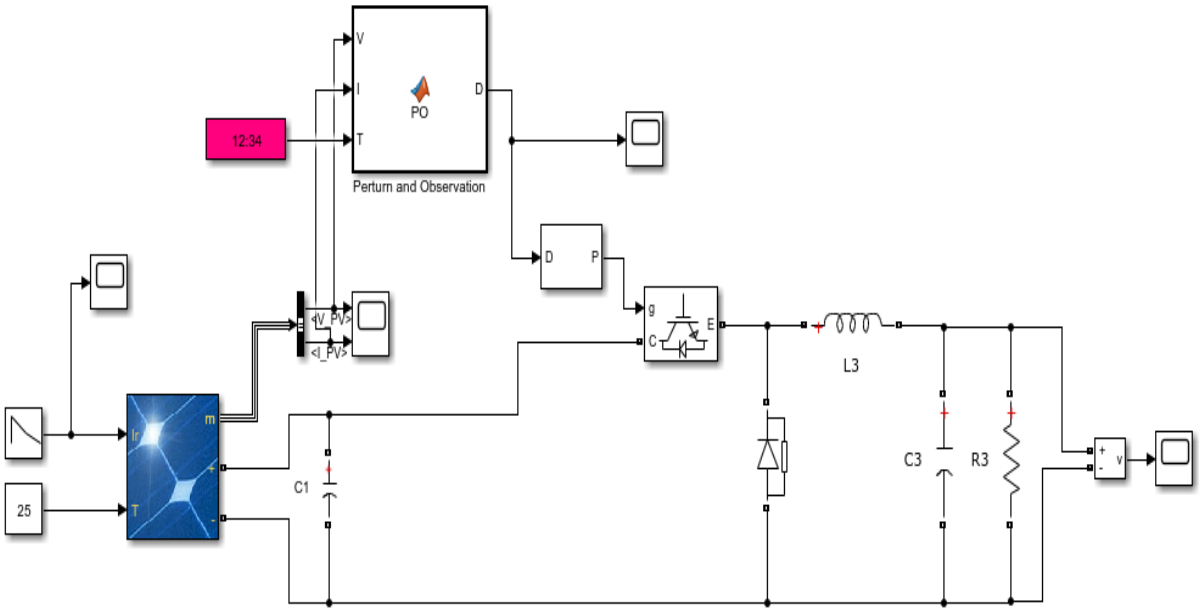

Figure 4.12: MPPT with PV Module.

The output current and voltage for PV at MPP are shown in Figure 4.13.

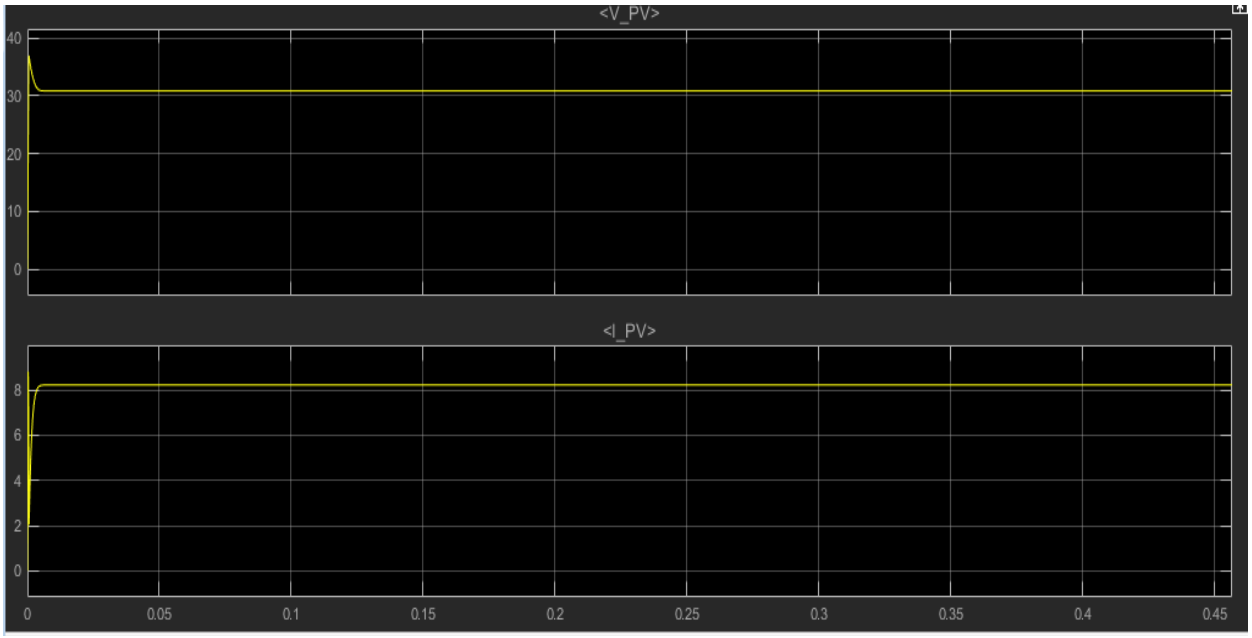

Figure 4.13: The output current and voltage for PV.

Comparing these results with the merits of Samsung SDIPV-MBA1CG255, we can see that they have constant values of I_{mpp}, V_{mpp} with nominal irradiance - 1000 and temperature 25C, as shown in Table 4.4.

Table 4.4: Impp, Vmpp values with MMPT and merits of PV collective

unit	Samsung SDIPV	P&O with Buck
I_{mpp} A	8.30	8.23
V_{mpp} V	30.5	30.8

4.4.2 Open Voltage

In this design, we used the voltage of open circuit of the PV power source without a load and separated the collective from the working PV panels using a Buck converter. In general, the MPP voltage in VOC is similar at 80% voltage for the open PV circuit; the reference voltage value will be 0.8xV_{OC}. Figure.4.14 shows the simulation of this collective in MATLAB/Simulink.

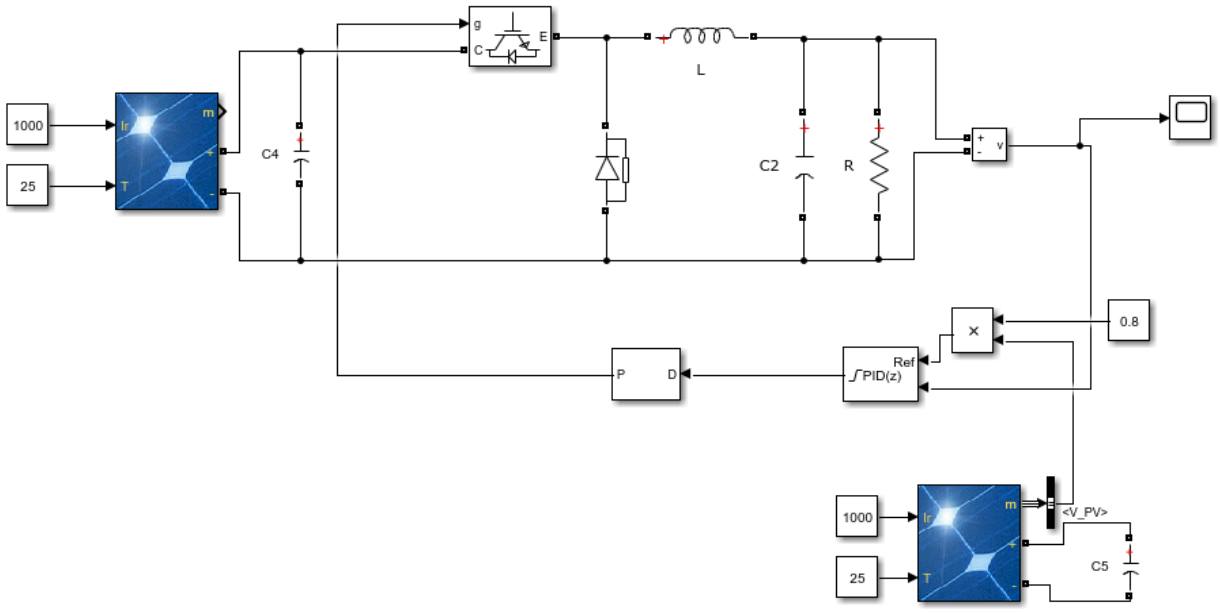

Figure 4.14: Simulation of open voltage method.

The output current and voltage at MPP are given in Figure 4.15; so, we'll see the results that are similar to the previous method but despite the simplicity of the open voltage method, it is obvious from the diagram that there are drawbacks. The first drawback is depending on unloaded PV module, and the second is using PID controller; besides, the collective is not used through a direct method. In this simulation, we are using the P&O algorithm for VOC for duty cycle of the whole system.

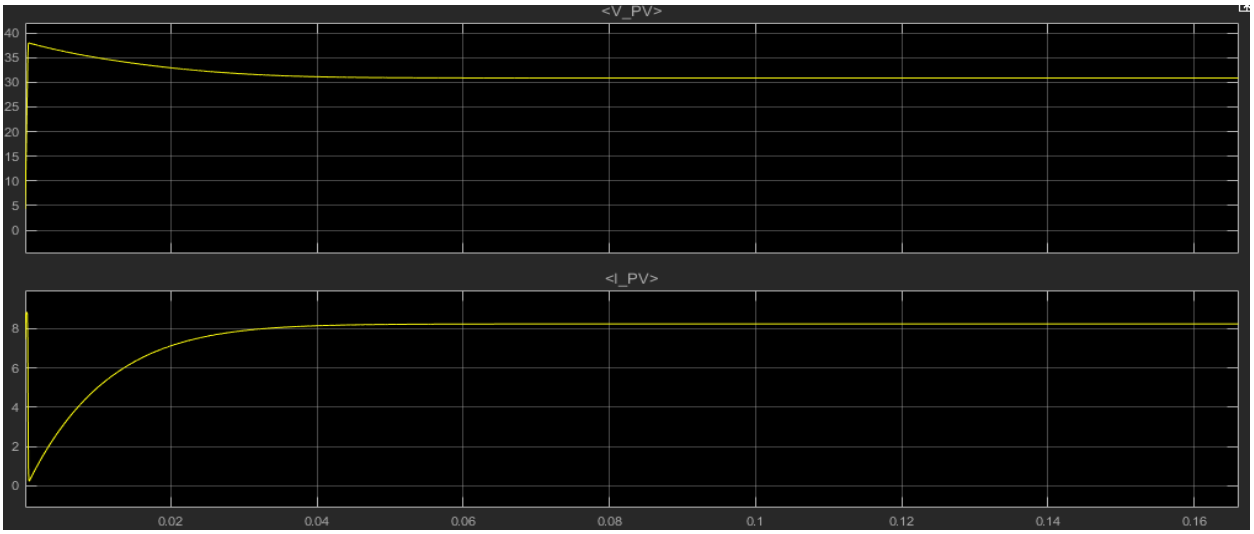

Figure 4.15: The output current and voltage of PV.

4.5. UTILITY GRID

The utility grid is the main power system, which is connected with the photovoltaic system. The power system has parameters (Voltage- Frequency- Power flow). This parameter will be affected by the active power produced in the PV system. The grid utility consists of many components:

- Power plants
- Transformer stations
- Power lines
- Electrical loads

In the simulation, we will consider the utility grid at medium voltage for distribution network with 66/20kV and nominal frequency 50Hz, the different power lines have different lengths, which are connected to stack loads at the end of each power line.

4.5.1 Synchronization Slashes

Before connecting any three-phase AC power source to the PV system, four conditions should be fulfilled:

a) The amplitude should be constant.
b) The phase angle differential should be zero.
c) The frequency of the systems should be constant.
d) The phase arrangement should be similar; it means that A, B, and C phases in a PV system should be connected to the A, B, and C in the other system.

The first three situations apply to the three-phase inverter, and the fourth is guaranteed in the simulation. The modeling of utility grid by MATLAB/Simulink has been shown in Figure.4.16; using three-phase AC sources will produce unlimited active and fusty power (66kV) in the first side of the transformer and 22kV on the other.

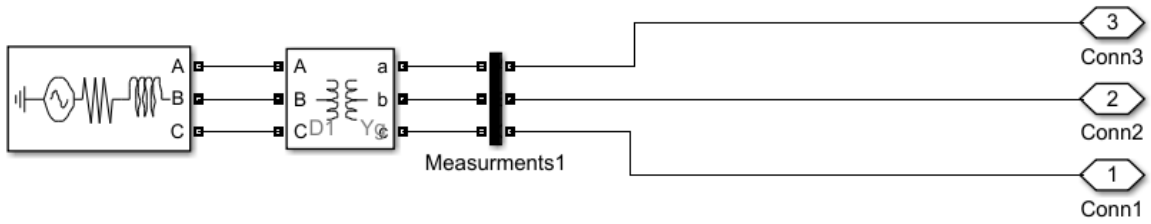

Figure 4.16: The main source in the utility grid.

Adjusting these components in the subsystem of simulation, and connecting it to the power lines with the loads, the utility grid will be as shown in Figure 4.17.

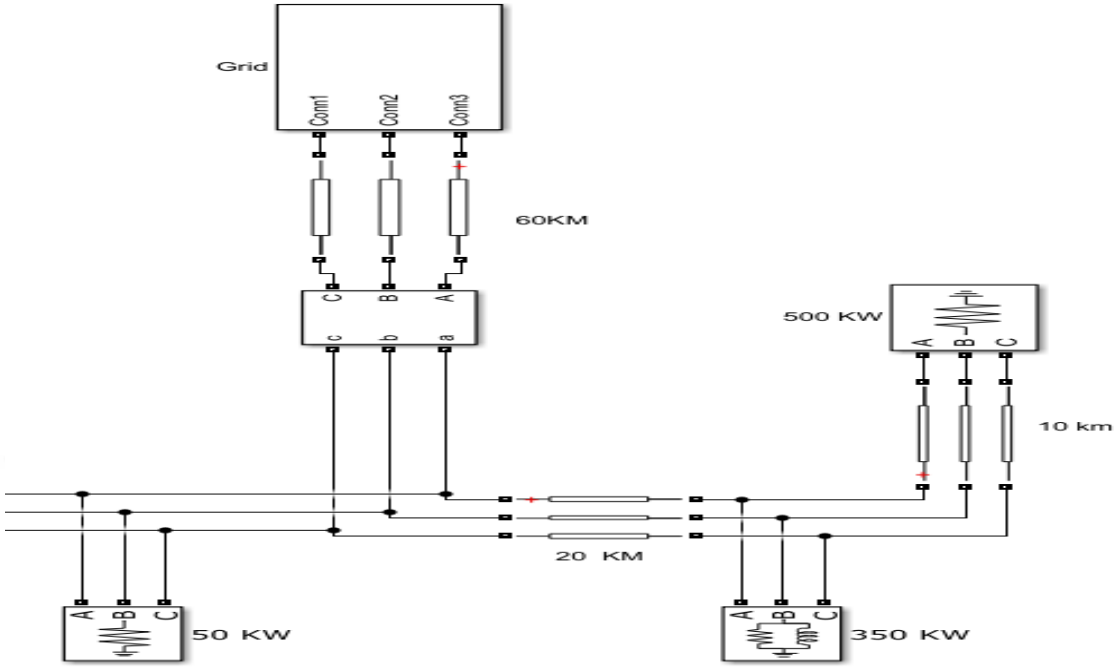

Figure 4.17: Utility grid simulation.

4.6. THREE PHASE INVERTER WITH CONTROLLER

4.6.1 Power Circuit of Inverter

The power circuit for the inverter consists of 12 transistors (4 in each phase) operating with a pulse width modulation PWM; the diagram of this circuit is simulated in MATLAB/Simulink, which is given in Figure 4.18, and it will be connected to coupling indictors and measurements by observing the changes in current, voltage and output electrical power.

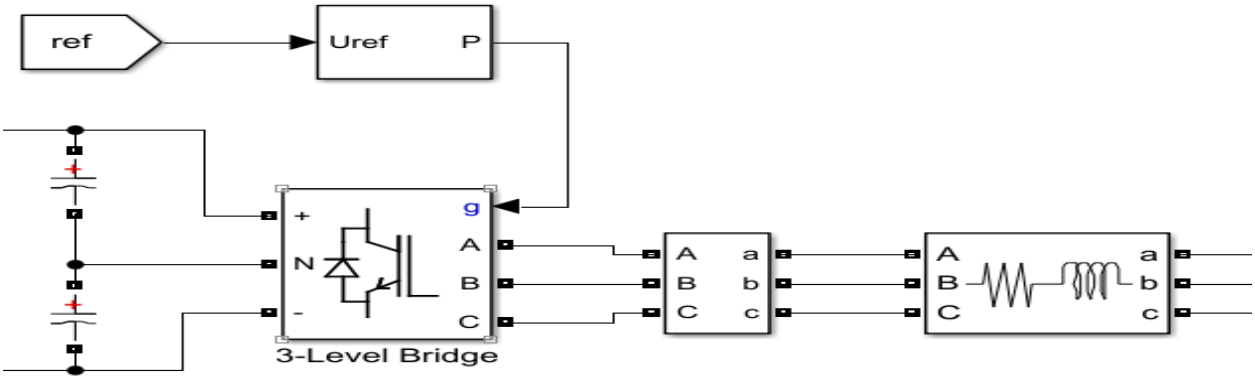

Figure 4.18: Three-phase inverter with coupling indictors.

4.6.2 Inverter Controller

Inverter controller is the most important component in this simulation because it can fulfill three synchronization conditions, and also guarantees the active power flow out of a PV system. Voltage loop is the first loop of controller, which provides the active power quantity, it is added to the utility grid, and it maintains the amplitude of output voltage equal to the utility grid voltage. The second loop is the current loop which assures that the current is flowing form the PV system to the utility grid. The frequency slash of synchronization will be fulfilled with PLL technique, which can control the frequency of PWM for the inverter. The controller has four main parts:

- Park's transformations
- Voltage loop
- Current loop
- Invert Park's transformer and pulse generator

The simulation was included in the PU system, and all the parameters were controlled and adjusted at suitable values.

The nominal value of PV power is the base value, and utility grid voltage is the base value for PU system. Figure 4.19 shows voltage of the loop in the controller.

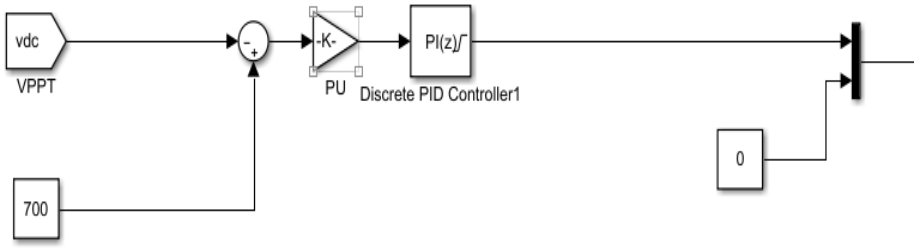

Figure 4.19: Voltage of loop .

As Figure 4.19 indicates, the output of controller PI is $I_{d\text{-}ref}$ (active power produced from the PV) and $I_{q\text{-}ref}$=0, which means there is no fusty power in the DC voltage, and all the adjustment will be applied to the active power in the next step through the current loop. Figure 4.20 shows Park's transformations, PU calculations and current loop, which compares the output current of the

inverter with $I_{d\text{-}ref}$ and $I_{q\text{-}ref}$. A PI controller helps deciding the adjustment needed in the output voltage in (d,q,0)

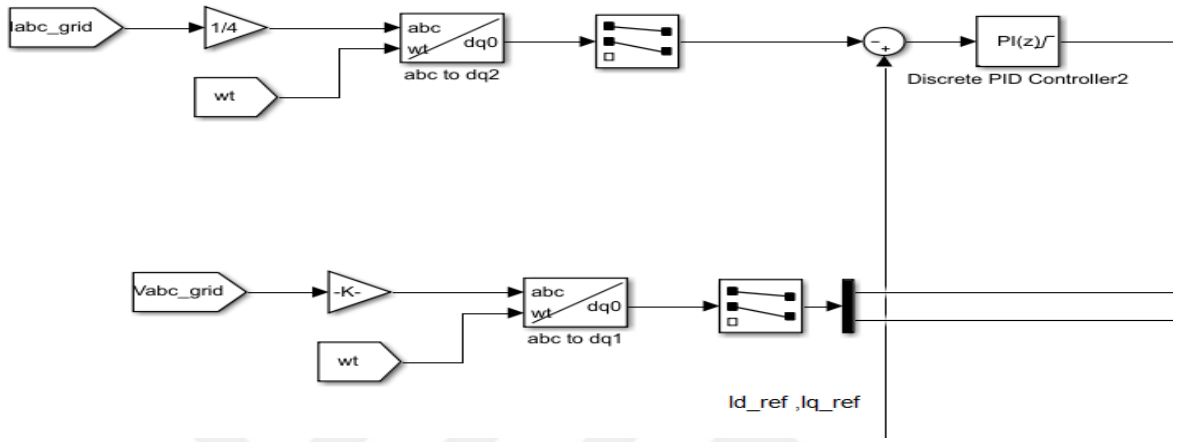

Figure 4.20: Park's transformations, PU calculations and current loop.

The diagram is used to eliminate the third sequence in the space (d,q,0), which isn't needed in normal conditions. The output voltage of PI controller flows into the output voltage of the inverter as an adjustment signal. The inverter voltage (d,q) has been modeled according to the grid voltage value (d, q) with the voltage drop in the coupling indictors, as Figure 4.21 indicates.

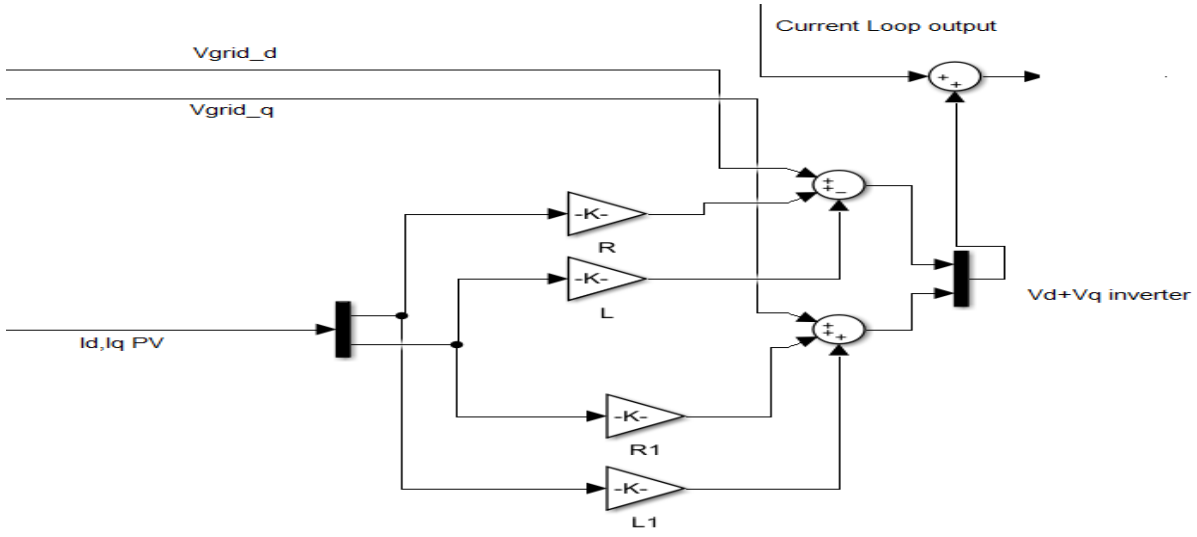

Figure 4.21: Modeling inverter for output voltage in (d,q).

The last part of the controller is the Inverse Park's transformations and pulse generation. In the inverse Park's transformations, we use PLL techniques to provide the transformations with w_t, and the output voltage has the same frequency. Figure.4.22 shows PWM generation in the controller.

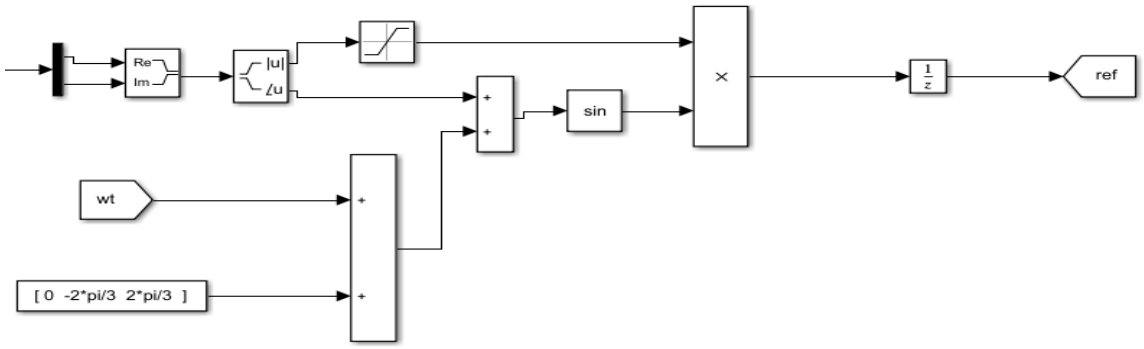

Figure 4.22: PWM generation in the controller **.**

Now, all the components for the PV power source and utility grid have been modeled and it is ready to inject active power from the PV system to the utility grid.

4.7. CASE STUDY

We used 66/20kV distributing transformer power system with several lines and stacked electrical loads. Now we assume that a 125kW PV system includes a 500 PV model with nominal power 250W, the PV array has 25 strings in parallel and 20 series of connecting collectives for each string (25x20=500). This array works with the MPPT using algorithm of the P&O through buck converters' interconnection to the DC-link side. The DC link connects to the central inverter, which interfaces between the utility grid and the PV. The study has two stages:

a) The first part was conducted before synchronization.

b) The second was conducted after synchronization.

We compared the performances of the utility grid with and without the PV system, and how it could be affected.

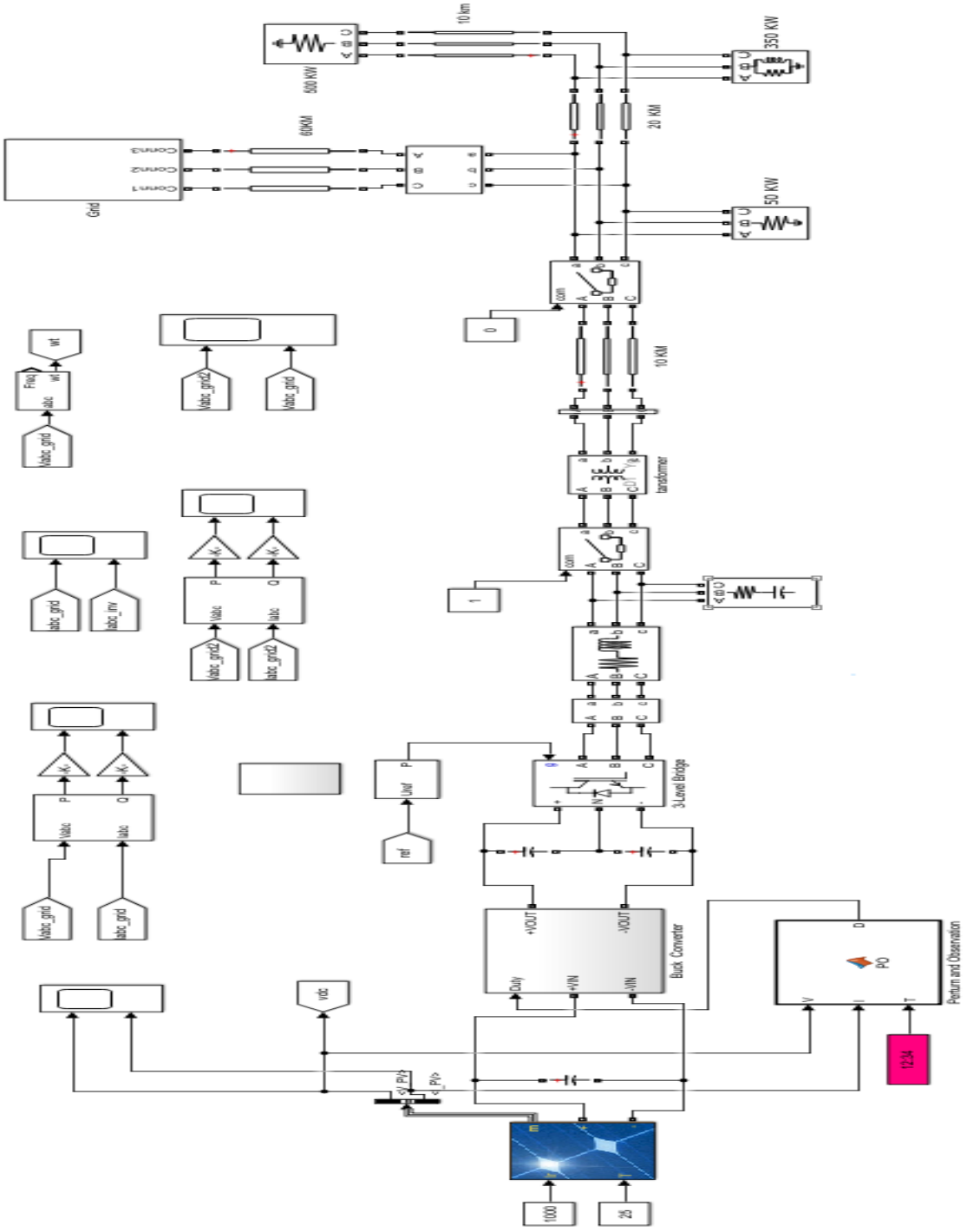

Figure 4.23: The full simulation of the system.

We used two switches to control these stages of study; the full simulation of the system is shown in Figure 4.23.

4.7.1 Before Synchronization

In this situation, the switches were in the off state that means the utility grid feeds all the loads in the system with active and fusty power. Figure.4.24 shows the flows of active power in kW and fusty power in kVAR in the grid.

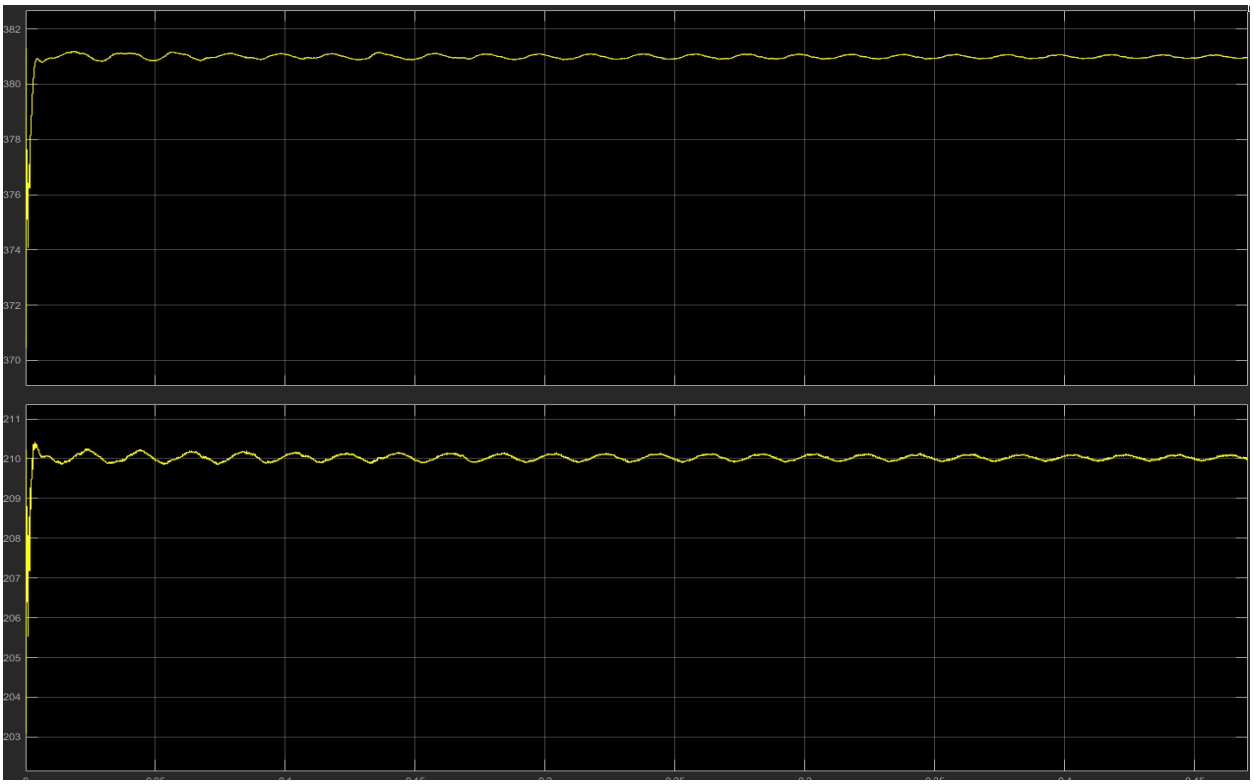

Figure 4.24: Active and reactive power produced from the grid.

The active of power is 382 kW and reactive power is 210kVAR, which flow across the power lines in the grid.

The frequency and amplitude of voltage are the most important parameters, and they should be in the acceptable range (Figure 4.25). We can see the first part of the three-phase AC voltage in the power lines since the pure sine wave has no THD but constant amplitude. In the second part of Figure 4.25, the frequency in the utility grid has constant value - 50Hz.

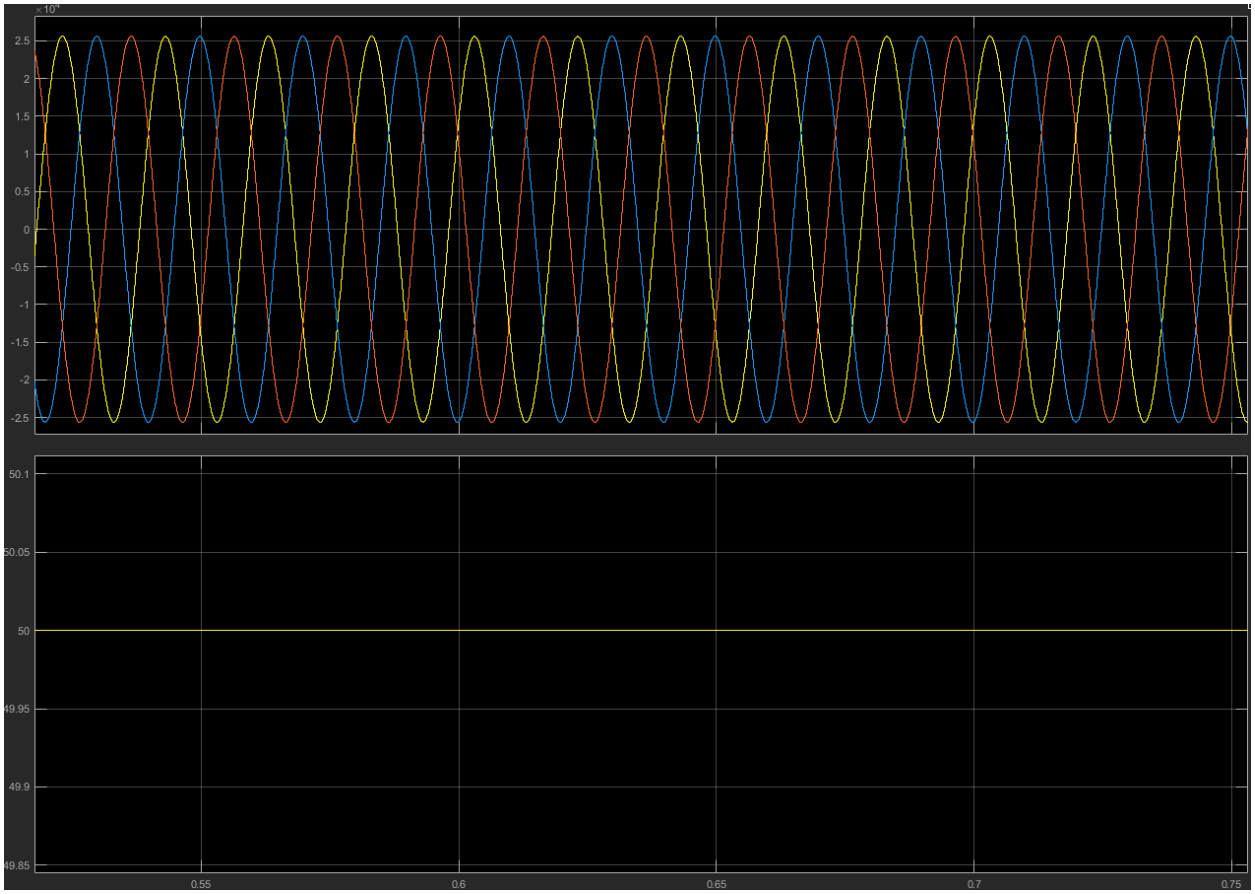

Figure 4.25: Voltage and frequency of of the utility grid.

The sine wave for phase current is shown in Figure 4.26. It is used for judging the performance of the PV system.

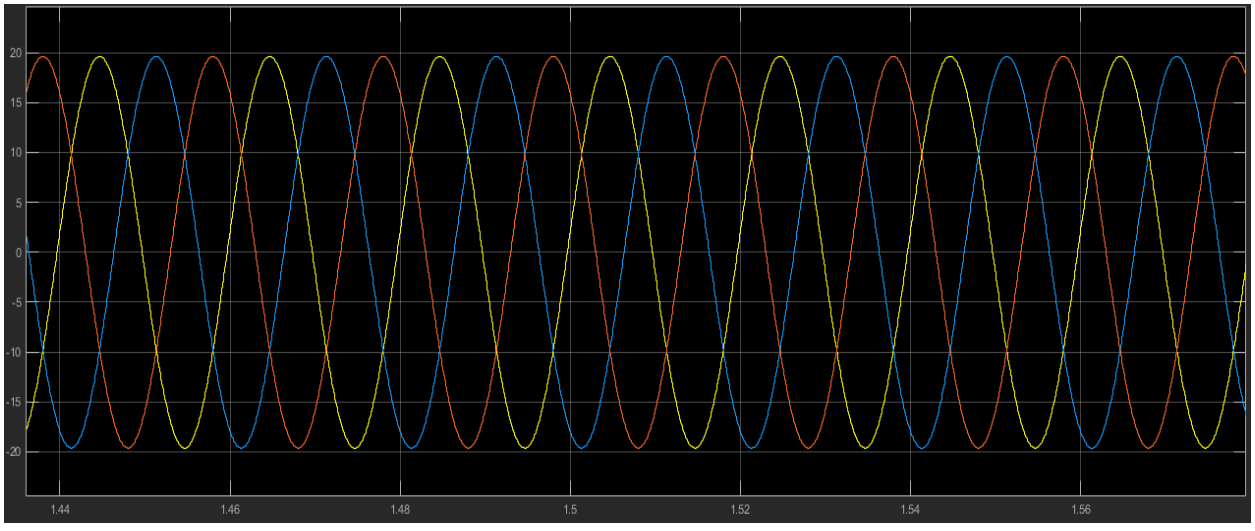

Figure 4.26: Overall current.

4.7.2 After Synchronization

When the switches are in the “ON” state, the inverter begins synchronizing, after which, the transit state of the PV system produces active power, which flows in the utility grid. Figure 4.27 shows the active power in kW and fusty power in kVAR, which flow in the grid after synchronization. Both of them will be lower than the first state (before synchronization) because equal amount of active power is produced by the PV.

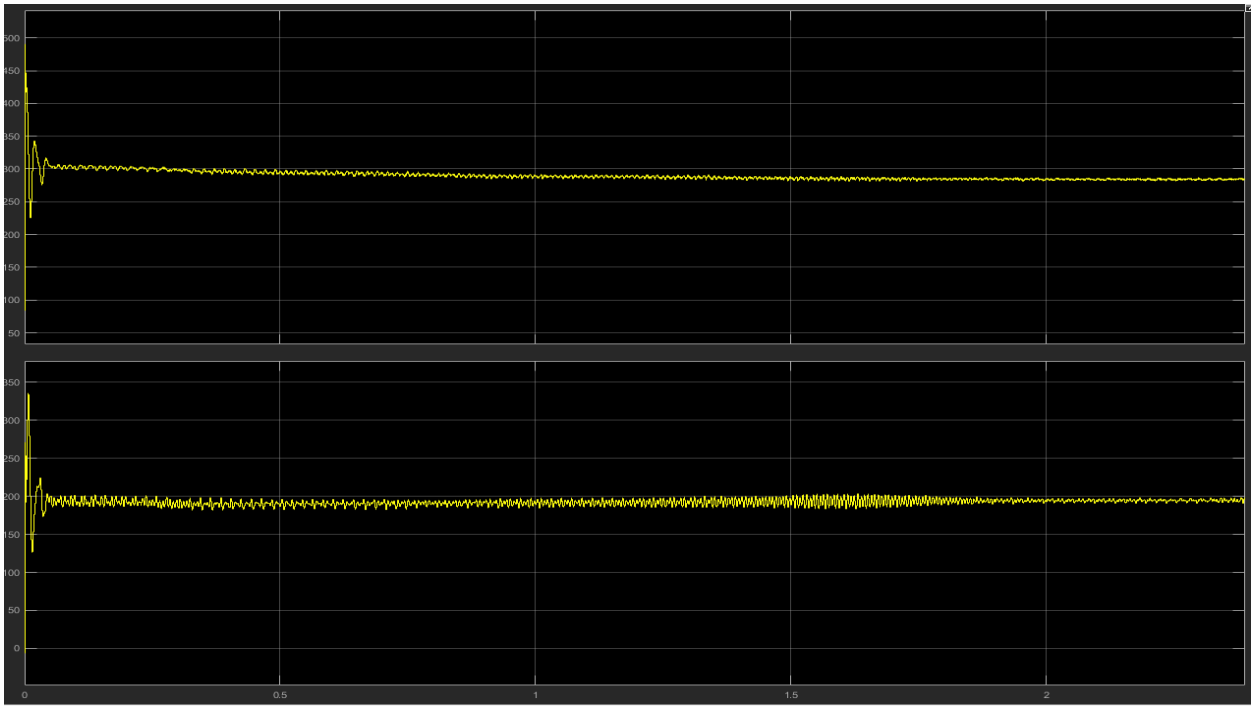

Figure 4.27: Active power in kW and reactive power.

Our results show that a lot of fusty power doesn’t affect despite consuming all the active power injected by the PV system. The reactive power gets slightly more than the power losses in the power line, which lowers the flow of active power from the PV, and it will reduce the active power from flowing in the utility grid. The active power is produced from the utility grid, and a similar power quantity is produced in the PV system. Before synchronization, the utility grid has almost 382kW active power and 210kVAR fusty power. After synchronization, the active power from the utility of grid was 265kW and the fusty power was 195kVAR, which indicates that using PV systems and distributed generation can improve the capability of power lines to

transmit the active power, and reduce the power losses. It also helps fusty power flows in the grid.

The parameters of the power system (voltage and frequency) were tested after synchronization. Figure 4.28 shows the voltage and the frequency after injecting the power from the PV system, and the new voltage is 20kV RMS value, while the frequency is 50Hz, the values were in the acceptable range. In a utility grid, the renewable energy generation systems support the power system to maintain the essential parameters at the nominal values for adjusting the power factor for inverters of the renewable energy system. It is likely to change the power flowing in the grid to keep the voltage and the frequency in the grid nodes at the nominal values.

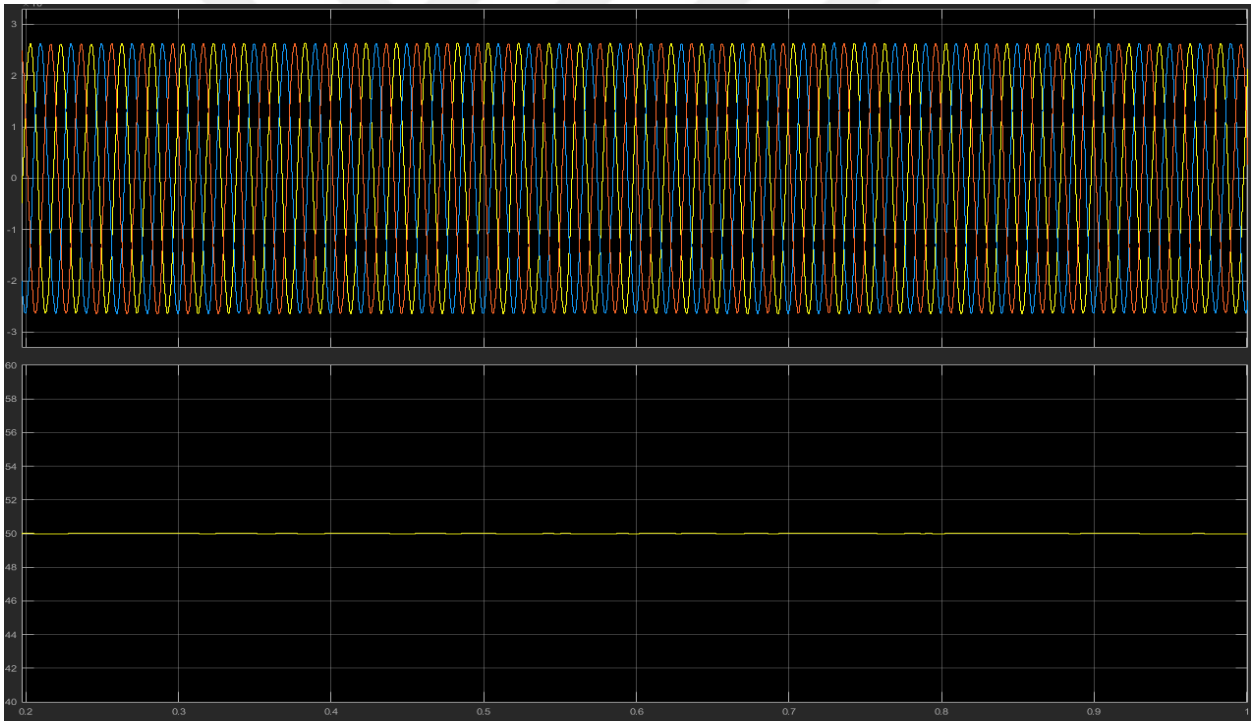

Figure 4.28: Voltage and frequency after synchronization.

When the power flow changes the current in the utility grid, the two currents change in a similar way. Figure 4.29 shows the current from the utility grid and the current, which is produced by the PV system. We can figure out that the utility grid receives the same quantity of current from the PV system. Before synchronization, the current had the tip value about 20 Amp on the 20kV side

while after synchronization; the tip value was 15 Amp. The current produced from PV has tip value 5 Amp, as Figure 4.29 shows.

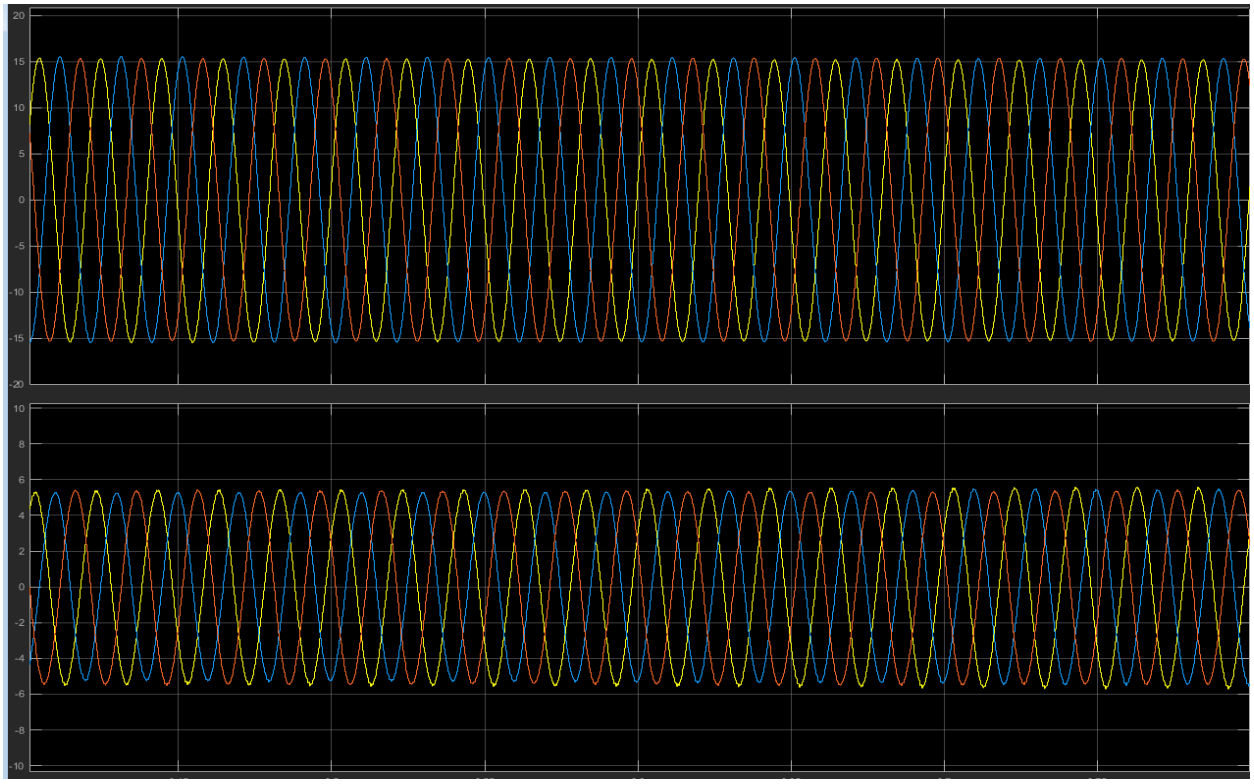

Figure 4.29: Current from the grid and PV after synchronization.

5. CONCLUSION

In this research, we performed complete and detailed study of grid-connected photovoltaic systems, starting from an equivalent circuit that has five parameters (solar irradiance, series resistance, temperature, ideality factor, parallel resistance) and compared the results with a PV module in the MATLAB/Simulink. We found that they were very close to each other.

We studied three types of converters for DC-DC (Buck-Boost, Buck/Boost) conversion with the PID controller to regulate the output voltage in DC 540 volts; so it can be applied to a standalone three-phase AC voltage system. The compared output voltage and the buck converter performed with the least ripple but the boost and buck/boost converters have a wide range of ripple. Since we can't use the boost converter for MPPT because Vmpp<Voc, the buck converter is suitable for our study.

Two of the maximum power points for tracking MPPT collectives, which have been applied with a buck converter, include perturb and observe (P&Q), and the open voltage method. Both of them were suitable for MPPT but P&O is more efficient and doesn’t need an interface between the controller and pulse generator.

Full bridge three-phase inverter with two control loops depends on Park's transformations; so, PLL has been modeled. The first one is a voltage loop that determines the current that the PV can produce while the second is the current loop that assures that the current will flow to the utility grid. PLL techniques were applied to adjust the frequency; so, both the PV system and the utility grid worked with each other.

A medium-voltage three-phase disturbing network 66/20kV has been applied as a case study with different power lines and loads. We connected a PV system using 10kM transport power line. The study has two steps: the first is before synchronization and the second is after synchronization. Based on the results, we concluded the following:

Using renewable power generation systems can add more power to the main distribution utility grid, and it produces active or fusty power according to the need of the system because it changes the power factor of the working inverter. Before synchronization, the utility grid produced 382kW, 210kVAR and 20A tip current value when the frequency was 50Hz but after

synchronization, the photovoltaic system injected nearly 125kW and 5A tip current value while the frequency remained constant at 50Hz; so the load and the flowing current changed. The utility grid produced 265kW, 195kVAR and 5A current tip value, which indicates that active power was generated from the PV module system, and it was injected in the utility grid.

Finally, we concluded the following for future researches:

- Modeling PV cells' performance is a useful way to study different parameters, which affect the active output power created by the PV systems.
- Suitable PV array model can be successfully applied to predict the generated power and deriving the cost function for optimal economic purposes; so, we can get the maximum benefit out of large-scale PV systems.
- The DC-DC buck converters show better performance than the other converters due to low ripples in the output voltage and fast response for changing in the environment of a working PV system.
- Applying maximum power tracking algorithm can substantially improve the amount of absorbed active power from the PV system, especially when it is connected with the closed-loop DC/AC inverter.
- Inverters are essential components for controlling the power factor of generated power (lagging or leading) according to power systems' parameters (voltage and frequency).

Large and small-scale photovoltaic devices can be very useful for voltage and frequency support but they should be installed in the closest node of loads.

The study of a DC-DC converter was conducted to analyze its practical applications but most of the experiments showed inaccurate results [22], [28]. Besides, we were unable to find credible previous researches on DC-DC converters other than a few descriptions on some websites. Most of power sources converted DC into AC at low voltages, and then converted the output voltage to high voltages (230kV or more). During this stage, the inverter increases the reactive power because of three stages of voltage inversion: DC to low voltage, low to medium voltage, and medium to high voltage. Every stage has its own reactive power, and during the process of our research, we found that reactive power was at least 10% [27]. In our approach, we handled this problem in two stages of inversion (DC-AC low voltage and low–medium voltage), and the

reason is: In DC-DC conversion, we do not have reactive power (zero reactive power) while at medium-high voltage, the reactive power in the simulation was approximately 5%, which means that the reactive power decreased by 5% and the active power increased by 5%. Moreover, the power losses were less despite long-distance [29], heat in wires, and inappropriate weather conditions. In the nutshell, the results improved by reducing the power offset, which was provided to the electrical networks and besides, the kind of electronic circuits (buck circuits) helped us overcome many losses. The important thing in this study is its focus on reducing the power losses in the electrical networks while most of the previous studies did not focus on such an important aspect. The results showed improvement when the power losses were successfully reduced, which also means that the renewed power generation was almost equal to the load on the transfer line because we successfully decreased the losses across the power line.

REFERENCES

[1] M. A. Green, K. Emery, Y. Hishikawa, W. Warta, E. D. Dunlop, "Solar cell efficiency tables (version 43)", *Progress in Photovoltaic: Research and Applications*, vol. 22, no. 1, pp. 1-9, 2014.

[2] "Technology Roadmap - Solar Photovoltaic Energy," *International Energy Agency - IEA, Technical Report*, 2014.

[3] S. Liu, R. A. Dougal, "Dynamic Multiphysics model for a solar array", *IEEE Trans. Energy Convers.*, vol. 17, no. 2, pp. 285-294, 2002.

[4] M. G. Villalva, J. R. Gazoli, E. F. Ruppert, "Comprehensive approach to modeling and simulation of photovoltaic arrays", *IEEE Trans. Power Electron.*, vol. 24, no. 5, pp. 1198-1208, 2009.

[5] A. Chatterjee, A. Keyhani, D. Kapoor, "Identification of photovoltaic source models", *IEEE Trans. Energy Convers.*, vol. 26, no. 3, pp. 883889, 2011.

[6] R. Kadri, J. P. Gaubert, G. Champenois, "An improved maximum power point tracking for photovoltaic grid-connected inverter setup on voltage-oriented control", *IEEE Trans. Ind. Electron.*, vol. 58, no. 1, pp. 66-75,2011.

[7] F. Bradaschia, E. A. Silva, M. C. Cavalcanti, A. J. Nascimento, and F. A. S. Neves, "Parameters estimation method for photovoltaic modules," in *2015 IEEE 13th Brazilian Power Electronics Conference and 1st Southern Power Electronics Conference (COBEP/SPEC)*, pp. 1–6.

[8] M. Hejri, H. Mokhtari, M. R. Azizian, M. Ghandhari, and L. Soder, "On the Parameter Extraction of a Five-Parameter Double-Diode Model of Photovoltaic Cells and Modules," *IEEE J. Photovolt.*, vol. 4, no. 3, pp. 915–923, May 2014.

[9] D. S. H. Chan, J. C. H. Phang, “Analytical methods for the extraction of solar cell single- and double-diode model parameters from i-v characteristics”, *IEEE Trans. Electron. Devices,* vol. 34, no. 2, pp. 286-293,1987.

[10] Y. A. Mahmoud, W. Xiao, H. H. Zeineldin, “Analytical methods for the extraction of solar cell single- and double-diode model parameters from i-v characteristics”, *IEEE Trans. Ind. Eletron.*, vol. 60, no. 12, pp.5708-5716, 2013.

[11] Y. A. Mahmoud, W. Xiao, H. H. Zeineldin, “A simple approach to modeling and simulation of photovoltaic collectives”, *IEEE Trans. Sustain. Energy*, vol. 3, no. 1, pp. 185-186, 2012.

[12] W. Xiao, W. G. Dunford, A. Capel, “A novel modeling method for photovoltaic cells”, *in Proc. IEEE PESC*, pp. 1950-1956, 2004.

[13] S. Zaineb and S. Lassad, “P&O controller for the maximum power point tracking in photovoltaic system,” *IEEE International Conference on Green Energy Conversion Systems, Hammamet, Tunisia*, 23-25 March, 2017.

[14] J. Ahmed and Z. Salam, “An enhanced adaptive P&O MPPT for fast and efficient tracking under varying environmental conditions,” *IEEE Transactions on Sustainable Energy*, Vol. PP, Issue. 99, 2018.

[15] J. Ahmed, and Z.Salam, “An improved perturb and observe (P&O)maximum power point tracking (MPPT) algorithm for higher efficiency,” *Applied Energy*, Vol. 150, pp. 97-108, 2015.

[16] V. R. Kota and M. N. Bhukya, “A novel linear tangents setup P&O scheme for MPPT of a PV system,” *Renewable and Sustainable Energy Reviews*, Vol. 71, pp. 257-267, 2017.

[17] M. S. Sivagamasundari, P. M. Mary, and V. K. Velvizhi, “Maximum power point tracking for photovoltaic system by perturb and observe method using buck boost converter,” *International Journal of Advanced Research in Electrical, Electronics and Instrumentation Engineering,*” Vol. 2, Issue 6, pp. 2433-2439, 2013.

[18] N. E. Zakzouk, et al., “Improved performance low-cost incremental conductance PV MPPT technique,” *IET Renewable Power Generation*, pp. 1-14, 2015.

[19] K. Vishweswara, “An investigation of incremental conductance setup maximum power point tracking for photovoltaic system,” *4 International conference on advances in energy research, Energy Procedia, Elsevier,* Vol. 54, pp. 11-20, 2014.

[20] K. A. Aganah and A. W. Leedy, “A constant voltage maximum power point tracking method for solar powered systems,” *IEEE 43rd Southeastern Symposium on System theory, Auburn, USA,* 14-16 March 2011.

[21] M. Lasheen, A. K. A. Rahman, M. Abdel-Salam, and S. Ookawara, “Performance Enhancement of Constant Voltage Based MPPT for Photovoltaic Applications Using Genetic Algorithm,” *Energy Procedia,* vol. 100, pp. 217–222, Nov. 2016.

[22] A. K. Rai, N. D. Kaushika, B. Singh and N. Agarwal, “Simulation model of ANN setup maximum power tracking controller for a solar PV system,” *Solar Energy Materials & Solar Cells,* Vol. 95, pp. 773-778, 2011.

[23] M. Allouche, et al., “Fuzzy observer-setup control for maximum power-point tracking of a photovoltaic system,” *International Journal of Systems Science, Taylor and Francis,* Vol. 49, 2018.

[24] M. Nabipour, M. Razaz, S. GH Seifossadat and S. S. Mortazavi, “A new MPPT scheme setup on a novel fuzzy approach,” *Renewable and Sustainable Energy Reviews,* Vol. 74, pp. 11471169, 2017.

[25] P. Kumar, G. Jain and D. K. Palwaliya, “Genetic algorithm setup maximum power tracking in solar power generation,” *IEEE International Conference on Power and Advanced Control Engineering, Bangalore, India,* 12-14 August 2015.

[26] P. S. Gavhane, et al., “EL-PSO setup MPPT for solar PV under partial shaded condition,” *Energy Procedia, Elsevier,* Vol. 117, pp. 1047-1053, June 2017.

[27] G. Cao, Z. Guo, Y. Wang, K. Sun and H. J. Kim, "A DC/DC conversion system for high power HVDC-connected photovoltaic power system," *2017 20th International Conference on Electrical Machines and Systems (ICEMS), Sydney, NSW,* 2017, pp. 1-6.

[28] H. Choi, M. Ciobotaru, M. Jang and V. G. Agelidis, "Performance of Medium-Voltage DC-Bus PV System Architecture Utilizing High-Gain DC–DC Converter," *in IEEE Transactions on Sustainable Energy*, vol. 6, no. 2, pp. 464-473, April 2015.

[29] X. Huang et al., "Large-scale photovoltaic generation system connected to HVDC grid with centralized high voltage and high-power DC/DC converter," *2017 20th International Conference on Electrical Machines and Systems (ICEMS), Sydney, NSW*, 2017, pp. 1-6.

[30] S. Du, B. Wu, K. Tian, D. Xu and N. R. Zargari, "A Novel Medium Voltage

Modular Multilevel DC–DC Converter," *in IEEE Transactions on Industrial Electronics*, vol. 63, no. 12, pp. 7939-7949, Dec. 2016.

[31] W. Chen, A. Q. Huang, C. Li, G. Wang and W. Gu, "Analysis and Comparison of Medium Voltage High Power DC/DC Converters for Offshore Wind Energy Systems," *in IEEE Transactions on Power Electronics*, vol. 28, no. 4, pp. 2014-2023, April 2013.

[32] J. Thoma, D. Chilachava and D. Kranzer, "A highly efficient DC/DC converter for medium-voltage applications," *2014 IEEE International Energy Conference (ENERGYCON), Cavtat*, 2014, pp. 127-131.

[33] N. Denniston, A. M. Massoud, S. Ahmed and P. N. Enjeti, "Multiple Collective High-Gain High-Voltage DC–DC Transformers for Offshore Wind Energy Systems," *in IEEE Transactions on Industrial Electronics*,vol. 58, no. 5, pp. 1877-1886, May 2011.

[34] Silpa.N and Chitra.J, "An Improved Luo Converter for High Voltage Applications," *International Journal of Emerging Technology and Advanced Engineering*, vol. 4, no. 5, pp. 262-267, 2014.

[35] S. A. Nath and J. Pradeep, "PV setup design of improved positive output super-lift Luo converter," *2016 Second International Conference on Science Technology Engineering and Management (ICONSTEM)*, Chennai, 2016, pp. 293-297.

[36] F. L. Luo and H. Ye, *Advanced DC/DC converters. Boca Raton*: Taylor & Francis, CRC Press, 2017.

[37] Moslehi K and Kumar R "2010 A reliability perspective of the smart grid" *IEEE Trans. Smart Grid*. 1 pp 57–64

[38] Rocabert J, Luna A, Blaabjerg F. and Rodriguez P "2012 Control of power converters in AC micro grids" *IEEE Trans. Power Electron*. 27 pp 4734–4739.

[39] P. Sarvghadi and M. Monfared, “Load sharing control of parallel inverters with uncertainty in the output filter impedances for islanding operation of AC micro-grid,” in *2017 Conference on Electrical Power Distribution Networks Conference (EPDC)*, 2017, pp. 55–61.